Pnictazane Oligomers $[RNPnX]_n$ - Towards Polypnictazanes

by

Jeffrey C. Landry

Submitted in partial fulfilment of the requirements
for the degree of Doctor of Philosophy

at

DALHOUSIE UNIVERSITY
Halifax, Nova Scotia
June 2006

Your file Votre référence
ISBN: 978-0-494-19604-5
Our file Notre référence
ISBN: 978-0-494-19604-5

DALHOUSIE UNIVERSITY

To comply with the Canadian Privacy Act the National Library of Canada has requested that the following pages be removed from this copy of the thesis:

Preliminary Pages

Examiners Signature Page (pii)

Dalhousie Library Copyright Agreement (piii)

Appendices

Copyright Releases (if applicable)

Table of Contents

List of Figures

List of Schemes

List of Tables

Abstract

Reactions of primary amines (RNH_2; R = 2,6-dimethylphenyl; Dmp, 2,6-diisopropylphenyl; Dipp) and pnictogen trihalides (PnX_3, Pn = P; X = Cl, Br, Pn = As, Sb; X = Cl) were performed under various conditions. For Pn = phosphorus or arsenic, cyclodipnictazanes were formed in the presence of triethylamine. Subsequent addition of GaX_3 to the cyclodipnictazanes effected a ring expansion reaction to new cationic 6-membered pnictazane rings. Similarly, addition of GaX_3 to the cyclodipnictazanes, followed by *in-situ* addition of a strong Lewis base yields the neutral cyclotripnictazanes. Combinations of both cyclodipnictazanes (Pn = P, As) under ring expansion conditions produce cyclotripnictazanes with varying composition of both phosphorus and arsenic in the heterocycle as identified by mass spectrometry. The mechanism of the ring expansion has been explored leading to the isolation of a novel cationic 4-membered ring and a unique arsazene-arsine, which suggests cationic monomeric intermediates are involved in the reaction pathway.

Corresponding reactions of RNH_2 and $SbCl_3$ do not yield the cyclodipnictazane but rather, in the presence of triethylamine produce the corresponding cyclotripnictazane. A dipnictadiazane (for Pn = Sb) has also been identified, which provides insight into the mechanism of dehydrohalide coupling reactions between primary amines and pnictogen trihalides.

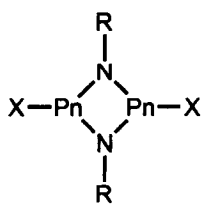

cyclodipnictazane

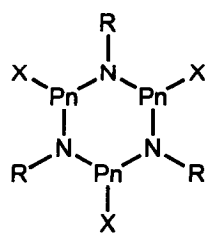

cyclotripnictazane

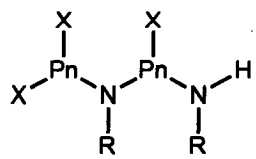

dipnictadiazane

List of Abbreviations and Symbols Used

$^{31}P\{^{1}H\}$	^{1}H decoupled ^{31}P NMR	m.p.	melting point
Å	Angstrom	MALDI-TOF	matrix assisted laser deionization mass spectrometry
amu	atomic mass unit	Mes*	2,4,6-tritertbutylphenyl
BF_{20}	tetrakispentafluorophenylborate	MS	mass spectrometry
BPh_4	tetraphenylborate	NMR	nuclear magnetic resonance
n-BuLi	n-Butyllithium	N,N-DMEDA	N,N-dimethyl ethylenediamine
δ	chemical shift	OTf	trifluoromethanesulfonate
°	degrees	ppm	parts per million
d	doublet	s	singlet
DMAP	4-dimethylaminopyridine	sept	septet
Dipp	2,6-diisopropylphenyl	t	triplet
Dmp	2,6-dimethylphenyl	TMS	trimethylsilyl
EA	elemental analysis	VT	variable temperature
EI-MS	electron ionization mass spectrometry	X	any halogen, F, Cl, Br, I
eq.	equivalents		
Fmes	1,3,5-tris(trifluoromethyl)phenyl		
GPC	gel permeation chromatography		
Hz	hertz		
IR	infrared		
m	multiplet		

Acknowledgements

I am truly grateful for the support, guidance and tolerance of my friends and co-workers while at Dalhousie. My time here would not have been the same without them.

First and foremost, I would like to extend the utmost gratitude to my supervisor, Neil Burford. In a world where research produces publications, which is needed for grant money, his philosophy "the student is the product, not the research" has provided an environment to learn and develop, and not surprisingly produced great results, scientific and otherwise.

I would like to thank all the past and present members of the inorganic lab groups at Dalhousie especially; Dr. Paul Ragogna, Dr. Melanie Eelman, Dr. Jan Weigand, Korey Conroy, Heather Phillips, and Katie Groom. My time at Dalhousie has produced some great friendships and scientific discussion. I would like to especially thank Ezra Edelstein, who provided a valuable experimental contribution to this thesis. Thanks to Adam Dyker, I can't imagine a better person to have spent the past four years working along side. In the end, we both became good scientists; too bad only one of us became a great squash player.

I am deeply indebted to all the crystallographic work done by Drs Robert McDonald and Michael Ferguson at the University of Alberta. How two people I have never met could have had such an impact on my research is quite eerie.

I would also like to thank the Atlantic Regional Magnetic Resonance Centre and Drs Mike Lumsden and Bob Berno for help with solution and solid-state NMR.

To Jurgen Müller, Brian Millier, Rick Conrad and Mike Boutiltier thank you for providing your glassblowing, electronics or mechanical expertise, the lab would not have run smoothly in your absence.

The office staff, Giselle, Deanna, Shelly, Cheryl and Gail, thank you for helping to solve the problems that arose when I only thought I was here to attend a few classes and do a little research.

To my previous research supervisors, Dr. Ignacio Vargas-Baca at McMaster University and Dr. Sheryl Tucker at the University of Missouri. Thank you for providing me the opportunity to get my hands wet in a research lab.

Finally to my wife Marie, I tried to separate research from the rest of my life as much as possible, thank you for not listening when I wouldn't talk. You support was unmatched in all the ways that mattered.

Chapter 1 – Introduction

1.1 – General introduction

Organic polymers comprise much of the synthetic and natural world around us with the conversion of ethylene to polyethylene being perhaps the most industrially important polymerization reaction. In terms of bond enthalpies, the polymerization of ethylene is energetically favourable as a carbon-carbon single bond has a bond energy of 347 kJ/mol, while a carbon-carbon double bond is 611 kJ/mol.[1] The cycloaddition of ethylene to cyclobutane (Scheme 1.1) is the simplest oligomerization for ethylene taking two double bonds and forming four single bonds. Considering only bond energies, the process is exoenthlapic by 166 kJ/mol, while if all factors are considered, including ring strain energy, the process is favourable by 76.2 kJ/mol.[2]

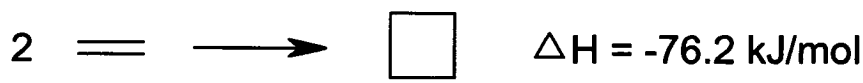

Scheme 1.1 – Cycloaddition of ethylene to form cyclobutane.

Ethylene can be stored indefinitely under ambient conditions and does not undergo cycloaddition or polymerization reactions. The stability of ethylene is not thermodynamic but results from kinetic factors due to limited orbital availability and consequential orbital-symmetry restriction, preventing ethylene from undergoing

oligomerization reactions. The kinetic barrier can be easily overcome under appropriate conditions, making ethylene an excellent monomer for polymerization reactions.

The thermodynamics that govern the polymerization of ethylene are also one of the significant problems facing synthetic inorganic chemists. The challenge known as the "double bond rule" commonly states that π bonds of the heavier elements (those beyond the second row) are thermodynamically unstable with respect to the corresponding σ bonds.[3]

Unfortunately, unlike ethylene, the heavier elements often have low lying, unoccupied orbitals, precluding any significant inherent kinetic stabilization, making multiple bonds of the heavy elements a difficult synthetic target. The problem has been overcome, often recognized by the preparation of the first silicon – silicon double bond,[4] with kinetic stabilization coming by way of large, bulky substituents that physically prevent reactions from occurring at the π bond. Consequently, the addition polymerization of heavier main group element π bonds, while energetically favourable is prevented by the sterics needed to protect the π bond. Only recently, Gates has shown that phosphalkenes containing a phosphorus – carbon double bond can undergo addition polymerization in a manner similar to ethylene.[5]

While other routes such as ring opening and condensation polymerizations have been used to prepare inorganic polymers,[6] addition polymerization still remains an attractive goal given the significance to organic polymers. While suitable inorganic monomers may be difficult to obtain, reactions that mimic addition polymerizations may be the key to understanding the thermodynamic and kinetic factors that govern

relationships between monomers, dimers and oligomers en-route to polymers containing the heavier elements.

1.2 – The pnictogens

The pnictogens comprise the group 15 elements; nitrogen, phosphorus, arsenic, antimony and bismuth and are often abbreviated "Pn" or using the suffix "pnict". This nomenclature will be used throughout the thesis, however in all cases, Pn will signify one of the heavier pnictogens (P-Bi) and not nitrogen.

The chemistry of group 15 elements can often be divided into two categories, nitrogen and the remaining pnictogens. This trend is best explained through a comparison of electronegativities for each element; nitrogen 3.0, phosphorus 2.1, arsenic 2.1, antimony 1.9 and bismuth 1.8, clearly showing a line that separates nitrogen from the latter four. Nitrogen often forms compounds with hydrogen (amines), while heavier pnictogen-halide compounds are readily observed. Reactions of amines and halopnictines which lose HX are common and heterocatenated nitrogen-pnictogen compounds are often seen.

1.3 – Nitrogen – pnictogen compounds

Nitrogen – pnictogen compounds are those containing a nitrogen atom directly bound to a pnictogen atom, which often heterocatentate, forming chains and rings with a backbone of alternating nitrogen and pnictogen atoms. This class of compounds can be broadly subdivided into two categories; pnictazenes, which are described as those containing alternating double and single bonds between the nitrogen and pnictogen atoms

(as example **1.1**), while pnictazanes are those hetercatenated nitrogen – pnictogen compounds that are connected exclusively by single bonds (as example **1.2** & **1.3**).

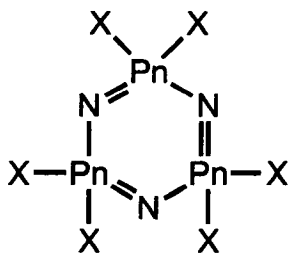

1.1

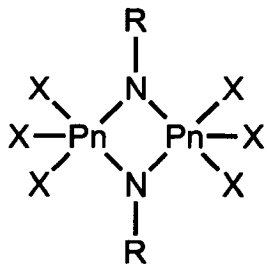

1.2

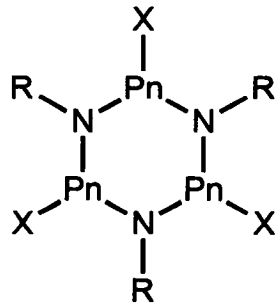

1.3

Pnictazenes are primarily thought of as the outcome of reactions of NH_3 and pnictogen pentahalides (PnX_5). As is common for all nitrogen – pnictogen compounds, the chemistry of pnictazenes is dominated when pnictogen = phosphorus and the amount of literature rapidly decreases down the group. Phosphazenes have been the subject of intense study due to their extensive polymer chemistry that has found industrial applications.[6]

Pnictazanes can be divided into two sub categories, pnict(V)azanes (**1.2**) and pnict(III)azanes (**1.3**) based on the oxidation state of the pnictogen atom. Pnict(V)azanes are formally derived from reactions of primary amines (RNH_2) and pnictogen pentahalides, while pnict(III)azanes are produced from primary amines and pnictogen trihalides.

The remainder of this thesis will focus on pnict(III)azane compounds. For simplicity, all compounds from this point on referred to by the pnictazane nomenclature will be the family of compounds, pnict(III)azanes. Also, unless otherwise specified, the scope of this thesis will deal with pnictazanes derived from primary amines and pnictogen trihalides. In this context, pnictazanes derived from secondary amines and/or primary or secondary pnictogen halides will be specified. As a consequence, any unspecified or unnamed substitution at either a nitrogen or pnictogen atom can be assumed to be a hydrogen or halide, respectively.

1.4 – Synthetic methods to the formation of nitrogen – pnictogen bonds

The synthesis of pnictazanes always begins with a primary amine (RNH_2) and pnictogen trihalide (PX_3), with the exception of a few cases where ammonia is used as the amine. The common routes to N-Pn bonds are outlined Scheme 1.2 with some of the techniques requiring the primary amine or pnictogen trihalide to be modified prior to the N-Pn bond formation step.

The direct reaction between RNH_2 and PnX_3 is perhaps the simplest method for N-Pn bond formation, referred to as a dehydrohalide coupling reaction (route A). The loss of HX in the reaction often occurs below room temperature but is regularly promoted by the use of heat or a base, which drives the reaction to completion. Similarly, hydrohalide salts of primary amines (RNH_3X) can undergo dehydrohalide coupling reactions with PnX_3 (route B), which is especially useful if the primary amine is a gas at room temperature as with ethylamine ($EtNH_2$).[7] While easily accomplished, the dehydrohalide coupling of primary amines and pnictogen trihalides can be difficult to

control with multiple reaction sites at both the primary amine and pnictogen trihalide. Dehydrohalide coupling reactions are also less effective for SbX_3 and BiX_3 with the remaining N-Pn bond forming reactions often overcoming the aforementioned problems.

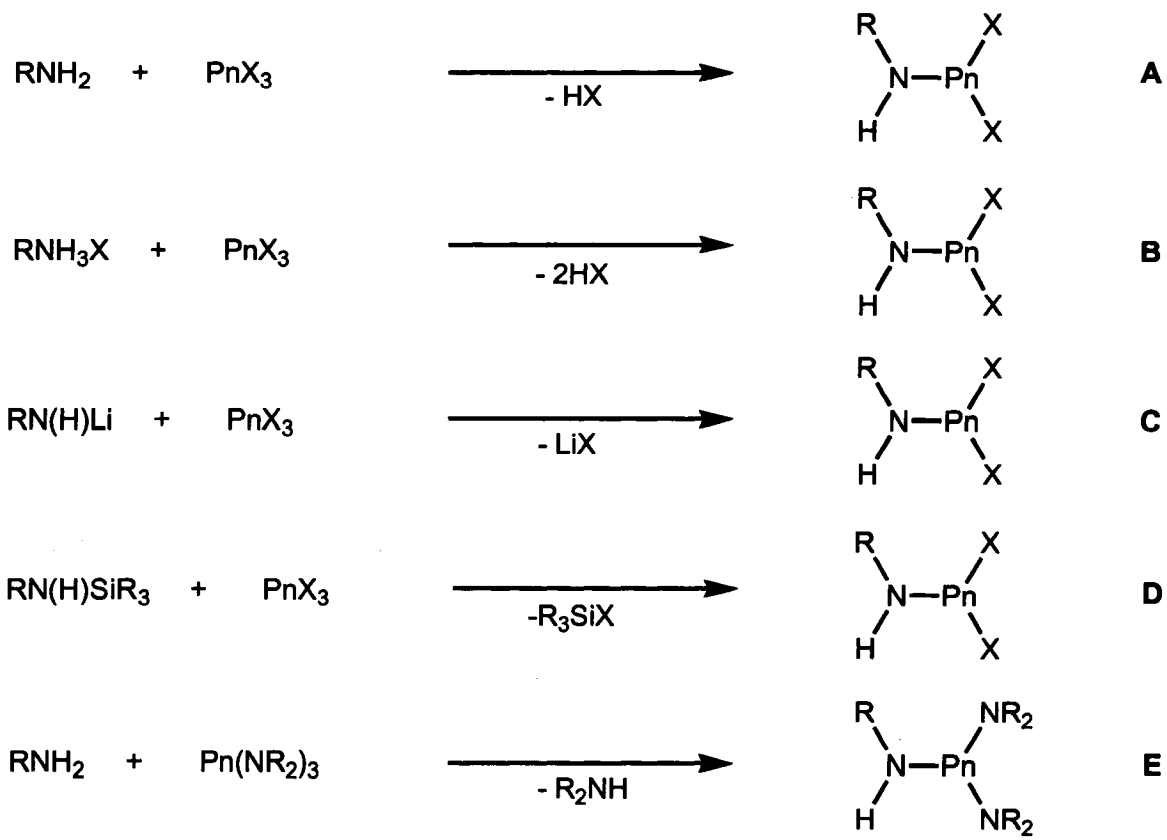

Scheme 1.2 – Synthetic routes to nitrogen – pnictogen bonds.

Primary lithium amides (RN(H)Li) also readily react with PnX_3 losing LiX to yield a N-Pn bond (route C). If done under conditions that circumvent further dehydrohalide coupling reactions, this synthetic route is often the most selective to the

formation of only one N-Pn bond at a time. Likewise, primary amines can be transformed into silylamines ($RN(H)SiR_3$) which readily undergo the loss of silylhalides (Me_3SiX) in the presence of a Pn-X bond to yield the desired N-Pn bond (route D).

Transamination reactions have also been used in the formation of N-Pn bonds (route E). These reactions involve tris(trialkylamino)pnictines ($Pn(NR_2)_3$) with N-Pn bond exchange occurring in the presence of a primary amine, liberating R_2NH. If R is small (usually methyl), the secondary amine is easily removed as a gas from the reaction, driving the formation of the new N-Pn bond.

1.5 – Acyclic pnictazanes

Acyclic pnictazanes can be defined as those in which the nitrogen and pnictogen atoms in the backbone are arranged in a linear fashion. Aminopnictines (**1.4**) are the simplest of acyclic pnictazanes of which there is only one comprehensively characterized example; ($DippN(H)PCl_2$) prepared from the dehydrohalide coupling of $DippNH_2$ and PCl_3 in a 2:1 ratio.[8] Many examples of substituted aminopnictines have been prepared using secondary amines or secondary halopnictines which prevent further reactions to large acyclic pnictazanes. Other substituted aminopnictines containing functionality at nitrogen, such as $-SiMe_3$ groups, which can undergo further N-Pn bond formation reactions have been prepared for Pn = P, As and Sb.[9-15] To date no examples of aminobismuthines (**1.4**Bi) or derivatives have been reported.

From an aminopnictine, the next step to larger acyclic pnictazanes is the addition of a unit of RNH_2 or PnX_3. Formation of bis(pnictino)amines (**1.5**) is well studied as they are readily prepared from excess PnX_3 and primary amine and extensive work has been

done for Pn = phosphorus.[16] On the other hand, formation of a bis(amino)pnictine (**1.6**), containing both Pn-X and N-H bonds has yet to be observed. Substitution of the N-H bonds in **1.6** for $SiMe_3$ groups[17,18] or again by limiting reactivity using secondary amines or secondary halophosphines has allowed the isolation of substituted derivatives of **1.6**.[19-22]

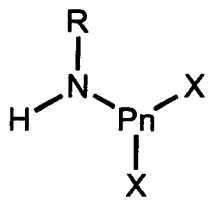

1.4

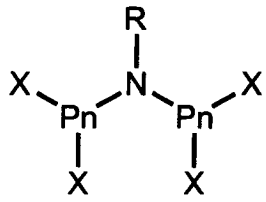

1.5

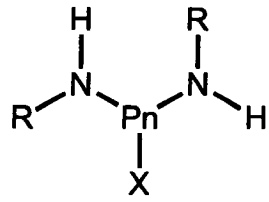

1.6

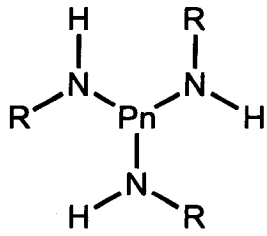

1.7

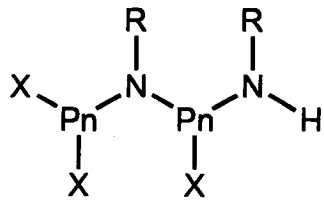

1.8

Further extension of linear pnictazane chains can be accomplished through the addition of RNH_2 to either **1.6** or **1.5** to yield the tris(amino)pnictine (**1.7**) or dipnictadiazane (**1.8**), respectively. Consequently tris(amino)pnictines (**1.7**) are typically prepared from excess amine and PnX_3, however examples of **1.7** with N-H or N-Si bonds are limited to rare examples for Pn = P,[23] Sb[24,25] and Bi[24,25]. More commonly, secondary amines can be reacted in excess with PnX_3 to yield substituted tris(amino)pnictines.[25-33]

No examples of the dipnictadiazane (**1.8**), have been comprehensively characterized although they have been observed by ^{31}P NMR spectroscopy,[8] Longer chains have been observed using amines and pnictines with limited reactivity combined with selective N-Pn bond forming reactions they are however quite rare.[15,23,34]

1.6 – Cyclic pnictazanes

1.6.1 - Iminopnictines

The simplest "cyclic" pnictazanes to be considered are the iminopnictines (**1.9**) which are formally acyclic and contain a double bond between the nitrogen and pnictogen atoms. Given their monomeric relationship with larger cyclic pnictazanes, while also being derived from a primary amine and pnictogen trihalide, iminopnictines are often best included in the category of cyclic pnictazanes.

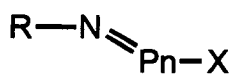

1.9

Large steric groups on nitrogen are required to stabilize the multiple bond between the nitrogen and pnictogen atoms. The most common iminopnictine is when Pn = phosphorus and is formed using the bulky amine Mes^*NH_2 (Mes^* = 2,4,6-tri-tertbutylphenyl) in the presence of excess PCl_3 and NEt_3 to yield (Mes^*NPCl).[35] Extensive studies have been done on iminophosphines, including substitution at both the

R and X position. The chemistry of iminophosphines is diverse including reactions with Lewis acids to form iminophosphenium cations $[RNP]^+$.[36,37]

Monomeric iminoarsines have also been prepared, the simplest derivatives (RNAsX) (**1.9**As) have yet to be observed, however amino or aryl substituted derivatives (RNAsR') (R' = NR_2, Aryl) are known.[38,39] To date no examples of iminostibines **1.9**Sb, iminobismuthines **1.9**Bi or their derivatives have been reported.

1.6.2 – 4-membered pnictazane rings

The 4-membered cyclodipnictazanes $(RNPnX)_2$ (**1.10**) and bis(amino)cyclodipnictazanes $(RNPnNRR')_2$ (**1.11**) are the most commonly observed structures in pnictazane chemistry. The cyclodipnictazane formulation was first suggested in 1894 from the reaction of $PhNH_3Cl$ and PCl_3, yielding $(PhNPCl)_2$,[40] which was later confirmed.[41] More recently, the phosphorus analogues of both **1.10** and **1.11** have been the focus of significant research, with their preparation, structural and spectroscopic features and reactivity being well reviewed.[16,42,43]

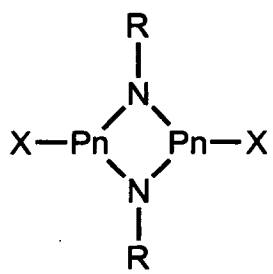

1.10

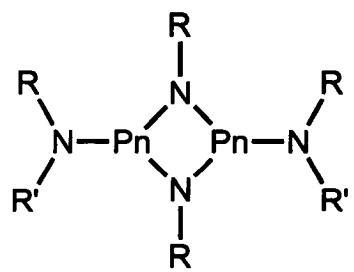

1.11

Cyclodipnictazanes and bis(amino)cyclodipnictazanes are successfully prepared through all of the N-Pn bond formation reactions discussed earlier. Their extensive observation is likely a consequence of aminopnictines (**1.4**) and bis(amino)pnictines (**1.6**) readily undergoing intermolecular cyclization reactions to yield cyclodipnictazanes (**1.10**) and bis(amino)cyclodiphosphazanes (**1.11**), respectively. In contrast, intermolecular cyclization reactions for bis(pnictino)amines (**1.5**) are not available which is the reason they are the most widely observed acyclic pnictazane.

Well characterized examples of cyclodipnictazanes $(RNPnX)_2$ are common for phosphorus and much of the literature is based around $(t\text{-BuNPCl})_2$[44] and $(PhNPCl)_2$[41]. For Pn = arsenic only four structurally characterized examples of cyclodiarsazanes are known; $(t\text{-BuNAsCl})_2$,[45] $(FmesNAsCl)_2$,[46] $(2\text{-pyridyl(Me-6)NAsCl})_2$[25] and $(Mes^*NAsCl)_2$.[47] One example of a cyclodistibazane has been prepared $(t\text{-BuNSbCl})_2$, but is has not been structurally characterized,[48] while no examples of cyclodibismuthanes of the formulation $(RNBiX)_2$ have been prepared to date.

Bis(amino)cyclodiphosphazanes are often the outcome of N-P bond formation reactions where excess primary amine and PX_3 are combined. Derivatives of **1.11**, where R' = H, have found substantial use as starting points for complexes that coordinate main group[43] and transition metal complexes,[49] (**1.12**) (Scheme 1.3). The latter of which have been shown to be ethylene polymerization catalysts.[50]

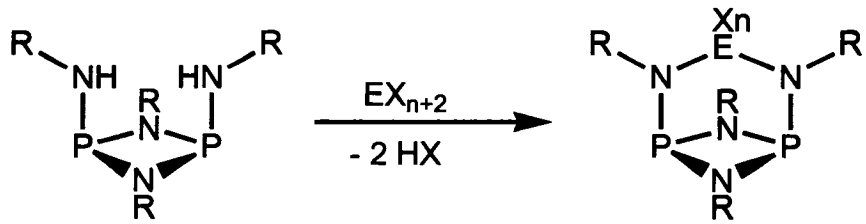

1.12

Scheme 1.3 – Formation of complexes of bis(amino)cyclodiphosphazanes.

The heavier bis(amino)cyclodipnictazanes are the most general 4-membered pnictazane frameworks and examples exist for all of the heavier pnictogens. The homologous series $(DippNPnN(H)Dipp)_2$ (Pn = P, As, Sb, Bi)[51,52] along with $(DmpNSbN(H)Dmp)_2$[53] and $(RNSbNMe_2)_2$ {R = Dipp,[54] 2-pyridyl(Me-4),[55] $C_6H_2(OMe)_3$-3,4,5[55]} have all been isolated. The remaining heavier cyclodipnictazanes that have been reported are substituted at the pnictogen with organic, azido or alkoxy groups and include $(MeNAsR)_2$ (R = C_5H_5, C_5i-Pr_4H),[56] $(PhNAsC_6H_4Br\text{-}4)_2$,[57] ($t$-$BuNSbR)_2$ (R = Ph,[20] t-Bu,[58] N_3,[48] Ot-Bu[48]) and (t-$BuNBiPh)_2$.[20]

Structurally cyclodipnictazanes or bis(amino)cyclodipnictazanes can exist in one of two configurations; *cis* or *trans* defined by the relative orientation of the two exocyclic Pn-X or Pn-N bonds being either on the same (*cis*) or opposite (*trans*) sides of the 4-membered N_2Pn_2 core (Figure 1.1).

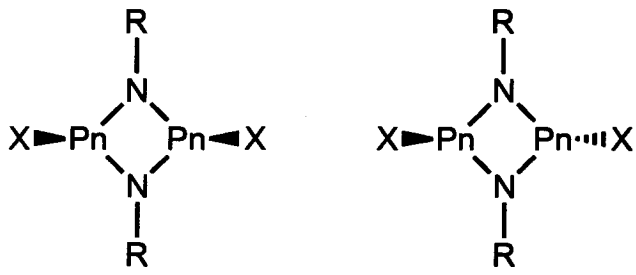

Figure 1.1 – *Cis* versus *trans* cyclodipnictazanes.

Approximately 100 cyclodiphosphazanes (regardless of substitution at phosphorus) are known and the configuration (either *cis* or *trans*) in solution can be assigned in virtually all cases. ^{31}P NMR chemical shifts in the range of 200 – 220 ppm are generally observed for *cis*-$(RNPX)_2$ (X = F, Cl) while the phosphorus nuclei in compounds with the *trans* configuration are more deshielded by 80 - 90 ppm.[42] The same trend is observed for bis(amino)cyclodiphosphazanes, where the phosphorus nuclei in compounds with *cis* configurations have chemical shifts in the range of 100 – 130 ppm. In solution there is a slight preference for the *cis* configuration, however chemical shifts for both configurations are often observed to be in equilibrium by VT ^{31}P NMR spectroscopy. For cyclodiphosphazanes isolated in the solid-state, there is a distinct preference for the thermodynamically favoured *cis* configuration.[43]

The preference changes down the group. Of the eight As_2N_2 frameworks isolated in the solid-state $(Mes^*NAsCl)_2$,[47] $(FmesNAsCl)_2$[46], $(MeNAsC_5i\text{-}Pr_4H)_2$[56] and $(PhNAsC_6H_4Br\text{-}4)_2$[59] are observed as the *trans* configuration, while the remaining four

have a *cis*-configuration. For the antimony and bismuth analogues, the *trans* configuration is observed more often in the solid-state as only one of twelve Sb_2N_2 or Bi_2N_2 cores, $(DippNSbNMe_2)_2$[54] has been characterized as the *cis* configuration. With the exception of *cis*-$(DippNSbNMe_2)_2$,[54] NMR studies have yet to be reported identifying the configuration of any heavier cyclodipnictazanes (Pn = As, Sb, Bi) in solution, which is possible given the appropriate exocyclic substituents.

In the solid-state, 4-membered N_2Pn_2 rings are planar in the case of the *trans* configuration, while they become puckered for the *cis* configuration. Different proposals have been made[43] but it appears sterics and ring flexibility play the greatest role in deciding whether cyclodipnictazane is *cis* or *trans*.

1.6.3 – 6- and 8-membered pnictazane rings

Cyclotripnictazanes (**1.13**) have also been the prepared, however they are limited to examples where R is small (Me, Et, *n*-Pr) and only for Pn = phosphorus and arsenic. Phosphazane examples include $(MeNPX)_3$ (X = Cl, Br) prepared through reactions of PX_3 and $MeN(SiMe_3)_2$,[60] while $(EtNPX)_2$ (X = F, Cl) and $(n\text{-}PrNPCl)_3$ are prepared from PCl_3 and the corresponding amine hydrochloride, followed by halide exchange for X = F.[7] Cyclotriphosphazanes can also be substituted at phosphorus with alcohols to yield alkoxy derivatives such as $(MeNPOMe)_3$[61] and $(EtNPOC_6H_4Br\text{-}4)_3$.[62] The cyclotriarsazane $(MeNAsCl)_3$, is the only example of a 6-membered arsazane ring and is prepared from $As(NMe_2)_3$, $MeNH_2$ and HCl.[63,64]

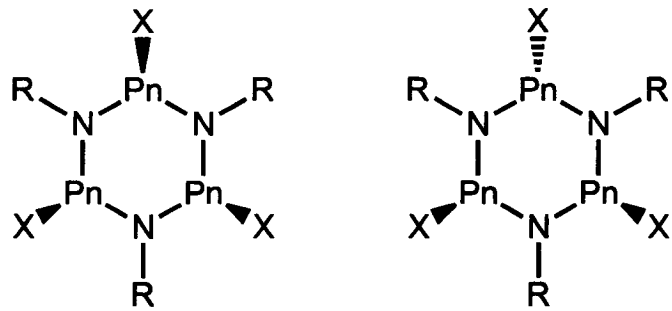

cis **1.13** *cis, trans*

As with cyclodipnictazanes, cyclotripnictazanes can exist as two different configurations. When all three Pn-X bonds are on one side of the N_3Pn_3 core, a *cis* configuration is defined, while if two Pn-X bonds are opposite the remaining P-X bond the cyclotripnictazane is said to have a *cis, trans* configuration. ^{31}P NMR spectroscopy easily distinguishes between the two configurations in solution (for Pn = P) as the *cis* exhibits a singlet peak, while the *cis, trans* configuration has two peaks, with a 1:2 relative integration. Though an AX_2 pattern is expected for the *cis, trans* configuration, this is only occasionally observed at low temperature.[7] For almost all cyclotriphosphazanes reported, ^{31}P NMR data indicates that mixtures of compounds having *cis* and *cis, trans* configurations are present in solution. Spectroscopic data for various cyclotriphosphazanes are shown in Table 1.1 showing the general chemical shift region (100 – 135 ppm) for both *cis* and *cis, trans* cyclotriphosphazanes, which compared to the *cis*-cyclodiphosphazanes (200 – 220 ppm), indicates that even though the local chemical environment (N-P(X)-N) may be similar, the geometry about phosphorus has significant influence on chemical shifts.

Table 1.1 – ^{31}P NMR data for select cyclotriphosphazanes.

Compound	δ ppm (*cis*)	δ ppm (*cis, trans*)	$^{2}J_{pp}$ Hz
$(MeNPCl)_3$	102	134, 129	-
$(MeNPBr)_3$	132	-	-
$(EtNPF)_3$	100	118, 111	6.2
$(EtNPCl)_3$	104	135, 129	6.7
$(n\text{-}PrNPCl)_3$	105	136, 131	-
$(MeNPOMe)_3$	94	117, 111	12.8
$(EtNPOC_6H_4Br\text{-}4)_3$	97	123, 118	6.8

The solid-state structures of three cyclotripnictazanes are known; $(EtNPCl)_3$,[65] $(MeNAsCl)_3$,[64] and the substituted $(EtNPOC_6H_4Br\text{-}4)_3$.[62] While both *cis* and *cis, trans* configurations have been observed in solution for $(EtNPCl)_3$,[7] only the *cis* configuration could be isolated in the solid-state as a chair conformation. In contrast, the cyclotriarsazane $(MeNAsCl)_3$[64] is observed as the *cis, trans* configuration in the solid-state however the configuration in solution has not been established. Fractional crystallization provided both the *cis* and *cis, trans* configurations in the solid-state for $(EtNPOC_6H_4Br\text{-}4)_3$.[62] The *cis* configuration is found to be a chair conformation, while the *cis, trans* configuration in a boat conformation.

Two examples of tetrameric cyclophosphazanes $(RNPR)_4$ have been observed,[66,67] and one example of a cyclotetraarsazane $(HNAsC_5H_5)_4$[56] however no halo-cyclotetrapnictazane $(RNPnX)_4$ derivatives are known.

1.7 – Transformations between oligomeric pnictazanes

Iminopnictines, cyclodipnictazanes, cyclotripnictazanes and cyclotetrapnictazanes represent a monomer, dimer, trimer and tetramer relationship. Scheme 1.4 shows

possible transformations between different ring sizes as first recognized by Zeiss.[61] Step A, the cycloaddition of an iminopnictine to a cyclodipnictazane was first observed by Scherer[15] and later by others,[47,68,69] and is proposed as a step en-route to cyclopnictazanes.[70] Step B, the interconversion of the dimer and trimer was first recognized by Zeiss,[61] who obtained bis(amino)cyclodiphosphazanes from distillation of the corresponding tris(amino)cyclotriphosphazanes. Step C, a monomer to tetramer relationship was recognized by Malavaud,[66] who observed the decomposition of a cyclotetraphosphazane to the iminophosphine through heating or exposure to a Lewis acid. Steps D and E have not been reported. Observation of steps A-C indicate that a subtle energetic interplay exists between oligomers, which could have a significant impact on accessing polypnictazanes.

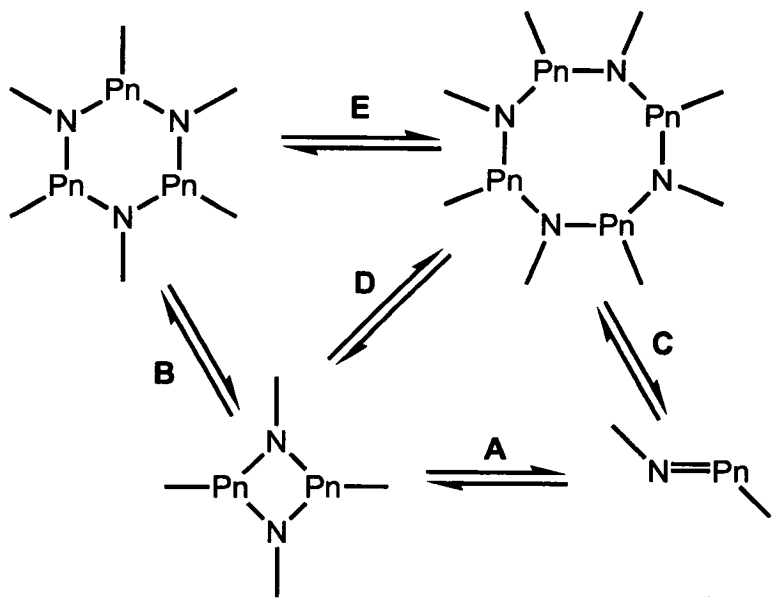

Scheme 1.4 – Interconversion of oligomeric pnictazanes taken from reference 61.

1.8 - Extended dipnictazane frameworks

Though widely discussed for Pn = phosphorus, polypnictazanes have yet to be realized.[34,71,72] In attempts to form extended frameworks based on Pn(III)-N backbones, two general methodologies have been applied; skeletal stabilization or the tethering of cyclodipnictazane rings.

Skeletal stabilization, has been widely exploited by Norman to form extended phosphazane chains (Figure 1.2).[73-79] Skeletally stabilized and geometrically restricted primary amines, often combined with the use of primary chlorophosphines, circumvent the formation of cyclic phosphazanes and have allowed larger acyclic chains to form. To date, such techniques have not been used with the heavier pnictogen analogues.

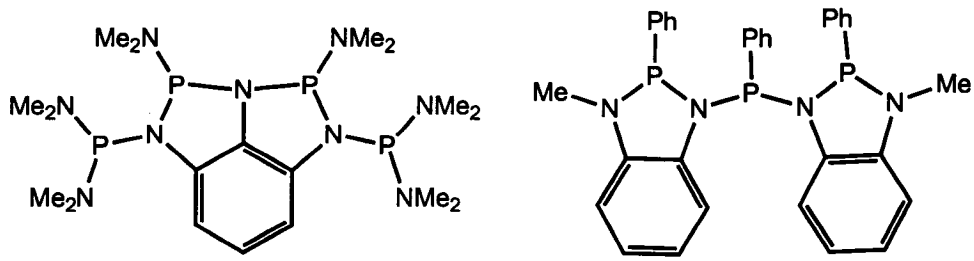

Figure 1.2 – Examples of skeletally stabilized phosphazanes.

Tethering of cyclodipnictazanes has also been used to form both linear and macrocyclic systems. The first linked ring systems (**1.14**) was prepared directly from $PhNH_2$ and PCl_3. Similarly, a reaction involving DmpN(H)Li and $SbCl_3$ yielded the macrocycle **1.15**,[53] of which a similar derivative had been prepared earlier through a

more obscure route.[80] Both **1.14** and **1.15** show the potential for reactions of primary amines and pnictogen trihalides to form larger, extended systems based on linked 4-membered rings.

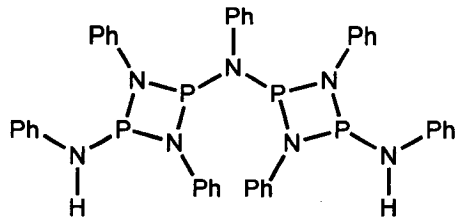

1.14

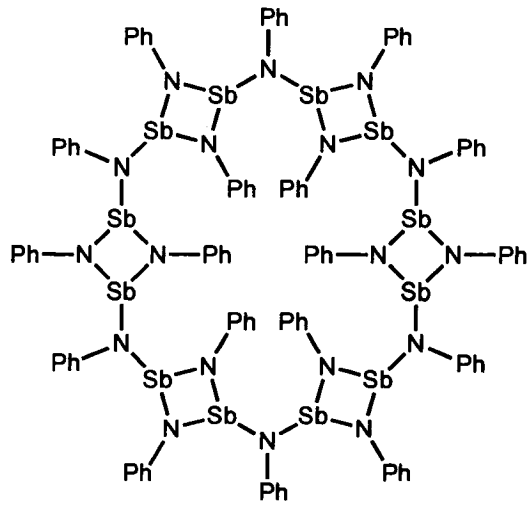

1.15

Cyclodipnictazanes rather than RNH_2 and PnX_3, have also been used as building blocks to prepare tethered cyclodipnictazanes. Perhaps the most interesting is the tetrameric macrocycle **1.16**,[81] formed through the condensation of the cyclodiphosphazane $(t\text{-BuNPCl})_2$ and the bis(amino)cyclodiphosphazane $(t\text{-BuNPNH}_2)_2$. The linear tris-tethered cyclodipnictazane **1.17**[82] is also unique and is formed from the transamination of the asymmetrically substituted bis(amino)cyclodiphosphazane *t*-$Bu(H)N(\mu\text{-}t\text{-BuNP})_2NH_2$ and $Sb(NMe_2)_3$. Both examples show the potential of bi-functional cyclodipnictazanes to undergo oligomerization reactions, potentially as a route to the formation of polymeric pnictazanes based on 4-membered ring monomers.

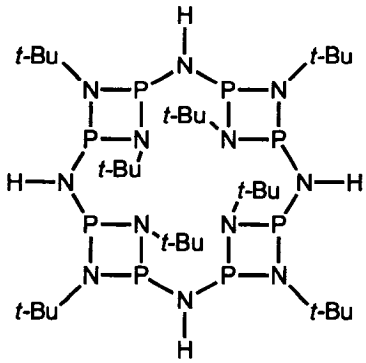

1.16

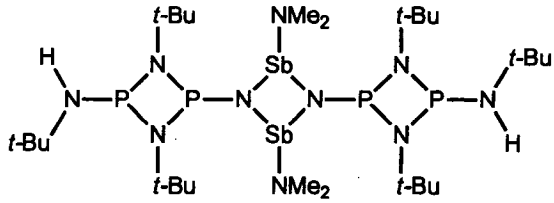

1.17

1.8 – Research goals and scope of the thesis

Given the availability of the cyclodipnictazanes and bis(amino)cyclodipnictazanes, the initial scope of the research project was to utilize the N_2Pn_2 core as a building block to larger pnictazane structures. Reactions were first explored towards rational synthetic routes to the sequential growth of tethered cyclodipnictazane frameworks or the inter-conversion of pnictazane oligomers with cyclodiphosphazanes given the *in-situ* ^{31}P NMR handle and research previously done. Based on the chemistry of phosphorus corresponding reactions with the heavier pnictogens (As, Sb and Bi) were then attempted.

Chapter 2 – Preparation of Cyclodiphosphazanes and Cyclodiarsazanes and their Reactions with Primary Amines

2.1 – Introduction

New cyclodipnictazanes were prepared as starting points to either tethered structures or for oligomer interconversion. The amines used almost exclusively throughout this thesis are $DmpNH_2$ (Dmp; 2,6-dimethylphenyl) and $DippNH_2$ (Dipp; 2,6-diisopropylphenyl), which are considered to have "moderate" steric protection at nitrogen.

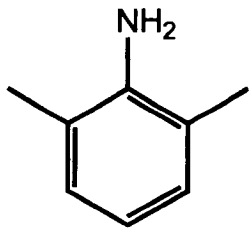

2,6-dimethyaniline

$DmpNH_2$

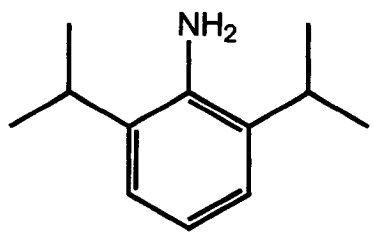

2,6-diisopropyaniline

$DippNH_2$

The synthesis of cyclodiphosphazanes is often most efficiently accomplished through the reaction of primary amines and pnictogen trihalides under dehydrohalide coupling conditions. For the heavier analogues, both $(t\text{-BuNAsCl})_2$[70] and $(t\text{-BuNSbCl})_2$[48] have been reported; however, these are the only examples of dehydrohalide coupling reactions used for the preparation of a cyclodiarsazane or a cyclodistibazane.

Many procedures have been reported for the preparation of $(t\text{-BuNPCl})_2$. While all are slightly different, they typically involve a one-pot synthesis containing the primary amine (or hydrochloride), phosphorus trichloride and a method to facilitate HCl loss (heat or base).[83-86] However, these methods are inconsistent with the preparation of $(DippNPCl)_2$ which requires a two step procedure. The first step (Scheme 2.1, step 2) uses $DippNH_2$ both as a reagent and base, yielding the aminophosphine $(Dipp(H)NPCl_2)$, which is then exposed to NEt_3, which promotes cyclization to the cyclodiphosphazane (step 3).[8]

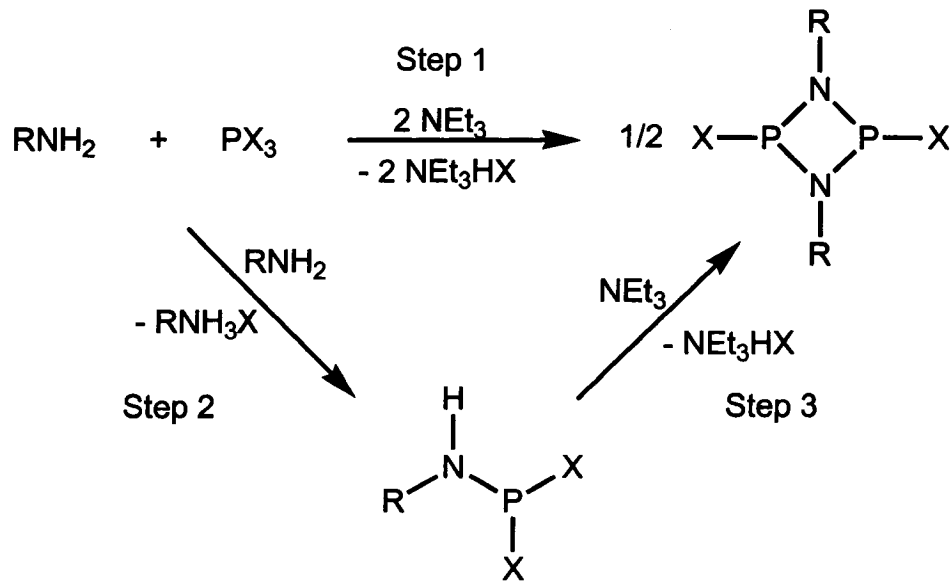

Scheme 2.1 – Select routes in the preparation of $(RNPX)_2$ (R = Dipp; X = Cl, R = Dmp; X = Cl, Br).

2.2 – Synthesis of cyclodiphosphazanes

Preparation of $(DmpNPX)_2$ (X = Cl, Br) was the first synthetic challenge. Following the route for $(DippNPCl)_2$ it was possible to prepare the aminophosphine $(DmpN(H)NPCl_2)$ from step 2, with cyclization readily occurring to the corresponding cyclodiphosphazane $(DmpNPCl)_2$ in the presence of NEt_3. Two steps were not needed and the synthesis of $(DmpNPX)_2$ (X = Cl, Br) was found to be most efficient through a one-pot procedure including $DmpNH_2$, PX_3 and NEt_3 (step 1). Under such conditions, quantitative formation of $(DmpNPX)_2$ is observed by use of ^{31}P NMR spectroscopy, (δ 210 ppm; X = Cl, δ 230 ppm; X = Br).

Isolation of the crude cyclodiphosphazanes was accomplished through filtration of the reaction mixture, removal of the solvent under vacuum followed by washing with pentane. At this point the product is sufficiently pure for further reactions and easily prepared on large scale (> 10 grams). The yields at this point (~ 50 %) could be better; however the solubility of the cyclodiphosphazanes represents a significant problem. In benzene and toluene, the solvents best suited for the reaction, the two compounds $(DmpNPX)_2$ (X = Cl, Br) are relatively insoluble and significant amounts of cyclodiphosphazane precipitate out of solution with NEt_3HCl and were lost during filtration. Washing the precipitate with benzene or toluene is usually ineffective unless excessive amounts are used. The cyclodiphosphazanes are very soluble in chlorocarbon solvents such as methylene chloride, which can be used as the reaction solvent or for washing however the by-product (NEt_3HCl) was also noticeably soluble in such solvents, causing purity issues. The most efficient method of obtaining better yields has been the use of a large-scale soxhlet extraction apparatus, equipped for air-sensitive requirements.

Depending on extraction duration, the crude yields have been increased by up 30 % by allowing the precipitate to be extracted with benzene for 18 hours. Given longer extraction periods, the yields could be further improved.

After isolation of the crude cyclodiphosphazanes, analytically pure samples as X-ray quality crystals can be readily obtained. As suggested by the ^{31}P NMR spectra, $(DmpNPCl)_2$ and $(DmpNPBr)_2$ are present in a *cis* configuration, which is confirmed by the solid-state structures. Minor peaks appeared in the spectra of re-dissolved crystals at 295 ppm; $(DmpNPCl)_2$ and 312 ppm; $(DmpNPBr)_2$ that were attributed to the *trans* configurations. Variable temperature NMR does not suggest an equilibrium exists between the two configurations.

Bond lengths and angles for $(DmpNPX)_2$ (X = Cl, Br) can be found in Table 2.1, along with $(DippNPCl)_2$.[8] All of the N_2P_2 cores are puckered, typical of *cis* cyclodipnictazanes. The endocyclic angles at the essentially planar nitrogen centers are larger than those at the pyramidal phosphorus centers. The geometry of each ring atom is indicated by the sums of the three angles, which define an almost planar geometry at nitrogen and a distinctly pyramidal geometry at phosphorus (substantially less than 360°). The nitrogen centers in derivatives of $(DmpNPX)_2$ are slightly distorted from planarity, perhaps due to the combination of ring strain and substituent steric strain.

Table 2.1 – Select bond lengths (Å) and angles (°) for derivatives of $(RNPnX)_2$.

	$(DmpNPCl)_2$	$(DmpNPBr)_2$	$(DippNPCl)_2$[8]	$(DmpNAsCl)_2$	$(DippNAsCl)_2$
N1-Pn1	1.703(3)	1.708(3)	1.71(3)	1.841(2)	1.845(1)
N2-Pn1	1.703(2)	1.708(3)	1.69(1)	1.847(2)	1.843(1)
N1-Pn2	1.713(2)	1.702(3)	1.73(1)	1.838(2)	1.845(1)
N2-Pn2	1.704(2)	1.706(3)	1.69(2)	1.842(2)	1.843(1)
Pn1-X1	2.111(1)	2.293(1)	2.017(8)	2.243(1)	2.239(1)
Pn2-X2	2.111(1)	2.301(1)	2.085(8)	2.244(1)	2.239(1)
N-Pn1-N	81.6(1)	81.4(1)	81.3(7)	79.7(1)	79.9(1)
N-Pn2-N	81.3(1)	81.6(1)	80.5(7)	80.0(1)	79.9(1)
Σ° at N1	355.5(2)	354.7(2)	355(1)	353.9(2)	352.8(2)
Σ° at N2	355.0(2)	354.7(2)	355(1)	354.3(2)	352.1(2)
Σ° at Pn1	290.1(2)	291.5(2)	290.1(7)	258.2(2)	284.6(2)
Σ° at Pn2	290.2(2)	291.3(2)	289.8(7)	284.7(2)	284.6(2)

2.3 – Synthesis of cyclodiarsazanes

As first recognised by Olah for alkyl derivatives, cyclodiarsazanes $(RNAsCl)_2$ are readily prepared by direct addition of excess primary amine to $AsCl_3$, however this is the only example of a dehydrohalide coupling reaction towards a cyclodiarsazane.[70] As described for the cyclodiphosphazanes, the dehydrohalide coupling of RNH_2 (R = Dmp and Dipp) and $AsCl_3$ can be facilitated and generalized in the presence of NEt_3 and exploited to obtain the new arsazane dimers $(RNAsCl)_2$ (R = Dipp, Dmp) (Figure 2.1). Both derivatives of $(RNAsCl)_2$ adopt a *cis* configuration, consistent with the phosphorus analogues $(RNPCl)_2$ (R = Dipp, Dmp).[39] ^1H NMR spectra provides no evidence to the presence of conformers having the *trans* configuration in solution. The geometries at nitrogen and arsenic in $(RNAsCl)_2$, like the corresponding cyclodiphosphazanes are distinguished by the sums of the three angles at each site, defining an almost planar geometry at each nitrogen center (almost 360°; Table 2.1) and a distinctly pyramidal geometry at each arsenic center (substantially less than 360°). The slight distortion of the nitrogen centers from planarity is due to a combination of ring strain and substituent steric strain.

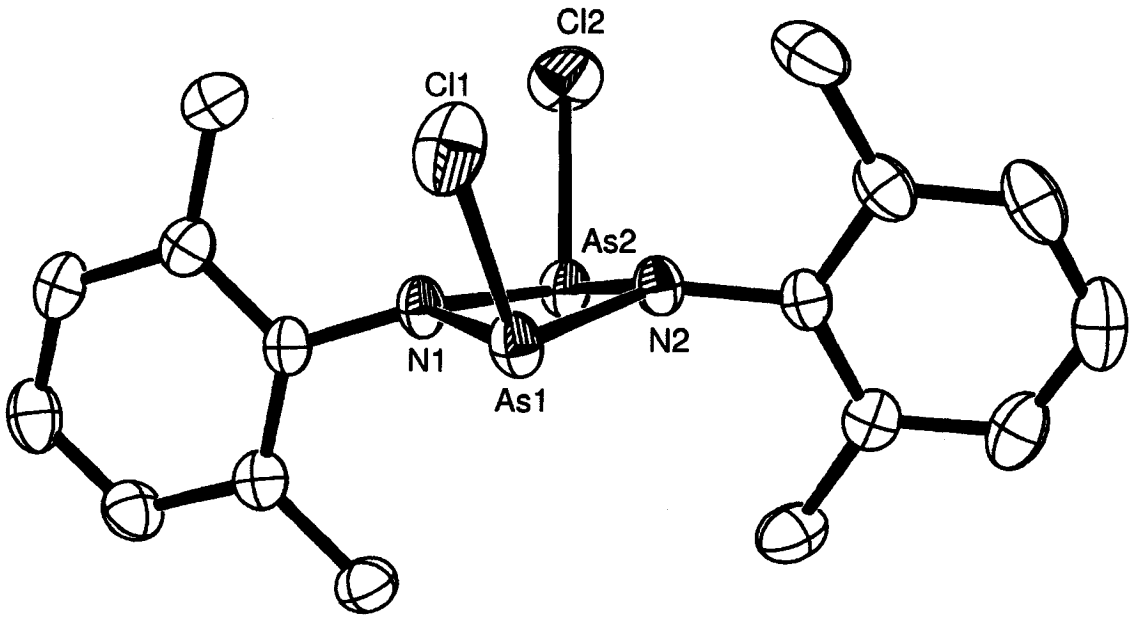

Figure 2.1 – Solid-state structure of $(DmpNAsCl)_2$. Hydrogen atoms omitted for clarity. Thermal ellipsoids drawn at 50 % probability.

2.4 – Reactions of cyclodiphosphazanes with primary amines

Attempts were made to prepare extended phosphazane systems using $(DmpNPCl)_2$ as a building block. Reaction of $DmpNH_2$ with $(DmpNPCl)_2$ yields the bis(amino)cyclodiphosphazane $(DmpNPN(H)Dmp)_2$.[87] Preliminary attempts were made to couple chorophosphines to the exocyclic N-H substituents to form an extended phosphazane chain away from the N_2P_2 core. Scheme 2.2 lists some of the synthetic approaches, including attempts at connecting the aminophosphine $(Ph(H)NPPh_2)$ to $(DmpNPCl)_2$, all proving unsuccessful. In most cases no reaction or decomposition of the bis(amino)cyclodiphosphazane back to the cyclodiphosphazane was observed.

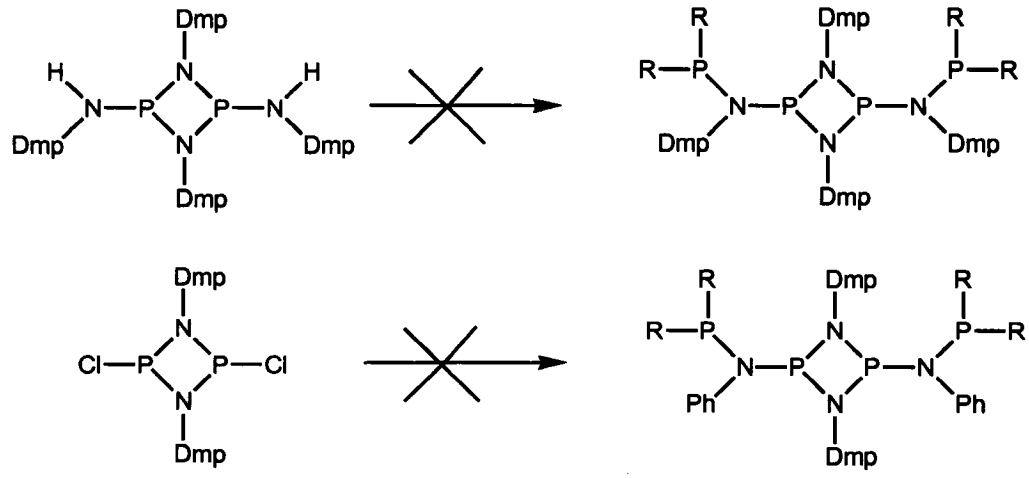

Starting material	Reagents, conditions
$(DmpNPN(H)Dmp)_2$	Ph_2PCl, NEt_3
$(DmpNPN(H)Dmp)_2$	Ph_2PCl, NEt_3 – reflux in toluene
$(DmpNPN(H)Dmp)_2$	$PhPCl_2$, NEt_3
$(DmpNPN(H)Dmp)_2$	PCl_3, NEt_3
$(DmpNPN(H)Dmp)_2$	1) n-BuLi; 2) Ph_2PCl
$(DmpNPCl)_2$	$Ph_2PN(H)Ph$, NEt_3
$(DmpNPCl)_2$	$Ph_2PN(H)Ph$, NEt_3 – reflux in toluene
$(DmpNPCl)_2$	$Ph_2PN(Li)Ph$

Scheme 2.2 - Synthetic attempts at coupling chlorophosphines to bis(amino)cyclodiphosphazanes or aminophosphines to cyclodiphosphazanes.

Considering the solid-state structure of $(DmpNPN(H)Dmp)_2$ (Figure 2.2) it becomes apparent why substitution at the exocyclic N-H bonds is not possible. The endo orientation of the two protons; H4n and H3n, which represent the only potential sites for dehydrohalide coupling, are sterically inaccessible. Substitution at these sites would

require an impeded rotation of the exocylic Dmp substituents towards the centre of the cyclodiphosphazane ring, which is unfavourable.

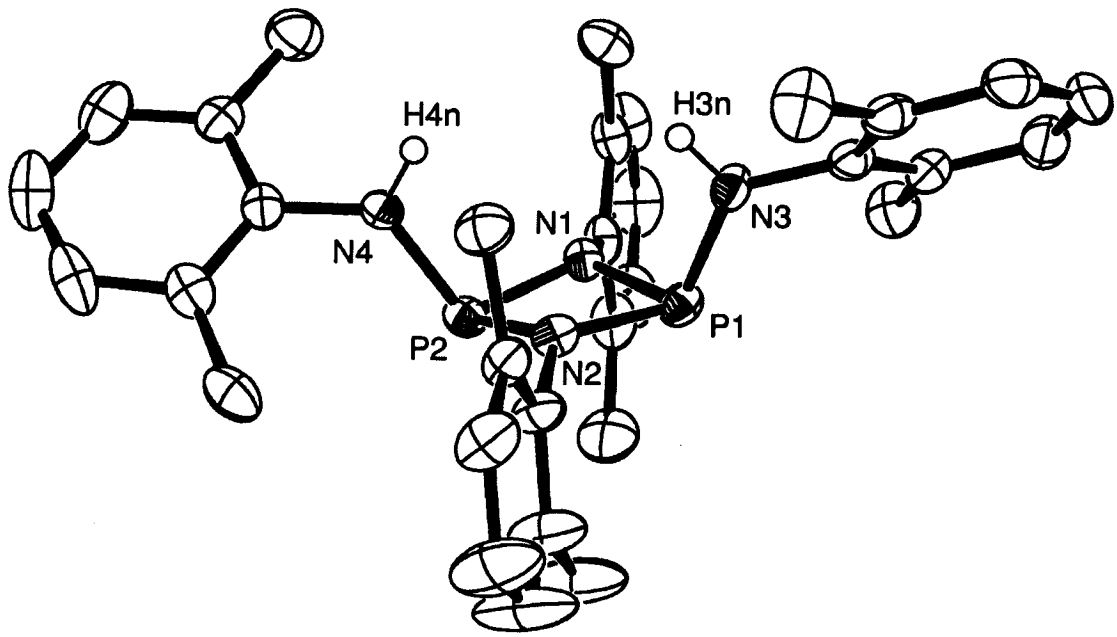

Figure 2.2 – Solid-state structure of $(DmpNPN(H)Dmp)_2$. Select hydrogen atoms omitted for clarity. Thermal ellipsoids are drawn at 50 % probability.

As reactions of $(DmpNPN(H)Dmp)_2$ with chorophosphines were unsuccessful, $(DmpNPCl)_2$ was reacted with primary amines bearing smaller substituents at nitrogen in attempts to form bis(amino)cyclodiphosphazanes with varying exocyclic substitution. Reaction products of $(DmpNPCl)_2$ with RNH_2 or RNH_3Cl (R = methyl, ethyl, *n*-propyl, *n*-butyl) in excess NEt_3 show a singlet at approximately 110 ppm in the ^{31}P NMR spectra,

consistent with chemical shifts observed for other bis(amino)cyclodiphosphazanes (*c.f.* $(DmpNPN(H)Dmp)_2$; δ 105 ppm). ^{31}P NMR chemical shifts for the new products along with melting point data were unusually broad (Scheme 2.3), while ^{1}H NMR spectroscopy gave no indication of exocyclic N-*H* protons (*c.f.* $(DmpNPN(H)Dmp)_2$; δ 4.88 ppm). Recognizing the potential for bi-molecular condensation oligomerization/polymerization reactions between primary amines and cyclodiphosphazanes, initially it was speculated that the outcome may have been the tethered cyclodiphosphazane **2.1** (Scheme 2.3) and not the corresponding bis(amino)cyclodiphosphazanes.

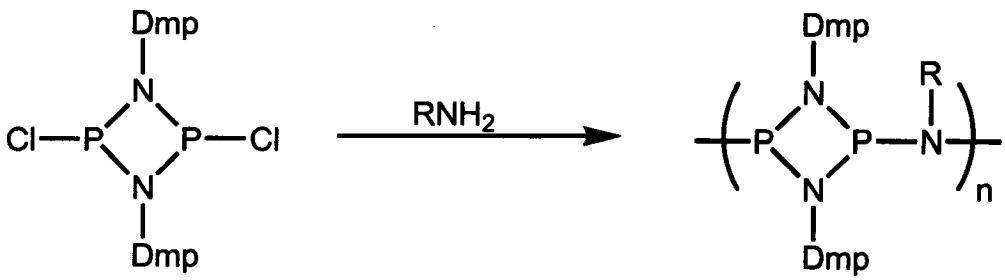

2.1

Compound	δ (ppm)	Peak width at half height (Hz)	Melting Point (°C)
$(DmpNPCl)_2$	211	13	218 - 222
$(DmpNPN(H)Dmp)_2$	105	11	135 – 140
2.1 Me	110	72	107 - 137
2.1 Et	111	83	70 - 91
2.1 Pr	112	70	59 - 79
2.1 Bu	112	68	94 - 101

Scheme 2.3 – Reaction of $(DmpNPCl)_2$ with primary amines; ^{31}P NMR spectroscopic and melting point data.

The new products were characterized by GPC and dynamic light scattering and indicated molecular weights below 1000 amu, however ^{31}P NMR spectroscopy indicated the samples were decomposing due to oxygen and water during the measurements. Elemental analysis gave results consistent with the bis(amino)cyclodiphosphazanes and not **2.1**. The product of $(DmpNPCl)_2$ and $MeNH_3Cl$ was also reacted with MeOTf and yielded two peaks in the ^{31}P NMR spectrum at 43 and 104 ppm. While it appeared that two products were being formed, crystals grown from the reaction were identified as the cyclophosphoniumphosphazane **2.2** (Figure 2.3).

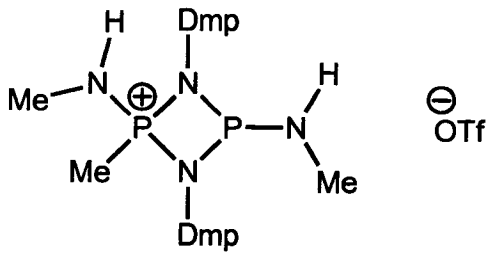

2.2

The solid-state structure of **2.2** shows the N_2P_2 core, which is substituted at each phosphorus with –N(H)Me groups. One of the phosphorus centres in the 4-membered ring has been oxidized by Me^+ to yield a phosphonium centre. Surprisingly, the phosphine and phosphonium centre do not couple in the ^{31}P NMR spectrum. Unfortunately the crystallographic data was insufficient for further discussion of structural data, however the connectivity indicates the reaction of primary amines with $(DmpNPCl)_2$ yielded the bis(amino)cyclodiphosphazanes and not **2.1** as was initially proposed.

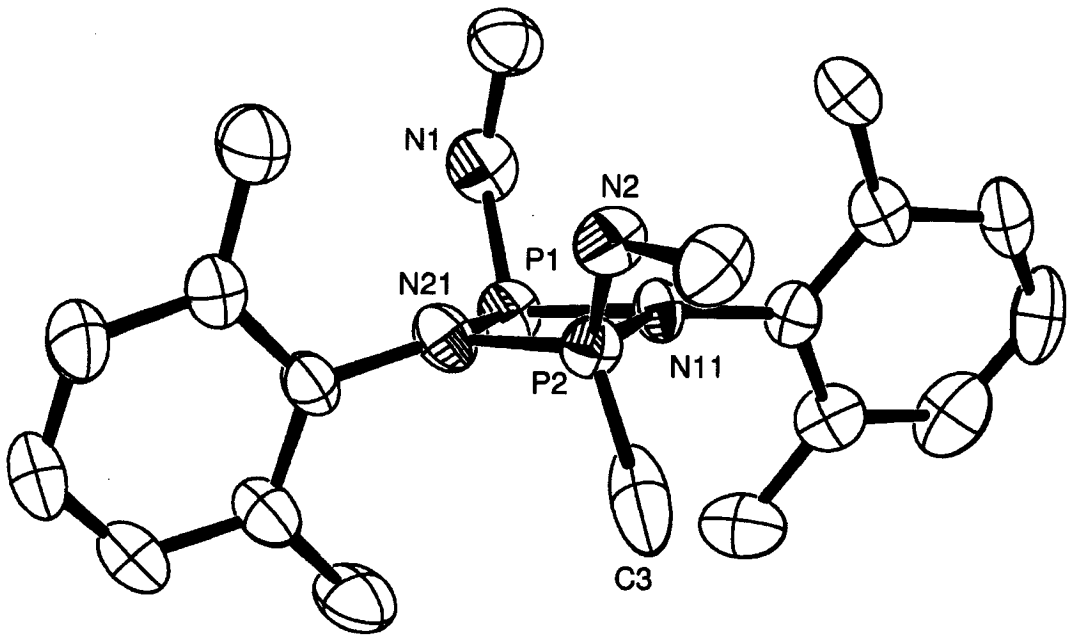

Figure 2.3 – Solid-state structure of **2.2**. Hydrogen atoms and $[OTf]^-$ anion omitted for clarity. Thermal ellipsoids drawn at 50 % probability.

Further reactions of $(DmpNPN(H)R)_2$ (R = Me, Et, *n*-Pr, *n*-Bu) with chlorophosphines have yet to be attempted but under appropriate conditions may lead to tethered cyclodiphosphazanes.

2.5 – Synthesis and reactivity of a mono(amino)cyclodiphosphazane

Reactions of $(DmpNPCl)_2$ with $MeNH_3Cl$ or $EtNH_3Cl$ yield the corresponding bis(amino)cyclodiphosphazanes after 2 hours. Under identical conditions with NH_4Cl the reaction proceeds at slower rate, with a pair of doublets beginning to arise after 2 hours in

the ^{31}P NMR spectrum (δ 144, 193 ppm, $^{2}J_{PP}$ = 44.6Hz) and the reaction is complete after 24 hours. The set of doublets have been assigned to the mono(amino)cyclodiphosphazanes **2.3** (Scheme 2.4). The doublet at 144 ppm corresponds to the *P*-NH_2 phosphorus and the doublet at 198 ppm corresponds to the *P*-Cl phosphorus, in accordance with previous examples of mono(amino)cyclodiphosphazanes.[8,88-90]

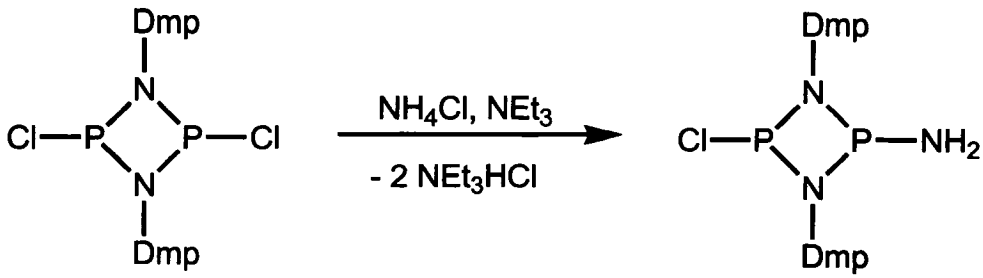

2.3

Scheme 2.4 – Selective amination of $(DmpNPCl)_2$ with NH_4Cl to yield **2.3**.

The solid-state structure of **2.3** is shown in Figure 2.4 and is distinguished by the asymmetric substitution (-Cl and $-NH_2$) at the two phosphorus centres of the 4-membered ring. The structure retains a puckered P_2N_2 core and the *cis* configuration of the starting cyclodiphosphazane $(DmpNPCl)_2$. Most structural parameters for **2.3** are consistent with other cyclodiphosphazanes. The notable exception was an asymmetric difference in the internal N-P bond lengths, where P2-N(1/2) [1.754(1) and 1.745(1) Å] are slightly longer

than P1-N(1/2) [1.681(1) and 1.687(1) Å] caused by the interaction of the lone pair of N3 with P2.

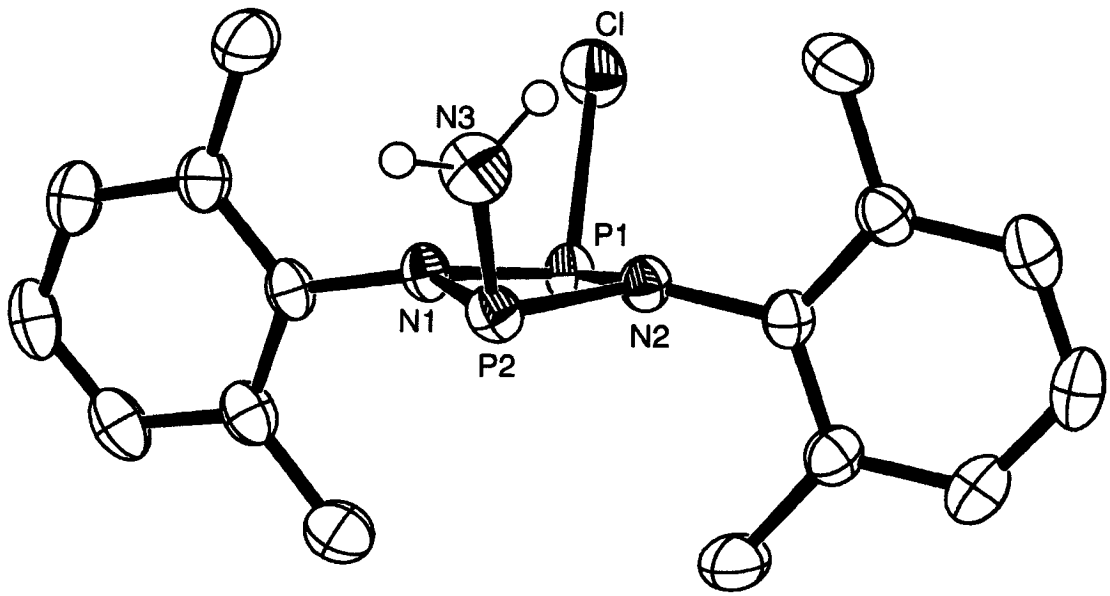

Figure 2.4 – Solid-state structure of **2.3**. Select hydrogen atoms omitted for clarity. Thermal ellipsoids drawn at 50 % probability.

The exocyclic $-NH_2$ group of **2.3**, compared to –N(H)Dmp group of $(DmpNPN(H)Dmp)_2$, minimize the unfavourable steric interaction with the endocyclic substituents at nitrogen in the N_2P_2 core. While initially optimistic that **2.3** might also be suited to undergo tethering reactions, all attempts to access the exocyclic N-H bonds with

chlorophosphines were unsuccessful under a variety of conditions. This is surprising considering the use of the mono(amino)cyclodiphosphazanes $Cl(\mu\text{-}t\text{-}BuNP)_2N(H)t\text{-}Bu$[89,91] and the bis(amino)cyclodiphosphazane $(t\text{-}BuNPNH_2)_2$[81,85] which bears two exocyclic -NH_2 groups, in the preparation of tethered cyclodiphosphazanes.

Summary

Reactions of RNH_2 (R = Dmp and Dmp) with PCl_3, PBr_3 or $AsCl_3$ proceed in a one step reaction in the presence of NEt_3 to yield the corresponding cyclodiphosphazanes on scales leading to > 10 g quantities. Reactions of $(DmpNPCl)_2$ with $MeNH_3Cl$, $EtNH_3Cl$, *n*-$PrNH_2$ and *n*-$BuNH_2$ yield the corresponding bis(amino)cyclodiphosphazanes, while an identical reaction with NH_4Cl produces the mono(amino)cyclodiphosphazane **2.3**. As of yet, attempts to prepare tethered cyclodiphosphazanes have been unsuccessful.

Chapter 3 – Lewis Acid Induced Transformation of Cyclodiphosphazanes to the Corresponding Cyclotriphosphazanes

3.1 - Introduction

Heterolytic cleavage of the P-Cl bonds in (Mes*NPCl) and bis(amino)phosphines is readily achieved by reaction with $AlCl_3$ or $GaCl_3$ to give the iminophosphenium cation **3.1**Mes*[35,92] and the bis(amino)phosphenium cations **3.2** (R = R' = Me, Et, *i*-Pr)[93,94] respectively. In this context, cyclodiphosphazanes $(RNPX)_2$ offer the possibility of dication formation, however, ^{31}P NMR spectra of reactions between $(t\text{-BuNPCl})_2$ and $AlCl_3$ show the presence of only phosphinophosphenium cation **3.3** (R = *t*-Bu, X = Cl) (δ doublets 177 and 366 ppm @ 233K, coalescence @ 343 K),[95] independent of reaction stoichiometry. Attempts were made to develop polyphosphorus cations with higher charges,[96] by examining reactions of GaX_3 and derivatives of $(RNPX)_2$ containing aryl substituents of medium steric load (R = Dipp; X = Cl, R = Dmp; X = Cl, Br).

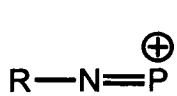

3.1

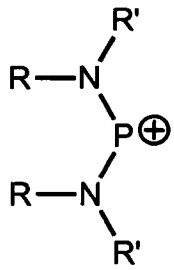

3.2

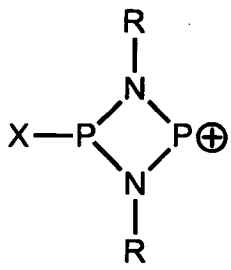

3.3

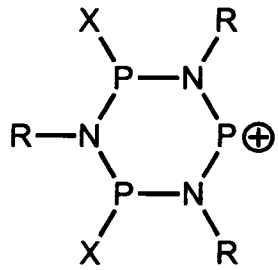

3.4

3.2 – Reactions of cyclodiphosphazanes with GaX_3; ^{31}P NMR spectroscopic evidence of heterolytic P-Cl bond cleavage

Colourless derivatives of $(RNPCl)_2$ (R = Dipp, X = Cl; Dmp, X = Cl, Br) react with gallium halides (GaX_3, X = Cl or Br) on mixing the solids at room temperature to give bright red liquids. In a molar ratio of 3:2 respectively, dissolving the red liquid in CH_2Cl_2, produces a red solution which exhibits a broad signal in the ^{31}P NMR spectrum at approximately 220 ppm (*c.f.* $(DippNPCl)_2$, 211 ppm;[8] $(DmpNPCl)_2$, 210 ppm; $(DmpNPBr)_2$, 231 ppm), as well as sharp signals of low relative integration at approximately 90 ppm (tentatively assigned to **3.1**Dipp and **3.1**Dmp, *c.f.* **3.1**Mes*, δ ^{31}P range 75-95 ppm)[92] and 270 ppm (tentatively assigned to **3.2**Dmp, and **3.2**Dipp; R' = H , *c.f.* **3.2**Mes*; R' = H, δ ^{31}P 272 ppm).[97] The spectra are independent of temperature over the range of 193 – 293 K, only changing with respect to the breadth of the peak at 220 ppm.

When a molar ratio of 1:2 is employed for combinations of $(RNPCl)_2$ (R = Dipp and Dmp) and $GaCl_3$, the red solutions in CH_2Cl_2 produce ^{31}P NMR spectra that become temperature dependent. For R = Dmp, the room temperature spectrum is dominated by a broad peak centered at 270 ppm. This peak collapses into the baseline at 253 K, while at 193 K a new peak appears at 220 ppm, which is reminiscent of reactions with 3:2 eq. of $(DmpNPCl)_2$ and $GaCl_3$. Another peak should be seen due to the coalescence, however the spectral window was likely not wide enough to observe this peak. For R = Dipp, the room temperature spectrum is again dominated by a broad peak at 270 ppm, as the temperature is cooled to 253 K, the peak also collapses into the baseline. As the temperature is further decreased a set of broad peaks rise at 185 and 335 ppm (Figure

3.1). While not resolved into doublets the two peaks are assigned to **3.3**Dipp exhibiting dynamic behaviour (*c.f.* **3.3***t*-Bu; 177 and 366 ppm).[95]

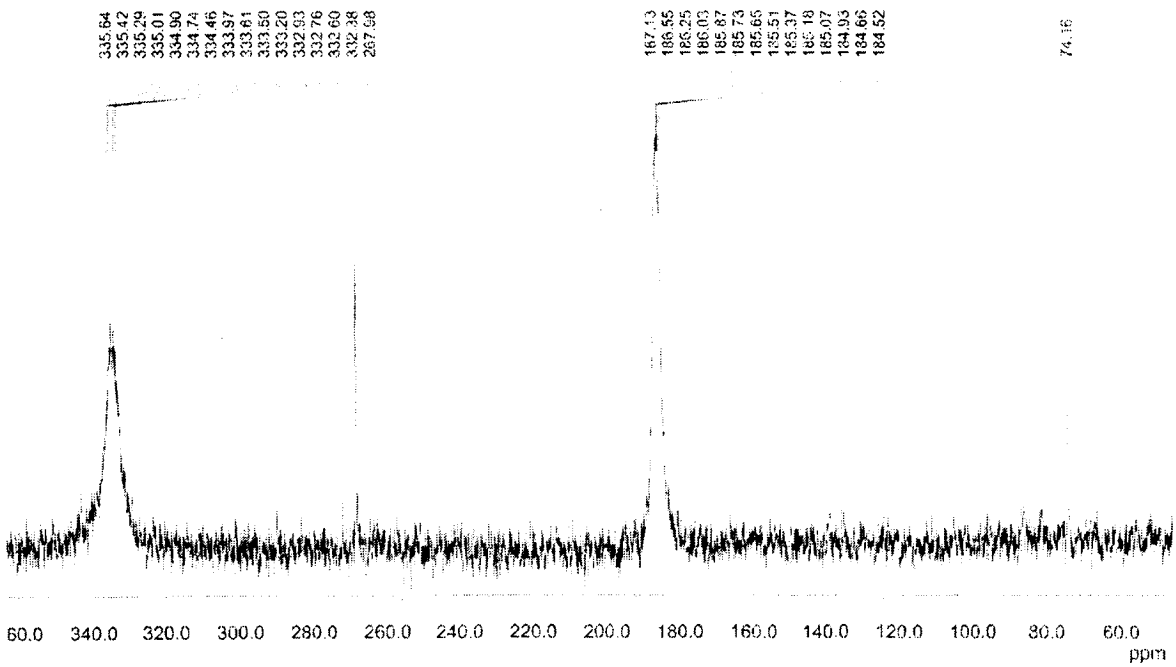

Figure 3.1 – ^{31}P NMR Spectrum of $(DippNPCl)_2$ + 2 $GaCl_3$ at 193 K.

Of interest is the difference imparted by stiochiometry and temperature in the VT ^{31}P NMR spectroscopy studies. When $(RNPCl)_2$ is in excess (3:2) over $GaCl_3$, regardless of temperature or substituent (Dmp, Dipp), the major peak in the spectra (220 ppm) is at a chemical shift characteristic of the starting cyclodiphosphazanes. If $GaCl_3$ is in excess (2:1) over $(RNPCl)_2$ (R = Dmp, Dipp), at room temperature both spectra show broad peaks at ~ 270 ppm, characteristic of a phosphenium centre. When the temperature is lowered, for R = Dipp, the peaks arising at 335 and 175 ppm, assigned to **3.3**Dipp suggest the interaction becomes more pronounced between the $GaCl_3$ and P-Cl bonds.

The same effect should be seen in the case of R = Dmp, however after coalescence the partner peak to that at 220 ppm has yet to be found.

3.3 – Isolation of cyclotriphosphazanes from the Lewis acid induced ring expansion of cyclodiphosphazanes

Removal of solvent from reaction mixtures of $(DippNPCl)_2$ with $GaCl_3$ at a stoichiometry of 3:2 gives an oil, from which a crystalline material has been obtained and characterized as **3.4**Dipp [$GaCl_4$], illustrated in Figure 3.2.[68] Although isolated in modest yield (27%), the formation of **3.4**Dipp [$GaCl_4$] can be rationalised in Scheme 3.1 (step 1) representing an unusual ring expansion process involving cleavage of a number of N-P bonds and transfer of an $[DippNP]^+$ fragment between molecules of $(DippNPCl)_2$, as well as abstraction of Cl^- by $GaCl_3$.

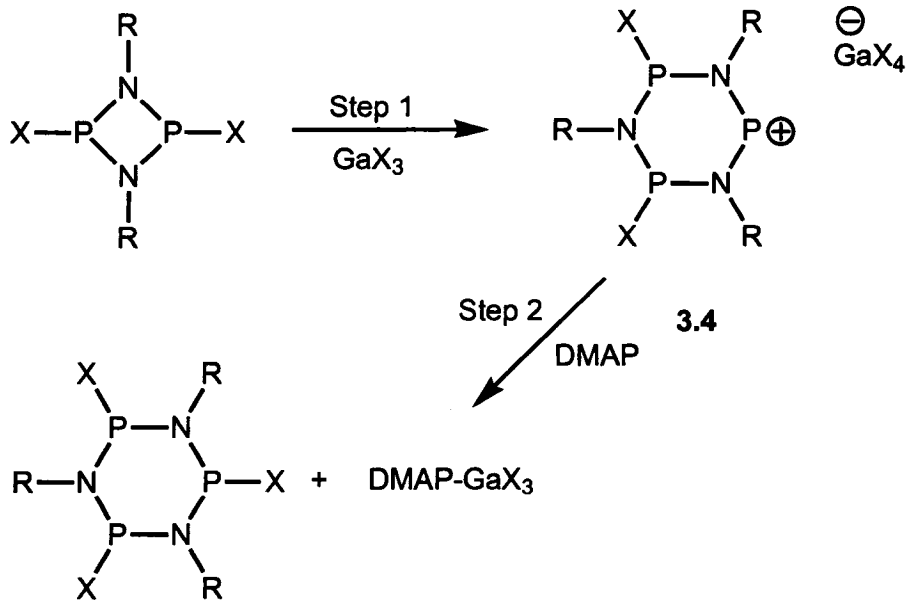

Scheme 3.1 – Reaction of $(RNPX)_2$ with GaX_3, followed by addition of DMAP.

Reaction of **3.4**Dipp [$GaCl_4$] with DMAP gives the corresponding cyclotriphosphazane $(DippNPCl)_3$, representing the preferential formation of the DMAP-$GaCl_3$ adduct, consequential release of chloride ion from the complex anion $[GaCl_4]^-$, and association of chloride with the phosphenium site of **3.4**Dipp in Scheme 3.1 (step 2). Preferential interaction of DMAP with the relatively strong Lewis acidic $GaCl_3$ (from $[GaCl_4]^-$) is expected, despite the demonstrated Lewis acceptor behaviour for phosphenium sites of the type present in **3.4**.[98]

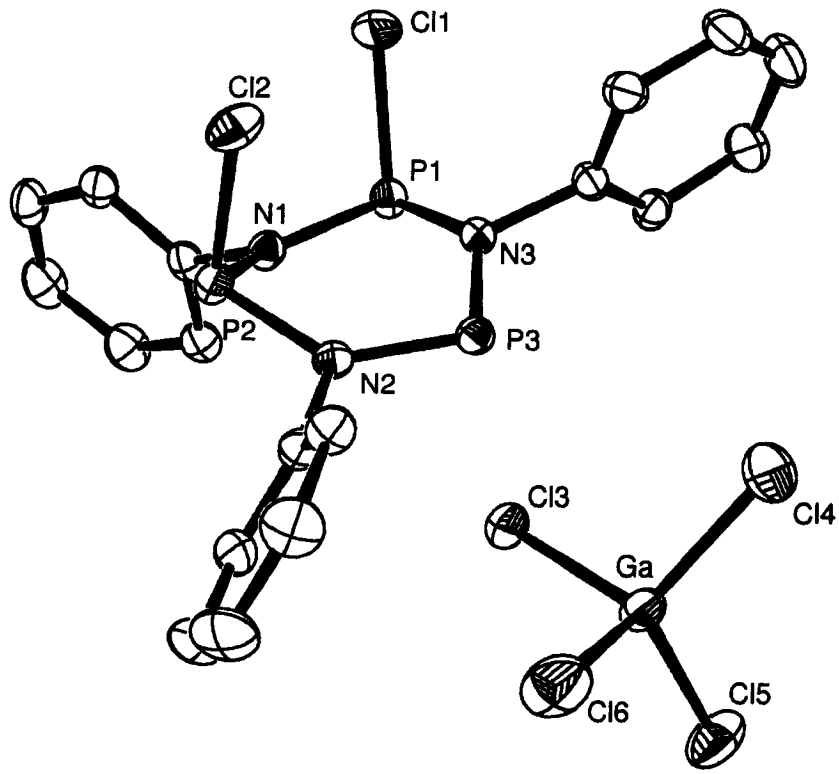

Figure 3.2. Solid-state structure of **3.4**Dipp [$GaCl_4$].[68] Hydrogen atoms and isopropyl groups omitted for clarity. Thermal ellipsoids are drawn at 50 % probability.

^{31}P NMR spectroscopic studies of analogous reaction mixtures containing 3 eq. of $(RNPX)_2$ with 2 eq. of GaX_3 followed by the addition of 1 eq. of DMAP show two signals with relative intensity of 1:2 indicating quantitative transformation to $(DippNPCl)_3$ [δ 110, 116 ppm], $(DmpNPCl)_3$ [δ 111, 116 ppm] and $(DmpNPBr)_3$ [δ 121, 134 ppm], respectively (Scheme 3.1 – step 1 and 2). Analogous reaction mixtures containing $(PhNPCl)_2$ show numerous phosphorus containing species that could not be isolated, indicating that the essentially quantitative process observed in the transformation of $(RNPX)_2$ to $(RNPX)_3$ is controlled by the steric limitations imposed by the relatively bulky Dipp and Dmp substituents.

Selected structural parameters (N-P and P-X distances, N-P-N angles, sum of angles at nitrogen and phosphorus centers) for **3.4**Dipp $[GaCl_4]$,[68] $(DmpNPCl)_3$, $(DmpNPBr)_3$ together with corresponding parameters for the rare example of a trimeric phosphazane $(EtNPOC_6H_4Br\text{-}4)_3$[9] are listed in Table 3.1. A *cis, trans* configuration of halogens is observed for both $(DmpNPX)_3$ (X = Cl, Br) in the solid-state (illustrated in Figure 3.3) and in solution, as demonstrated by the two distinct signals observed in the ^{31}P NMR spectra, with relative intensity of 1:2. There is no evidence of the *cis* isomer in the reaction mixtures, in contrast to previous reports of both *cis* and *cis, trans* configurations for $(EtNPOC_6H_4Br\text{-}4)_3$.[9] Interestingly, $^2J_{PP}$ coupling is not observed for $(DmpNPCl)_3$, $(DmpNPBr)_3$ or $(DippNPCl)_3$ over the temperature range of 80 to -80°C.

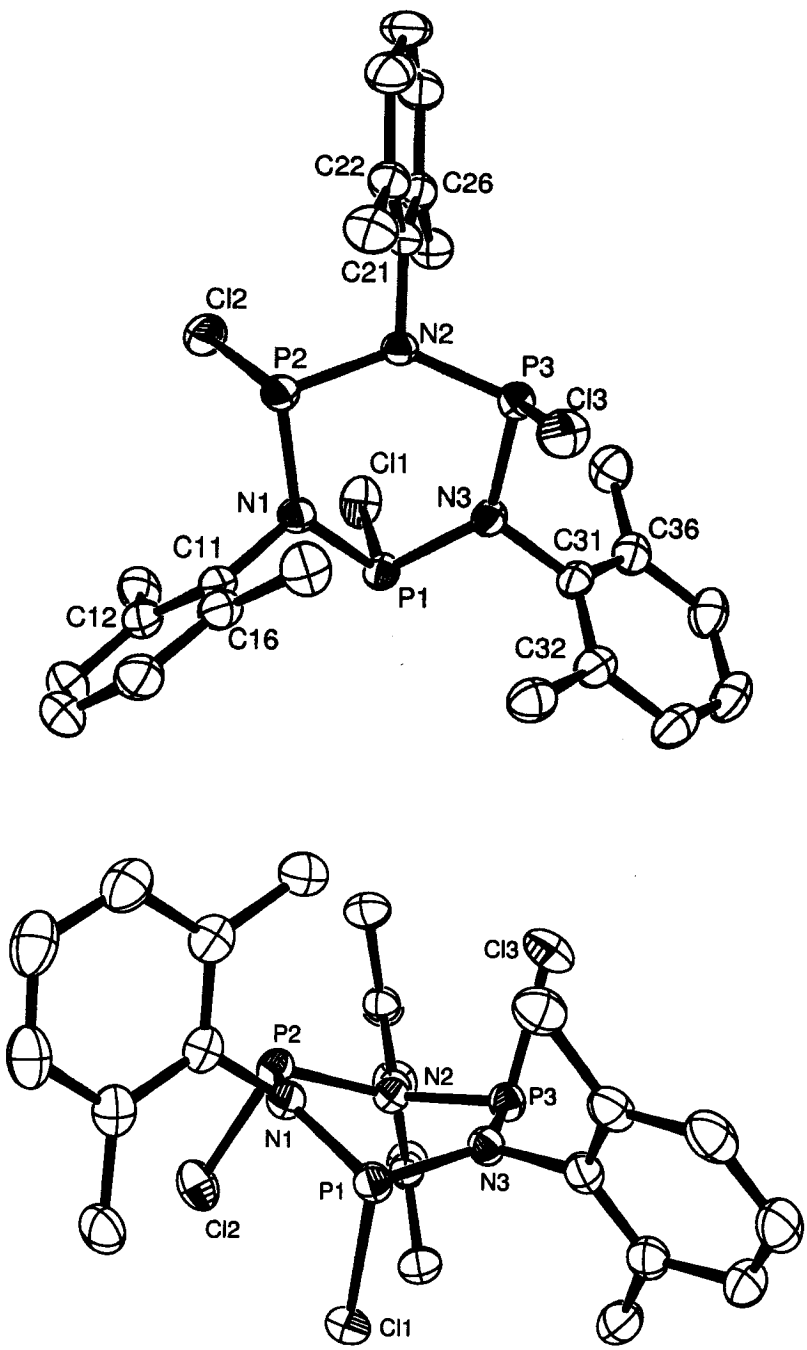

Figure 3.3. Two views of $(DmpNPCl)_3$ in the Solid-state. Hydrogen atoms omitted for clarity. Thermal ellipsoids are drawn at 50% probability.

Table 3.1 - N-P and P-X distances (Å), N-P-N angles (°), and sums of angles at phosphorus and nitrogen centers for derivatives of $(DmpNPCl)_3$ {including $(EtNPOC_6H_4Br\text{-}4)_3$[62] and **3.4**Dipp $[GaCl_4]$.[68]

	$(DmpNPCl)_3$	$(DmpNPBr)_3$	$[(DippN)_3P_3Cl_2][GaCl_4]$	$[EtNPOR]_3$ *cis*	$[EtNPOR]_3$ *cis, trans*
N1-P1	1.704(2)	1.689(3)	1.697(2)	1.68(1)	1.67(2)
N1-P2	1.687(2)	1.702(3)	1.703(2)	1.69(2)	1.69(2)
N2-P3	1.694(2)	1.707(3)	1.656(2)	1.68(1)	1.62(2)
N2-P2	1.717(2)	1.686(3)	1.736(2)	1.67(1)	1.67(2)
N3-P3	1.703(2)	1.696(3)	1.650(2)	1.68(2)	1.63(2)
N3-P1	1.693(2)	1.713(3)	1.753(2)	1.69(1)	1.68(2)
P1-X1	2.104(1)	2.308(1)	2.081(1)	1.67(1)	1.62(2)
P2-X2	2.116(1)	2.286(1)	2.088(1)	1.65(1)	1.65(2)
P3-X3	2.136(1)	2.324(1)	2.704(1)	1.67(1)	1.61(2)
N1-P1-N3	101.7(1)	100.6(1)	99.4(1)	101.9(8)	99.0(9)
N1-P2-N2	100.1(1)	101.8(1)	100.8(1)	102.0(7)	103.9(8)
N2-P3-N3	101.8(1)	101.8(1)	105.0(1)	101.2(8)	97(1)
Σ Angles P1	307.5(1)	307.9(1)	304.5(9)	302.3(8)	299.0(9)
Σ Angles P2	305.5(1)	306.0(1)	302.6(7)	302.0(8)	300.4(9)
Σ Angles P3	303.9(1)	305.2(1)		303.1(8)	297(1)
Σ Angles N1	360.0(1)	359.9(2)	359.7(2)	360(1)	359(1)
Σ Angles N2	358.1(1)	359.3(2)	359.0(2)	358(1)	355(2)
Σ Angles N3	359.6(2)	358.8(2)	359.6(2)	357(1)	356(1)

Although the P-Cl distances cannot be distinguished in the structure of $(DmpNPCl)_3$ (Figure 3.3), the *trans* configured P3-Cl3 in **3.4**Dipp $[GaCl_4]$ (Figure 3.2) is dramatically longer [2.704(1) Å] than the *cis* configured P-Cl distances [2.081(1), 2.088(1) Å] and is longer than a typical P-Cl distance [*cf.* PCl_3, 2.038(6) Å].[99] This

distinction in P3-Cl3 for **3.4**Dipp [$GaCl_4$] is due to interaction of Cl3 with gallium, although the Cl3-Ga distance is only slightly longer [2.249(1) Å] than the other three [Cl-Ga 2.149(1), 2.150(1), 2.156(1) Å]. Consistently, the N-P distances in $(DmpNPCl)_3$ and $(DmpNPBr)_3$ are essentially indistinguishable, while N-P3 distances in **3.4**Dipp [$GaCl_4$] [N2-P3 1.656(2) and N3-P3 1.650(2) Å] are significantly shorter than the neighbouring bonds [N2-P2 1.736(2) and N3-P1 1.753(2) Å]. Moreover, the endocyclic angle at P3 [105.0(1)°] in **3.4**Dipp [$GaCl_4$] is relatively wide compared with those at P1 and P2 and the corresponding angles in $(DmpNPCl)_3$ or $(DmpNPBr)_3$. Therefore, we assign an ionic formulation for **3.4**Dipp [$GaCl_4$], and describe the cation **3.4**Dipp as an assembly of a P1-N1-P2 phosphazane unit and a N2-P3-N3 'diaminophosphenium' unit, representing a six-membered analogue of **3.3**^{t}Bu.[95] In this context, the relatively short N2-P3 and N3-P3 distances implicate significant π interaction at the phosphenium site P3.

3.4 –Thermodynamic preference of cyclotriphosphazanes versus cyclodiphosphazanes

The thermodynamic preference for trimeric phosphazanes over the more familiar dimeric analogues due to the imposition of sterically loaded substituents such as Dipp and Dmp is counter-intuitive. Substituent steric strain is expected to favour monomers or smaller oligomers in which the substituents are spatially less restricted. The substituent steric strain in derivatives of $(RNPX)_3$ (R = Dmp, Dipp) destabilizes the dimer relative to the corresponding trimer $(RNPX)_3$ by virtue of relative N-P framework flexibility. The greater substituent steric strain in the dimers is evidenced (Table 2.2) by slight distortions

from planarity at the nitrogen centers (sum of angles at N < 356°), which results from interactions between the *cis* bromide substituents and the methyl groups at C16 and C22, as shown in Figure 3.4. In comparison, the environments for nitrogen in the trimers $(RNPX)_3$ are closer to planar (sum of angles at N > 358°).

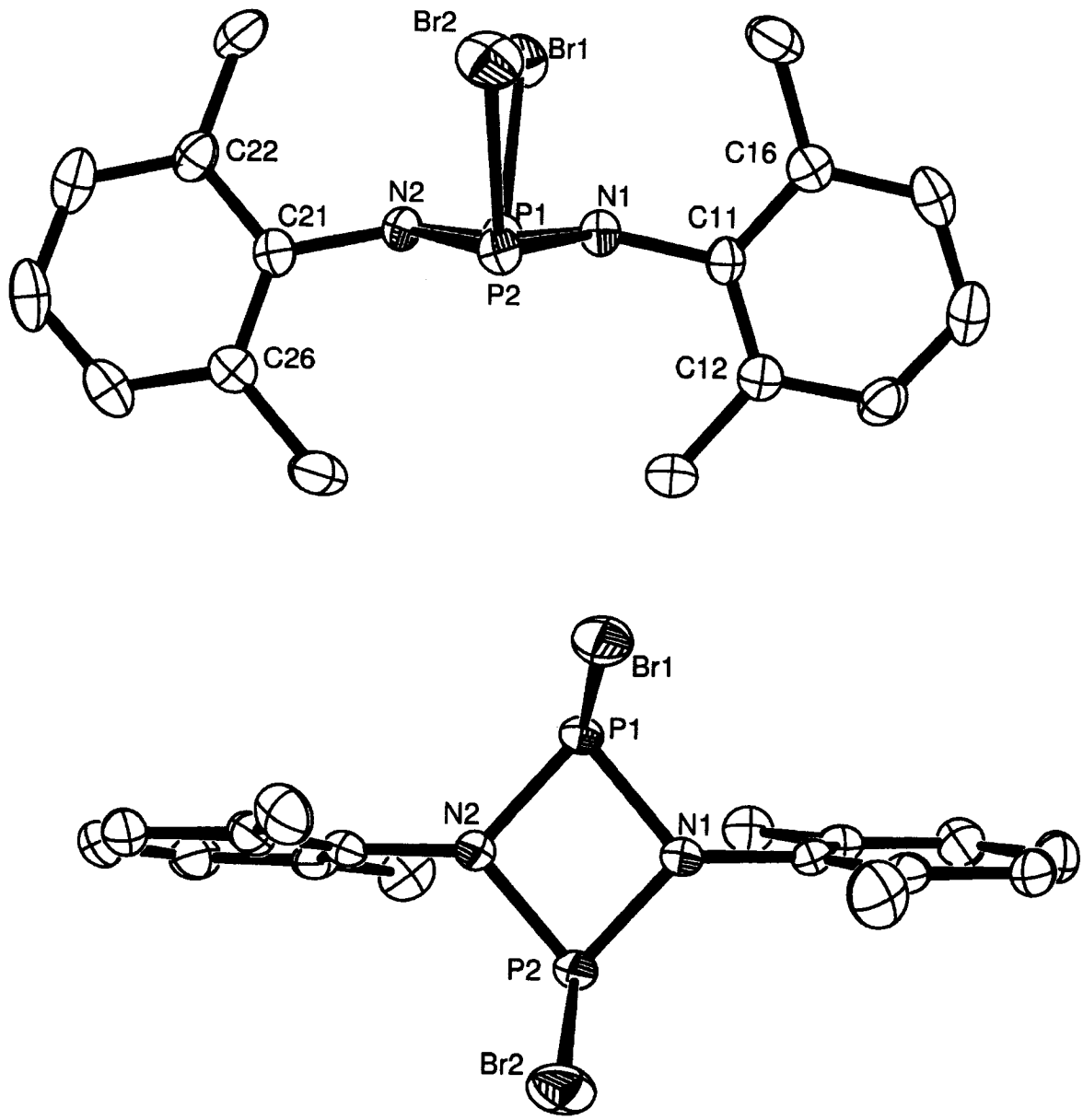

Figure 3.4 - Two views of $(DmpNPBr)_2$ in the Solid-state. Hydrogen atoms omitted for clarity. Thermal ellipsoids are drawn at 50 % probability.

More apparent are the differences in torsional angles about the N-P bonds (Table 3.2), which reveal the relative orientation of X and the *ipso* carbon center. The dimers exhibit X-P-N-C torsional angles all close to 90°, while the corresponding trimers demonstrate a more flexible framework with distortions (from 90°) as large as 29°.

Table 3.2 - X-N-P-C torsional angles (°) for derivatives of $(DmpNPX)_n$.

	$(DmpNPCl)_2$	$(DmpNPBr)_2$	$(DmpNPCl)_3$	$(DmpNPBr)_3$
X1-P1-N1-C11	90.1(3)	87.7(3)	119.5(1)	97.0(2)
X2-P2-N1-C11	94.6(3)	94.2(3)	97.3(1)	120.8(2)
X1-P1-N2-C21	94.7(3)	95.5(3)		
X2-P2-N2-C21	90.3(3)	88.8(3)	65.4(1)	103.4(2)
X3-P3-N2-C21			92.4(1)	66.3(2)
X1-P1-N3-C31			97.4(1)	67.6(2)
X3-P3-N3-C31			77.4(2)	84.3(2)

The consequences of these distortions include the twist of the aryl substituent away from the halide for C22 in Figure 3.3, which is limited in the more restricted frame of the dimers as shown in Figure 3.4. The boat shaped frameworks of the trimers reveal a non-symmetric twisting of the aryl substituents and a non-symmetric orientation of the halide substituents minimizing distortions from planarity at each nitrogen center without compromising the accommodation of substituent steric strain. We associate these subtle structural distinctions between dimer and trimer with the relative thermodynamic preference for the cyclotriphosphazanes over the cyclodiphosphazanes with Dmp and Dipp substituents at nitrogen.

Recently is has been shown $(EtNPCl)_3$ is readily converted to the corresponding dimer $(EtNPCl)_2$ under distillation at reduced pressure (10^{-5} mm Hg, 76 °C).[65] Heating the dimer (130 °C) at atmospheric pressure for 12 hours in solution results in dimer reverting back to the trimer, which can again be reversibly transformed to the dimer under distillation. This observation indicates the formation of the trimer under thermodynamic conditions and the dimer under kinetic control, which agrees with our conclusions of the thermodynamic preferences of the trimer over dimer.

Summary

Deep orange reaction mixtures of dimeric cyclodiphosphazanes $(RNPX)_2$ (R = Dipp; X = Cl, R = Dmp; X = Cl, Br) with GaX_3 become colourless on addition of DMAP and the corresponding trimeric cyclotriphosphazanes $(RNPX)_3$ have been isolated. An unusual cyclo-phosphazanium tetrachlorogallate salt **3.4**Dipp $[GaCl_4]$ $[(DippN)_3P_3Cl_2][GaCl_4]$ has been isolated and represents an intermediate in the disproportionation process. The lability of the N-P bond in derivatives of $(RNPX)_2$ is imposed by appropriate selection of substituents (R) with medium steric loading that thermodynamically destabilizes the dimer with respect to the corresponding trimer, but the substituents have insufficient steric bulk to favour the monomer. This ring expansion reaction is analogous to the gallium chloride induced ring opening polymerisation of a thionylphosphazene,[100] but represents an interesting contrast to the ring contraction of cyclocarbophosphazenes also facilitated by gallium chloride.[101] As phosphazane chemistry has been essentially limited to dimeric frameworks, the manipulation of

substituent steric strain to modify the relative stability of the phosphazane framework in favour of the trimer represents a new opportunity for diversification.

Chapter 4 – Ring Expansion of Cyclodiarsazanes to Cyclotriarsazanes

4.1 - Introduction

Compounds and materials containing phosphorus can be monitored by use of the sensitive ^{31}P NMR probe, but elucidation of the chemistry for compounds of arsenic, antimony and bismuth is less efficient. Therefore, comparisons in reactivity between homologous series of compounds are vital. In this context, synthetic methodologies devised for phosphorus can sometimes be extrapolated to analogous compounds for arsenic, antimony and bismuth. With the effective ring expansion reaction for cyclodiphosphazanes $(RNPX)_2$ to give the cyclotriphosphazanes $(RNPX)_3$, transferring this reaction to the corresponding cyclodiarsazanes would be significant in the development of pnictazane chemistry.

4.2 – Isolation of a cationic 6-membered cycloarsazane

Derivatives of $(RNAsCl)_2$ (R = Dmp, Dipp) react rapidly with 0.66 eq. of $GaCl_3$ to give dark red solutions, and crystalline materials have been isolated and characterized as **4.1**[$GaCl_4$] (Scheme 4.1). In addition, crystals of **4.1**Dipp [$GaCl_4$] were suitable for X-ray crystallography studies (Figure 4.1). The cation **4.1**Dipp is a six-membered As-N heterocatenated ring with two chloro-arsine centers and one arsenium center and its formation can be described as a ring expansion disproportionation that is induced by chloride ion abstraction.

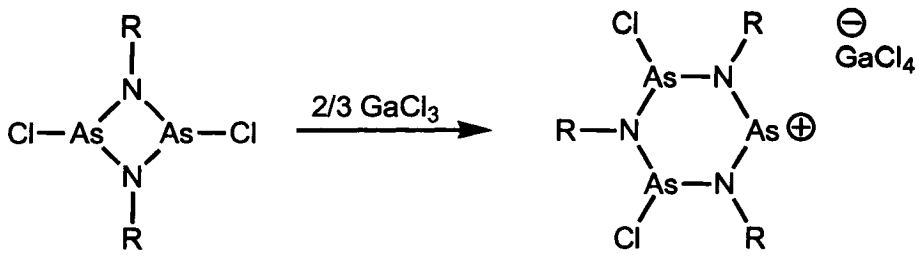

4.1

Scheme 4.1 – Reaction of $(RNAsCl)_2$ with $GaCl_3$ to yield the cationic 6-membered ring **4.1**.

As for **3.4**Dipp [$GaCl_4$],[68] the Solid-state structure of **4.1**Dipp [$GaCl_4$] (Figure 1) is distinctly ionic with two covalent As-Cl bonds [As-Cl 2.207(1) and 2.209(1) Å] in a *cis* configuration about the six-membered As_3N_3 heterocyclic frame, and a long *trans* configured As3---Cl3 contact [2.708(1) Å] representing the closest interaction between cation and complex anion (Table 4.1).

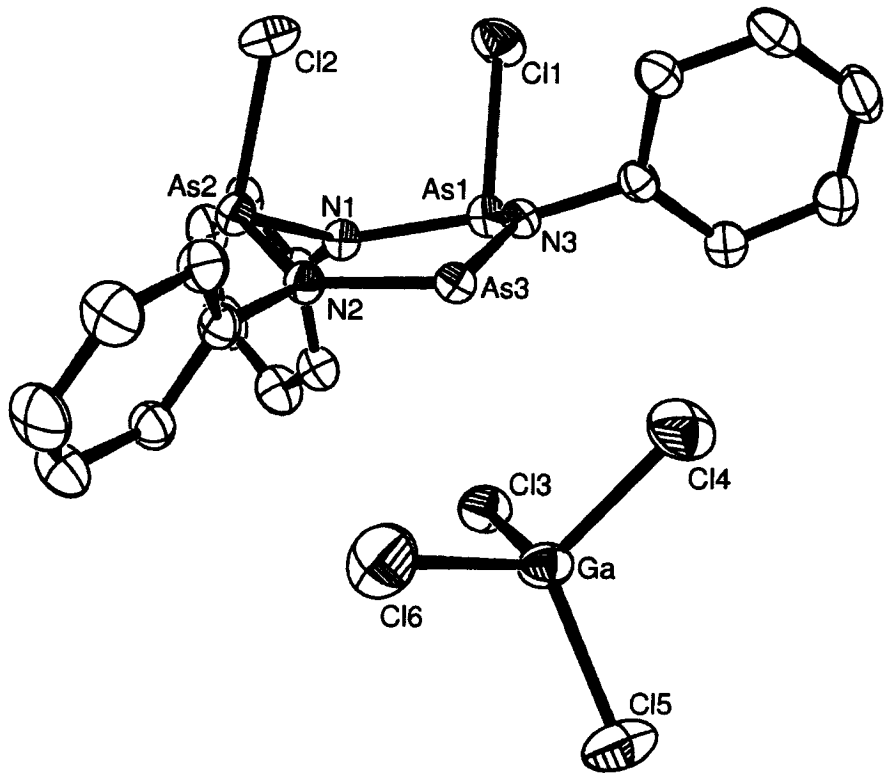

Figure 4.1 – Solid-state structure of **4.1**Dipp [$GaCl_4$]. Hydrogen atoms and isopropyl groups omitted for clarity. Thermal ellipsoids are drawn at 50%.

The N-As3 distances are correspondingly distinct and are shorter [1.793(2) and 1.786(2) Å] than the other four N-As bonds in the heterocycle [1.829(2), 1.834(2), 1.864(2), 1.881(2) Å], highlighting cation **4.1** as an arsazane/arsenium hybrid, and indicating a significant π interaction in the N-As3 bonds. In this context, the N2-As3 and N3-As3 bonds compare with those in previously reported examples of azarsenium salts [**4.2**, 1.776(4) Å;[102] **4.3**, 1.752(5), 1.949(4) Å this cation adopts a dimeric arrangement in the solid-state involving intermolecular N-As interactions that effect disruption of one N-As π interaction;[103,104] **4.4**, 1.68(3), 1.67(2)].[104]

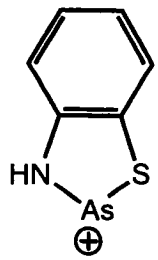

4.2

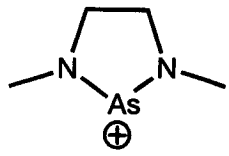

4.3

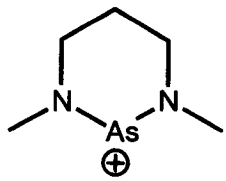

4.4

4.3 – Isolation of cyclotriarsazanes

Equimolar combinations of DMAP and **4.1** [$GaCl_4$] (including *in situ* mixtures of $(RNAsCl)_2$ with 0.66 eq. of $GaCl_3$ give yellow solutions, from which the corresponding cyclotriarsatriazanes $(RNAsCl)_3$ (R = Dipp, Dmp) have been isolated. As with the phosphorus analogues, the reactions are envisaged to involve release of chloride ion from the gallate anion by formation of DMAP-$GaCl_3$ and consequential formation of a covalent As-Cl bond in $(RNAsCl)_3$. While the reaction stoichiometry [3 $(RNAsCl)_2$: 2 $GaCl_3$] is appropriate for the formation of **4.1**[$GaCl_4$], the ring expansion process is facilitated by increasing the relative amount of $GaCl_3$, from 0.66 eq, to 2 eq., given suitable reactions times (> 2 hrs) before addition of DMAP. Addition of DMAP to the reaction mixture after a short (< 30 min) reaction time gives $(RNAsCl)_2$ quantitatively. We speculate that the increase in the stoichiometric ratio of $GaCl_3$ promotes the formation of [$RNAs^+$] by chloride ion abstraction and ring cleavage, and drives the equilibrium toward the six-membered heterocyclic cation **4.1**.

Selected solid-state structural features for $(DippNAsCl)_3$, $(DippNAsCl)_3$ and **4.1**Dipp $[GaCl_4]$ are listed in Table 4.1, together with analogous features for $(MeNAsCl)_3$,[64] representing the only previous structural report of a cyclotriarsazane.

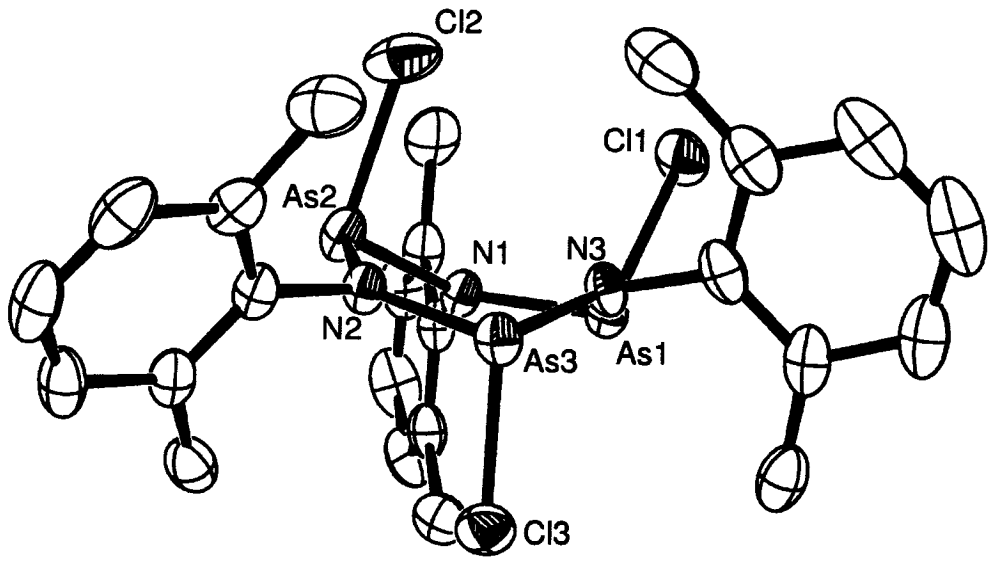

Figure 4.2 – Solid-state structure of $(DmpNAsCl)_3$. Hydrogen atoms have been omitted for clarity. Thermal ellipsoids are drawn at 50% probability.

Table 4.1 Selected bond lengths (Å) and angles (°) for derivatives of $(RNAsCl)_3$, **4.1** and **3.4**.

	$(DmpNAsCl)_3$	$(DippNAsCl)_3$	$(MeNAsCl)_3$[64]	$[Dipp_3N_3As_3Cl_2][GaCl_4]$ **4.1Dipp**	$[Dipp_3N_3P_3Cl_2][GaCl_4]$[68] **3.4Dipp**
N1-Pn1	1.834(3)	1.848(2)	1.79	1.829(2)	1.697(2)
N3-Pn1	1.836(3)	1.831(2)	1.85	1.881(2)	1.753(2)
N1- Pn2	1.846(3)	1.826(2)	1.83	1.834(2)	1.703(2)
N2-Pn2	1.826(3)	1.835(2)	1.88	1.864(2)	1.736(2)
N2-Pn3	1.828(3)	1.827(2)	1.76	1.793(2)	1.656(2)
N3-Pn3	1.829(3)	1.837(2)	1.86	1.786(2)	1.650(2)
N-Pn1-N	100.2(1)	99.5(1)	102.5	98.4(1)	99.4(1)
Pn1-Cl1	2.255(1)	2.230(1)	2.28	2.207(1)	2.081(1)
Pn2-Cl2	2.245(1)	2.270(1)	2.24	2.209(1)	2.088(1)
Pn3-Cl3	2.232(1)	2.235(1)	2.28	2.708(1)	2.704(1)
N-Pn2-N	98.5(2)	101.4(1)	99.7	99.1(1)	100.8(1)
N-Pn3-N	100.7(1)	100.3(1)	105.5	103.8(1)	105.0(1)
Σ° at N1	354.7(3)	356.6(2)	359.1	359.4(1)	359.7(2)
Σ° at N2	359.9(2)	359.5(2)	359.6	358.8(1)	359.0(2)
Σ° at N3	360.0(2)	359.4(2)	358.3	358.6(1)	359.6(2)
Σ° at Pn1	300.2(1)	301.4(1)	303.9	301.5(1)	304.5(9)
Σ° at Pn2	299.1(1)	302.4(1)	295.2	298.1(1)	302.6(7)
Σ° at Pn3	300.3(1)	300.5(1)	301.1	-	-

Interesting similarities and distinctions are apparent between $(DmpNPCl)_3$ $(DmpNPBr)_3$, $(DmpNAsCl)_3$ and $(DippNAsCl)_3$. All adopt a *cis, trans* configuration of the halogens that is maintained in solution. Four distinct ortho-methyl signals in the ^1H NMR spectra of $(DmpNPBr)_3$ and $(DmpNAsCl)_3$ (Figure 4.3), with relative intensity of 1:2:1:2, suggest restricted rotation of the 2,6-dimethylphenyl substituents. In contrast, $(DmpNPCl)_3$ exhibits only two signals in the ^1H NMR spectrum consistent with free rotation about the N-C bonds.

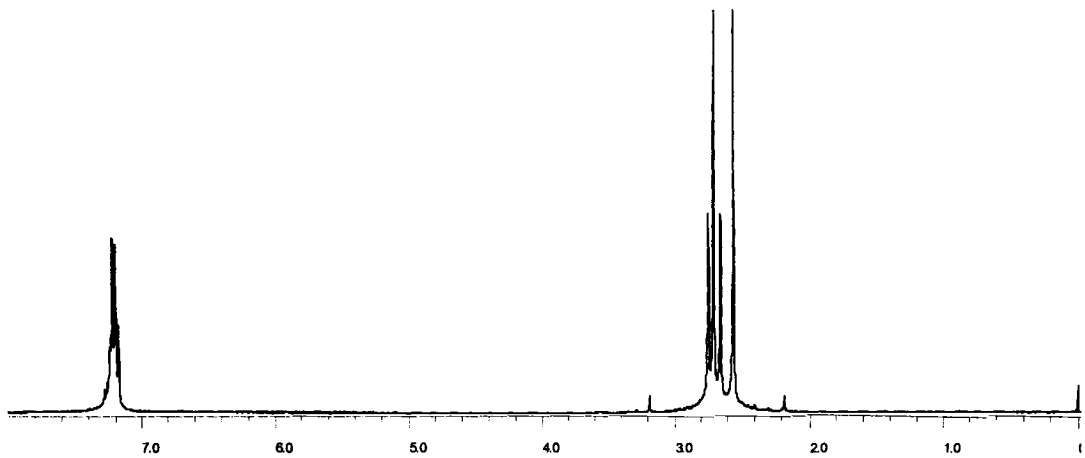

Figure 4.3 – ^1H NMR spectrum of $(DmpNAsCl)_3$ in $CDCl_3$ at 298K.

A combination of ring strain and substituent steric strain is likely responsible for the preferred *cis, trans* configuration in derivatives of $(RNAsCl)_3$, which enables maintenance of the almost planar geometry at each nitrogen center and the distinctly

pyramidal geometry at each arsenic or phosphorus center (substantially less than 360°; Table 4.1). All bond lengths (N-As, N-P, As-Cl and P-Cl) are essentially identical to those observed in the corresponding dimeric oligomers and are representative of single bonds.

Summary

The substituents 2,6-dimethylphenyl (Dmp) and 2,6-diisopropylphenyl (Dipp) impose "medium" substituent steric strain on derivatives of $(RNAsCl)_2$ influencing the relative thermodynamic stability of potential oligomers in favor of the trimers $(RNAsCl)_3$. Extrapolation of observations for phosphazanes to arsazanes demonstrates the general application of this new synthetic procedure for the development and diversification of pnictazane chemistry.

Chapter 5 - Identification of Cycloarsaphosphazanes, Cyclodiarsaphosphazanes and Cycloarsadiphosphazanes

5.1 - Introduction

Substitution of one or more phosphorus atoms by carbon or sulphur in the backbone of phosphazene heterocycles has been important to the diversification of inorganic polymers to include poly(carbophosphazenes), poly(thiophosphazenes) and poly(thionylphosphazenes).[6,105] In a similar fashion, preparing heterocycles containing nitrogen, phosphorus and arsenic would significantly diversify pnictazane chemistry. Small, linear arsino-phosphinoamines (**5.1**)[106-108] have been identified as well as rare examples of mixed cyclodipnictazanes (**5.2**)[109] and (**5.3**),[110] but solid-state structures have not been reported for **5.1** - **5.3** and little to no NMR data are provided. No example of a mixed cyclotripnictazane has been reported to date.

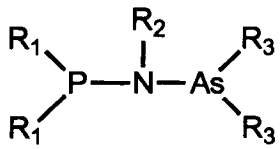

5.1

R_1 = tBu, N,N-DMEDA, CF_3
R_2 = Me, H
R_3 = Me, N,N-DMEDA, CF_3

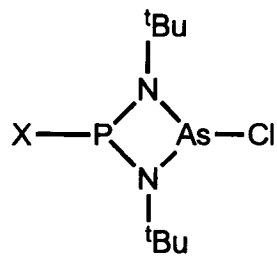

5.2

X = F, Cl

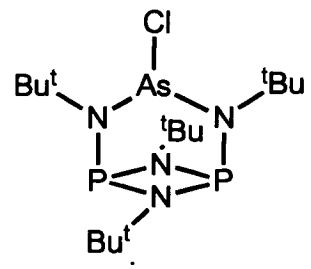

5.3

While the mechanism of the ring expansion shown in chapters 3 and 4 is not known, transforming a cyclodipnictazane into a cyclotripnictazane at some point requires a monomeric unit, formally derived from the cleavage of a cyclodipnictazane ring. Mixtures of cyclodiphosphazanes and cyclodiarsazanes therefore have the potential to undergo ring expansion reactions, in which a monomer unit for one pnictogen (for instance phosphorus), can be inserted into a cyclodipnictazane ring of the other pnictogen (arsenic). Such a mixture under ring expansion conditions has the potential to form cyclotripnictazanes $(RNPnX)_3$ with varying composition of phosphorus and arsenic at Pn. Shown in Figure 5.1 are the ten possible cyclotripnictazanes of the general formula $(RNP_nAs_{3-n}X)_3$ (n = 0 – 3) including both *cis* and *cis, trans* configurations. It might be expected that preparation of such a mixed ring system would produce a statistical distribution of all possible cyclotripnictazanes, depending on the relative proportions of either $(RNPX)_2$ and $(RNAsX)_2$ in the reactions mixture.

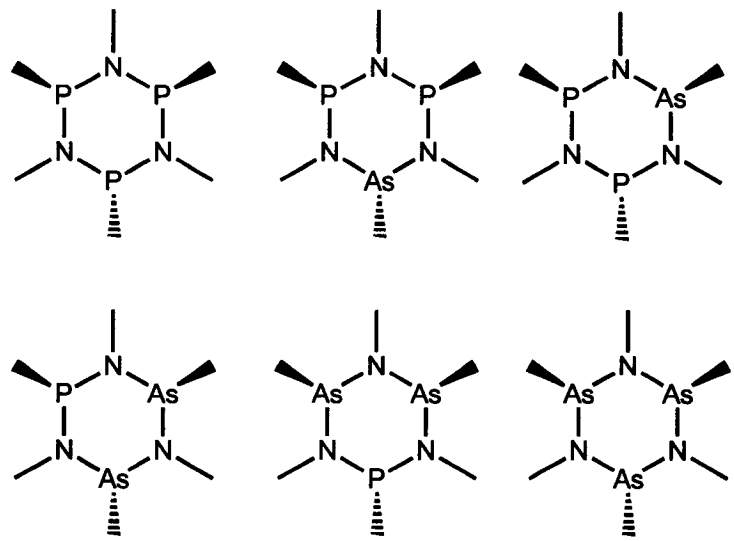

Cis, trans Cyclotripnictazanes

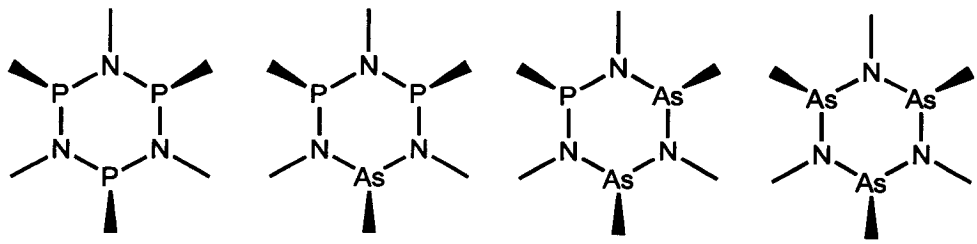

Cis Cyclotripnictazanes

Figure 5.1 – Potential derivatives of $(RNP_nAs_{3-n}X)_3$ (n = 0 – 3).

Factors may limit the potential numbers of the cyclotripnictazanes that could be formed under ring expansion conditions. *Cis* cyclotripnictazanes have not been observed, for R = Dmp or Dipp, suggesting only the *cis, trans* configurations would be seen under ring expansion conditions, reducing the number of potential cyclotripnictazanes from ten to six. Selectivity from the six remaining *cis, trans* cyclotripnictazanes may be possible under specific conditions. If certain intermediates, such as the proposed $[RNP]^+$ and

$[RNAs]^+$are found within the reaction mixture, the thermodynamic stability of one intermediate over another may allow the reaction to proceed on a pathway preferential to one of the remaining six mixed cyclotripnictazanes.

5.2 – ^{31}P NMR spectra of mixtures of $(RNPCl)_2$ and $(RNAsCl)_2$ under ring expansion conditions

Stoichiometries of 2:1 and 1:2 of $(RNPCl)_2$ and $(RNAsCl)_2$ (R = Dmp or Dipp) were combined with 2 or 6 eq. of $GaCl_3$ and allowed to stir for 2 hours. Alternatively, $(RNPnCl)_2$ was combined with 2 eq. of $GaCl_3$, allowed to stir for 15 minutes, after which 2 eq. of $(RNPn'Cl)_2$ was added to the solution. In either case, after two hours, the subsequent red solutions yielded broad peaks in the ^{31}P NMR spectrum. Attempts to crystallize cationic intermediates from either combination, which had been done for both phosphorus[68] and arsenic, were not successful yielding oily mixtures when $(RNPCl)_2$ was in excess. If $(RNAsCl)_2$ was in excess, crystals grown from the reaction mixture were consistent with the previously isolated all arsenic 6-membered cationic rings **4.1**Dmp or **4.1**Dipp.

Quenching the ring expansion reaction with DMAP and obtaining ^{31}P NMR yields spectra that vary depending on the initial reaction stoichiometries. When $(RNPCl)_2$ is in excess prominent peaks in the ^{31}P NMR spectrum are seen at 211 ppm $(RNPCl)_2$, 206 ppm (tenatively assigned to cyclomonoarsamonophosphaazane ($R_2N_2AsPCl_2$)) and a clustering of peaks in the range of 109 - 119 ppm. These latter peaks at lower chemical shift contain $(RNPCl)_3$ (110 & 116 ppm), with the remaining peaks tentatively assigned to variations of $(RNPnCl)_3$ as outlined in Figure 5.1. No peaks are seen that are more

shielded by 20-30 ppm than those centered around 110 - 119, suggesting that no *cis* configured cyclotripnictazanes were observed.[7,61,62]

^{31}P NMR spectra of reactions containing $(RNAsCl)_2$ in excess (2:1) over $(RNPCl)_2$ are less complicated than with $(RNPCl)_2$ in excess (Figure 5.2). Peaks at 211 ppm and 206 ppm are again seen, however peaks corresponding to $(RNPCl)_2$ are in lower relative intensity. In the chemical shift region associated with $(RNPCl)_3$, only one peak is seen at 109 ppm which is the highest relative intensity in the spectrum.

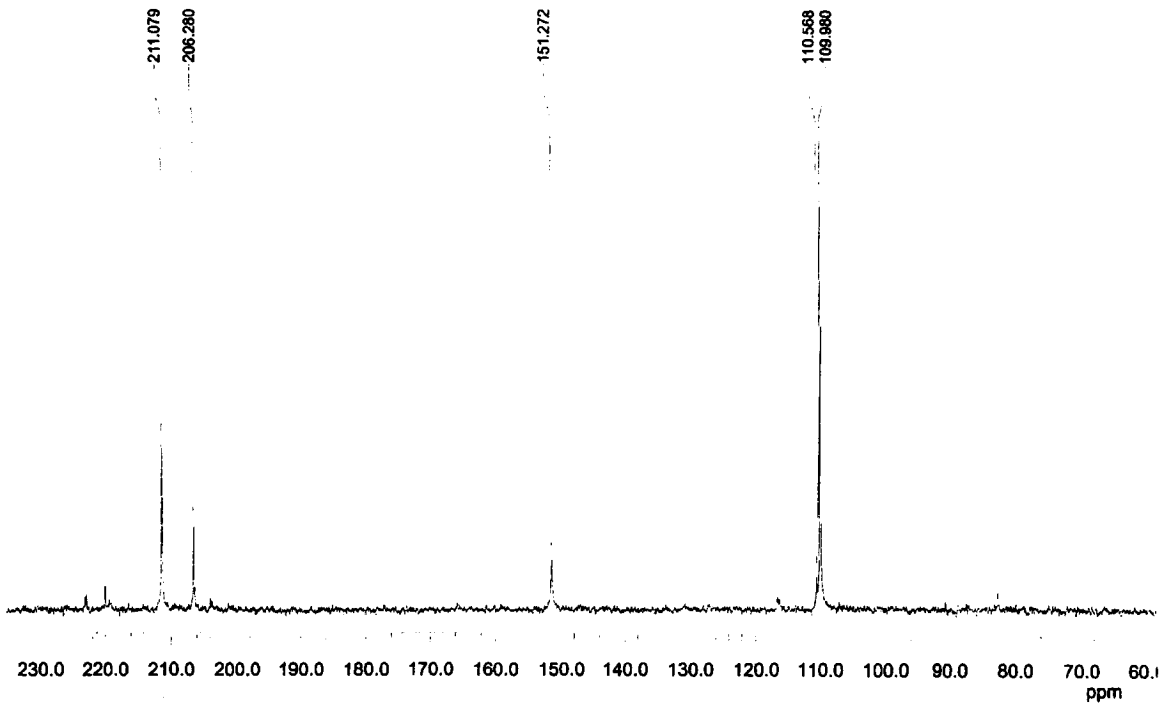

Figure 5.2 – ^{31}P NMR spectrum of the reaction mixture of $(DmpNPCl)_2$ + 2 $GaCl_3$ + $(DmpNAsCl)_2$ + 2 DMAP.

Considering the reaction stoichiometry, insertion of an (RNPCl) unit might be expected into a molecule of $(RNAsCl)_2$ to yield a cyclotripnictazane containing one phosphorus and two arsenic atoms. Two isomeric possibilities exist for a 6-membered ring with the composition ($R_3N_3As_2PCl_3$). Containing the P-Cl bond either *trans* to both As-Cl bonds or *cis* to one and *trans* to the other As-Cl bond. In the ^{31}P NMR spectrum of $(RNPCl)_3$ derivatives, by integration the two phosphorus with *cis P*-Cl bonds (110 ppm) are shifted up field to the phosphorus with a *trans P*-Cl bond (116 ppm). The peak found at 109 ppm in Figure 5.2 is therefore assigned to a composition ($Dmp_3N_3As_2PCl_3$) where the lone phosphorus is found in the P-Cl bond *cis* to one and *trans* to the other As-Cl bond. This observations may have mechanistic consequences as it would appear the once *cis* As-Cl bonds of a cyclodiarsazane are now trans to each other. Further studies showed, that while the peak at 109 ppm is dominate in the ^{31}P NMR spectra, the ^{1}H NMR spectra indicate that when $(RNAsCl)_2$ is in excess, substantial amounts $(RNAsCl)_3$ are formed with a relative intensity larger than any phosphorus containing species.

5.3 – MALDI-TOF analysis of mixed cyclic pnictazanes

To help identify derivatives of $(RNP_nAs_{3-n}Cl)_3$ (n = 0 – 3) that were postulated as an outcome in the reaction of mixtures of $(RNPCl)_2$ and $(RNAsCl)_3$ (R = Dmp) under ring expansion conditions, air-sensitive MALDI-TOF mass spectrometry was performed on isolated solids that contained a distribution of peaks in ^{31}P NMR spectrum in both the dimer (206 - 211 ppm) and trimer (109 - 119 ppm) region. The result was a MALDI-TOF spectrum that was complicated (Figure 5.3), however almost all peaks can be assigned

(Table 5.1). Assignments were done based on m/z^+ values for ions containing only hydrogen (^1H - 99.9%), carbon (^{12}C – 98.9%) nitrogen (^{14}N – 99.6%), phosphorus (^{31}P – 100%) and/or arsenic (^{75}As – 100%). For ions containing chlorine (^{35}Cl – 75.8%; ^{37}Cl – 24.2%), isotopic distributions were also used to help confirm the assignment of m/z^+ peaks by comparison of the experimental isotopic pattern to the calculated pattern (Figure 5.4).

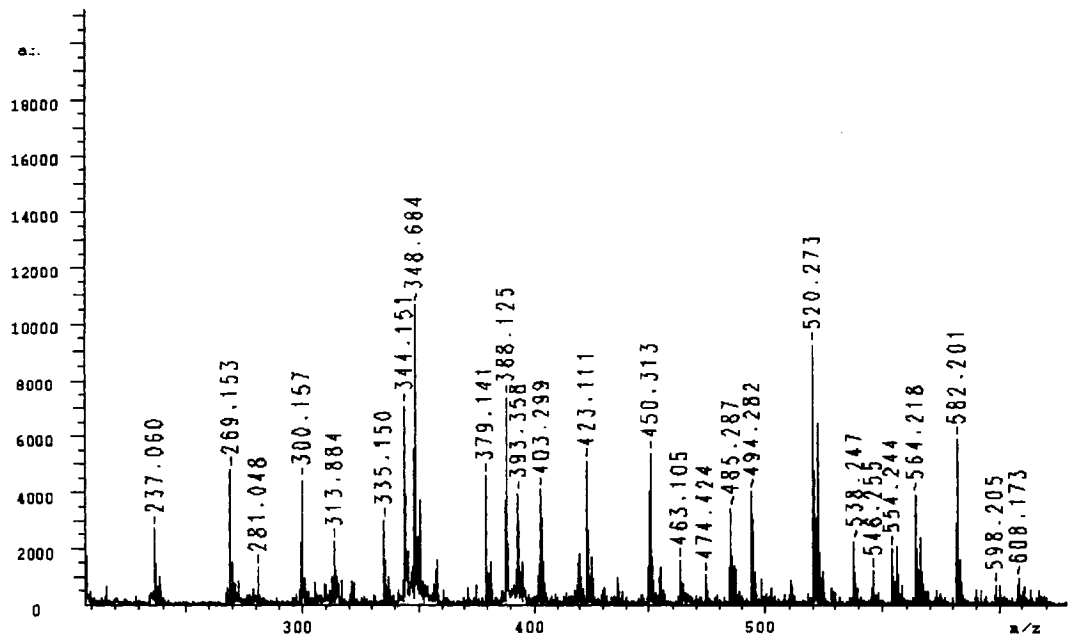

Figure 5.3 – MALDI-TOF mass spectrum of isolated solid of the reaction of 2 $(DmpNPCl)_2$ + $(DmpNAsCl)_2$ + 6 $GaCl_3$ + 6 DMAP.

At low m/z^+ values, (below those cyclotripnictazanes) a variety of fragment ions are observed including $[(DmpN)_2P]^+$, $[(DmpN)_2As]^+$ and $[(DmpNPn)_2X_n]^+$ (n = 0 or 1).

While these fragment ions could be derived from $(DmpNPnCl)_2$, the observation of the $[(DmpN)_2As_3]^+$ cation, which has formally lost a $[DmpN]^-$ fragment from $(RNAsCl)_3$ makes it difficult to conclude if the ions at lower m/z^+ are derived from cyclodipnictazanes or cyclotripnictazanes.

Table 5.1 - m/z^+ assignments for MALDI-TOF spectrum in Figure 5.4.

Assignment	m/z^+	Assignment	m/z^+
$[(DmpN)_2P]^+$	269.153	$[(DmpN)_2As_3]^+$	463.105
$[(DmpNP)_2]^{+\cdot}$	300.157	$[(DmpNP)_3Cl]^{+\cdot}$	485.287
$[(DmpN)_2As]^+$	313.884	$[(DmpN)_3P_2As]^+$	494.282
$[(DmpNP)_2Cl]^+$	335.150	$[(DmpNP)_3Cl_2]^+$	520.273
$[(DmpN)_2PAs]^{+\cdot}$	344.151	$[(DmpN)_3PAs_2]^+$	538.247
$[(DmpN)_2AsCl]^{+\cdot}$	348.684	$[(DmpN)_3P_2AsCl_2]^+$	564.218
$[(DmpN)_2PAsCl]^+$	379.141	$[(DmpNAs)_3]^+$	582.201
$[(DmpNAs)_2]^{+\cdot}$	388.125	$[(DmpN)_3P_2AsCl_3]^{+\cdot}$	598.205
$[(DmpNAs)_2Cl]^+$	423.111	$[(DmpN)_3PAs_2Cl_2]^+$	608.173
$[(DmpNP)_3]^+$	450.313		

At the highest m/z^+ values, peaks are observed that can be assigned to the fragmentation of $(DmpNPCl)_3$ or $(DmpNAsCl)_3$. More important, assignment of fragments from $(RNP_nAs_{3-n}Cl)_3$ (n = 0 – 3), namely the $[(DmpN)_3P_2As]^+$, $[(DmpN)_3PAs_2]^+$, $[(DmpN)P_2AsCl_2]^+$, $[(DmpN)_3P_2AsCl_3]^{+\cdot}$ and $[(DmpN)_3PAs_2Cl_2]^+$. $[(DmpN)P_2AsCl_2]^+$ cations, identify that cyclotripnictazanes with both arsenic and phosphorus atoms are formed from the ring expansion of mixtures of $(RNPCl)_2$ and $(RNAsCl)_2$.

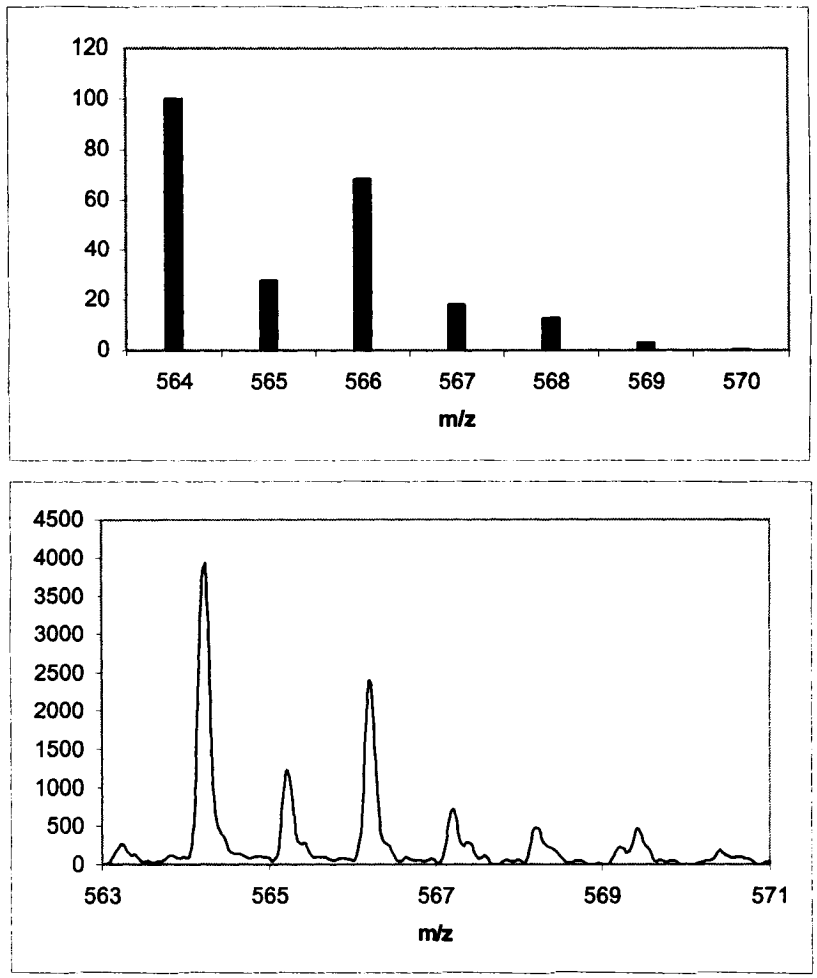

Figure 5.4 – Calculated (top) and experimental (bottom) isotopic distributions for the $[(DmpN)P_2AsCl_2]^+$ cation at m/z$^+$ 564.

5.4 – Solid-state structure of a mixed cyclotripnictazanes

The reaction of 2 $(DmpNAsCl)_2$ and 1 $(DmpNPCl)_2$ with 2 or 6 eq. $GaCl_3$ followed by addition of DMAP, yielded a mixture with one large peak in the ^{31}P NMR spectrum at 109 ppm was the most promising for isolation of a cyclotripnictazane containing both phosphorus and arsenic. Unfortunately, separation of the compound

having the peak at 109 ppm in the ^{31}P NMR spectrum from $(DmpNAsCl)_2$ and $(DmpNAsCl)_3$ was not possible. In cases where the removal of DMAP-$GaCl_3$ adducts was accomplished by running the reaction mixture down a small column of silica, the ^{31}P NMR spectrum on the ensuing products became more complicated in the region 110-119 ppm, indicating that the cyclotripnictazanes disproportionate further on the Lewis acid silica.

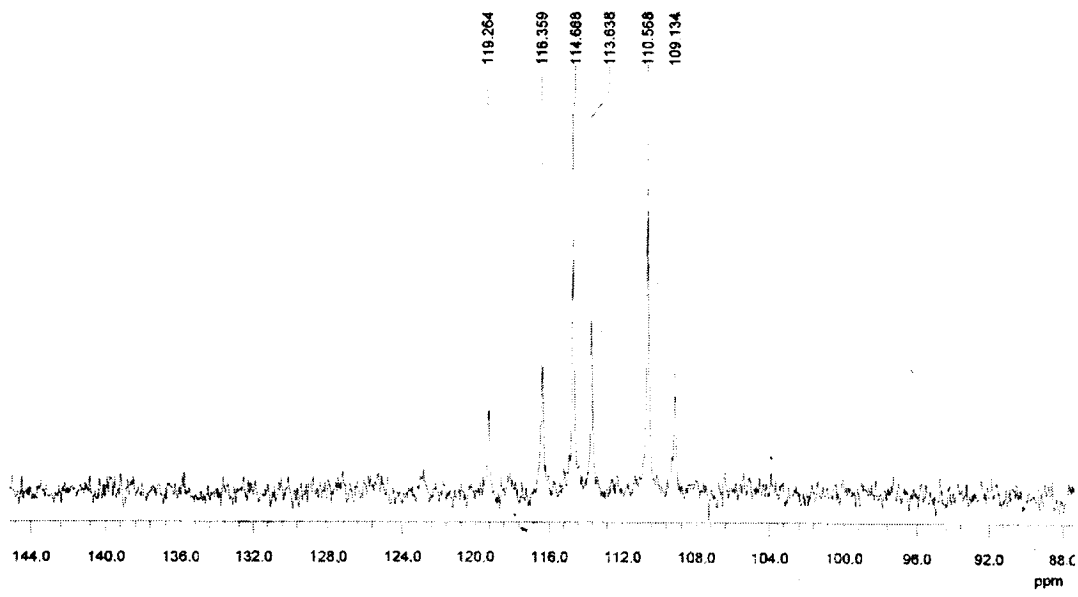

Figure 5.5 – ^{31}P NMR spectrum of re-dissolved crystals of $(RNP_nAs_{3-n}X)_3$ (n = 0 – 3).

Single crystals suitable for diffraction were grown after the product was passed through silica. While the ^{31}P NMR spectrum of the crystal showed they were phosphorus containing (Figure 5.5), ^{1}H NMR spectroscopy again indicated substantial amounts of $(DmpNAsCl)_3$. X-Ray crystallography produced a 6-membered cyclopnictazane

framework, identical to those previously observed for $(DmpNPCl)_3$ and $(DmpNAsCl)_3$ with a *cis, trans* configuration (Figure 5.6). The unit cell of the crystal was determined to be $P2_1/n$ as compared to I2/a for $(DmpNAsCl)_3$ and initially the structure was thought to be a different morphology of $(DmpNAsCl)_3$.

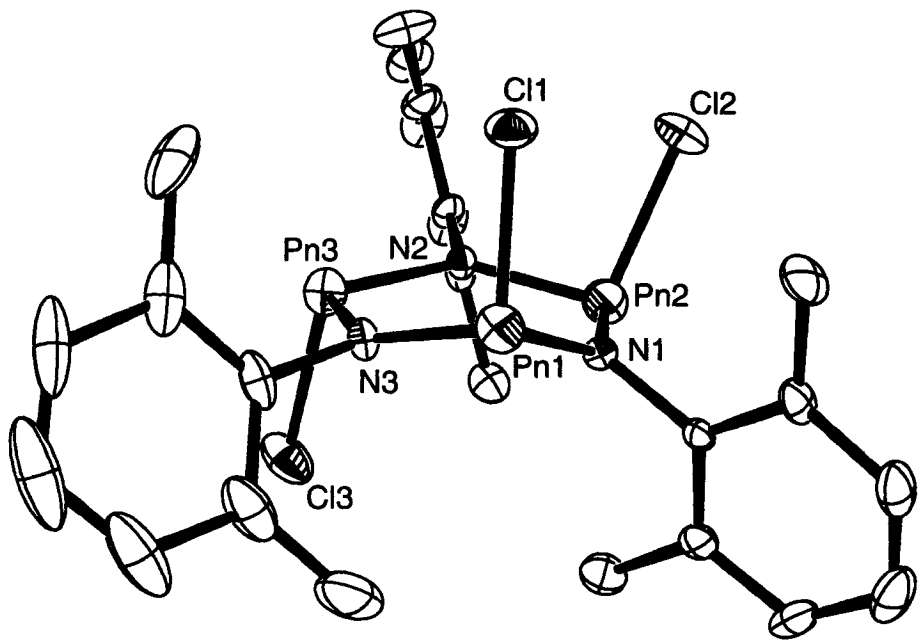

Figure 5.6 – Solid-state structure of $(RNP_nAs_{3-n}X)_3$ (n = 0 – 3). Hydrogen atoms removed for clarity. Thermal ellipsoids are drawn at 50 % probability.

After further investigation, refinement of 25 % Pn1 as phosphorus gave a better R factor than as 100 % $(DmpNAsCl)_3$ indicating that the crystal was likely a co-crystallite

of at least two derivatives of $(RNP_nAs_{3-n}Cl)_3$ (n = 0 – 3). Considering the refinement of Pn1 as 25% phosphorus and 75% arsenic, the N-Pn1 bond lengths should be significantly shorter than those for N-Pn2 and N-Pn3, however this was not the case. All of the N-Pn bonds showed an intermediate value for the aforementioned structure, compared to average P-N or As-N bond lengths in $(DmpNPCl)_3$ and $(DmpNAsCl)_3$ (Table 5.2). Similarly the average Pn-Cl bonds lengths and endocyclic N-Pn-N angles are intermediate between $(DmpNPCl)_3$ and $(DmpNAsCl)_3$, albeit closer to the later structure. Considering the solid-state parameters and the spectroscopic data it appears that while the crystal contains a large quantity of $(DmpNAsCl)_3$, it is likely a co-crystallite of potentially all $(RNP_nAs_{3-n}Cl)_3$ (n = 0 – 3) derivatives, such that each Pn position in the structure is a combination of both phosphorus and arsenic atoms.

Table 5.2 - Selected bond lengths (Å) and angles (°) for derivatives of $(RNPnX)_3$.

	$(DmpNPCl)_3$	$(DmpNAsCl)_3$	$(DmpNPnCl)_3$
Pn1 – N1	1.704(2)	1.834(3)	1.780(4)
Pn1 – N3	1.693(2)	1.836(3)	1.765(4)
Pn2 – N1	1.687(2)	1.846(3)	1.777(4)
Pn2 – N2	1.717(2)	1.826(3)	1.798(4)
Pn3 – N2	1.694(2)	1.828(3)	1.797(4)
Pn3 – N3	1.703(2)	1.829(3)	1.810(4)
Ave Pn-N	1.700	1.833	1.788
Pn1 – Cl1	2.104(1)	2.255(1)	2.179(2)
Pn2 – Cl2	2.116(1)	2.245(1)	2.203(2)
Pn3 – Cl3	2.136(1)	2.232(1)	2.224(2)
N1-Pn1-N3	101.7(1)	100.2(1)	99.9(2)
N1-Pn2-N2	100.1(1)	98.5(2)	98.9(2)
N2-Pn3-N3	101.8(1)	100.7(1)	100.4(2)
Pn1-N1-Pn2	132.0(1)	134.0(2)	134.0(2)
Pn2-N2-Pn3	134.5(1)	131.9(2)	137.4(2)
Pn1-N3-Pn3	131.8(1)	128.6(2)	132.5(2)

Summary

Under ring expansion conditions, combinations of either 1:2 or 2:1 molar equivalents of $(RNPCl)_2$ and $(RNAsCl)_2$ (R = Dmp or Dipp) are shown to disproportionate, yielding derivatives of $(RNP_nAs_{3-n}X)_3$ (n = 0 – 3). In most cases ^1H and ^{31}P NMR spectra indicate that the products are dominated by the homopnictino cyclotripnictazanes and the selective formation of one mixed derivative is not possible under the conditions studied.

Chapter 6 – Intermediates in the Lewis Acid Induced Ring Expansion of Cyclodipnictazanes to cyclotripnictazanes.

6.1 - Introduction

The ring expansion of cyclodipnictazanes to cyclotripnictazanes, being induced by a Lewis acid likely involves cationic pnictazanes in the reaction pathway. Beyond the isolation of new examples of structure and bonding, understanding the reaction mechanism has the potential to provide insight for reactions that might access larger oligomers and pnictazane polymers.

6.2 – Identification and isolation of a ligand stabilized cyclodiphosphazanes bearing a cationic phosphenium centre

As mentioned in chapter 3, ^{31}P NMR spectra of cyclodiphosphazanes with $GaCl_3$ at room temperature show a broad peak at 210 ppm, consistent with $(RNPCl)_2$ having relatively fast chloride exchange with $GaCl_3$. Lowering the temperature reveals two broad peaks that can be attributed to the phosphinophosphenium cation **6.1**[$GaCl_4$].

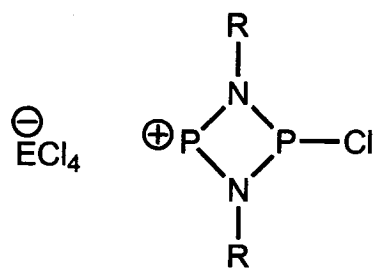

6.1

Reaction of cyclodiphosphazanes with $GaCl_3$ and addition of DMAP after less than 10 minutes yields the starting cyclodiphosphazane in the ^{31}P NMR spectra, while after 2 hours the cyclotriphosphazane is produced. For the same reaction, if DMAP is added after 15 - 30 minutes, two doublets, along with a broad peak at 210 ppm can be seen in the ^{31}P NMR spectra (Figure 6.1).

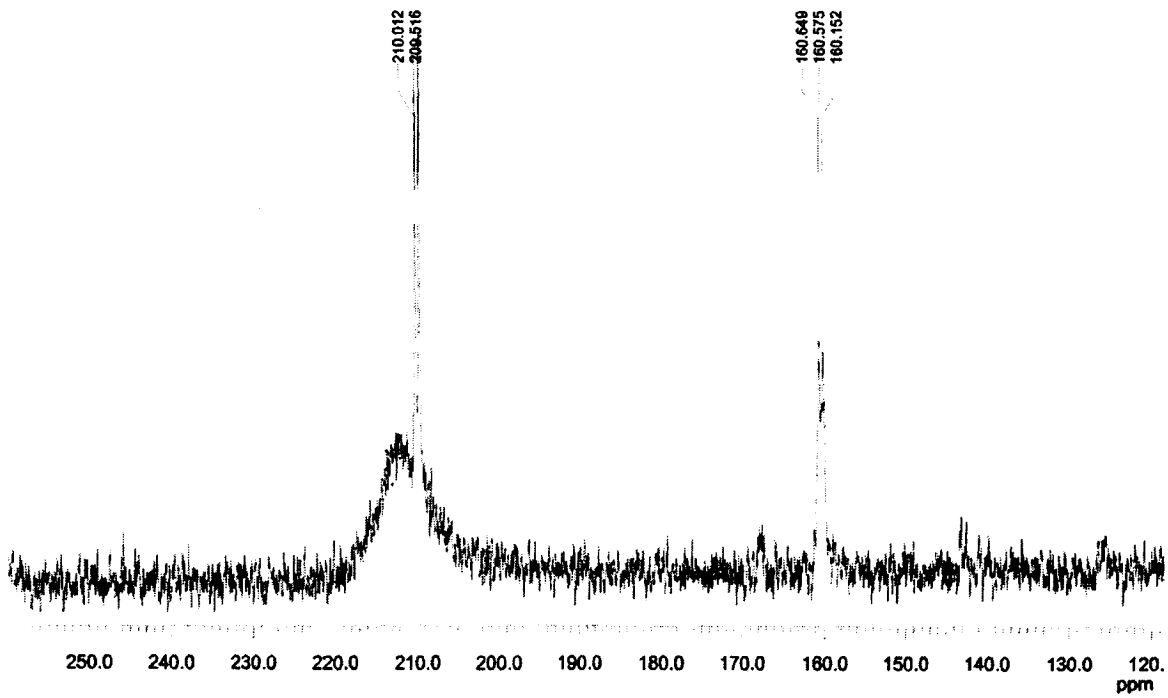

Figure 6.1 - ^{31}P NMR Spectrum of $(DmpNPCl)_2$ + 2 eq. of $GaCl_3$ with 2 eq. of DMAP added after ~ 15 minutes.

The broad peak at 210 ppm is typical for reactions of $(RNPCl)_2$ and $GaCl_3$ in the absence of DMAP, while the doublets centred at 160 and 210 ppm ($^2J_{pp}$ = 50.2 Hz) are reminiscent of those seen for **6.1**[$AlCl_4$] (R = *t*-Bu) [*c.f.* δ 177 and 366 ppm].[95] The new doublets are deshielded, suggesting if a complex similar to **6.1** was formed, the phosphenium cation is likely tri-coordinate, suggesting a base stabilized phosphenium cation. The doublets were therefore assigned to the 4-membered cationic ring, **6.2** where DMAP is acting a neutral donor to the phosphenium centre.

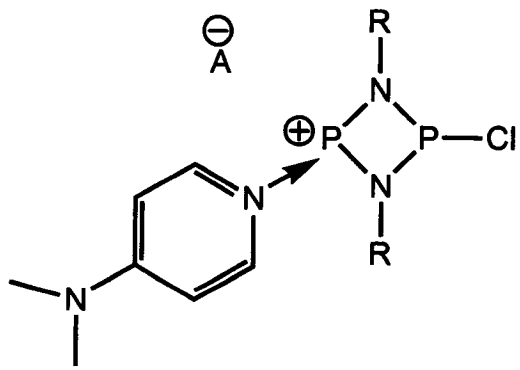

6.2

^{31}P NMR peaks associated with **6.2**[$GaCl_4$] (R = Dmp, Dipp) persist in solution, however attempts to isolate **6.2**[$GaCl_4$] in the solid-state were unsuccessful producing starting material $[RNPCl]_2$ or the DMAP.$GaCl_3$ adduct as identified by ^{31}P or ^1H NMR spectroscopy. Identification of **6.2**[$GaCl_4$] is unexpected as the ring expansion of $(RNPX)_2$ to $(RNPX)_3$ is completed by the coordination of DMAP to $GaCl_3$, suggesting $GaCl_3$ is a more favorable Lewis acid towards DMAP than towards the phosphenium centre in **6.1**. However, the Lewis acid strength of phosphenium cations compared to

$GaCl_3$ is dependent on both the acid and the base, as seen with phosphinophosphonium salts, in which phosphines preferentially coordinate to phosphenium cations over $GaCl_3$.[111] While the DMAP.$GaCl_3$ adduct is thermodynamically stable, the phosphenium centre in **6.1** under these circumstances appears to be Lewis acidic enough to form the kinetically stable DMAP adduct **6.2**[$GaCl_4$]. Since isolation of **6.2**[$GaCl_4$] was not possible due to the instability of the $[GaCl_4]^-$ anion, alternative derivatives of **6.2** were prepared using chloride abstracting agents with non-coordinating, non-Lewis acidic anions. Under such conditions, the anion would not complex with DMAP, preventing the reformation of starting material.

The reaction of $[RNPCl]_2$ (R = Dipp, Dmp) and 1.2 eq. of TMSOTf showed no change by ^{31}P NMR spectrum over a period of days. If DMAP was added to the same reaction and stirred, ^{31}P NMR spectroscopy showed the quantitative conversion of the starting material have a chemical shift of 210 ppm to a set of doublets at 159 and 209 ppm ($^2J_{P\text{-}P}$ = 51.2 Hz) (Figure 6.2; R = Dmp) after 3 days. The new doublets are similar in chemical shift and coupling constant to **6.2**[$GaCl_4$] and were assigned to **6.2**[OTf], where the anion is now the Lewis base stable $[OTf]^-$. In the reaction, DMAP acts as a donor to effect the heterolytic cleavage of the P-Cl bond, forming the base stabilized phosphenium cation and TMSCl as a by-product.

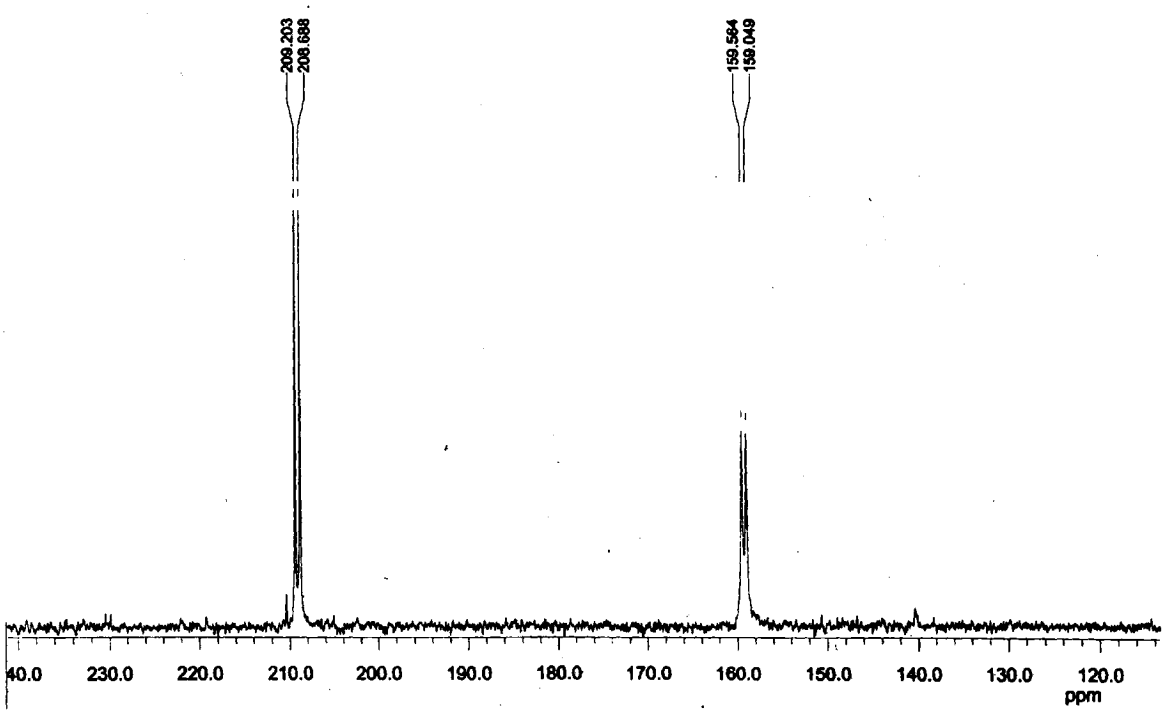

Figure 6.2 - ^{31}P NMR Spectrum of redissolved crystals of **6.2**[OTf] (R = Dmp).

Preparation of derivatives of **6.2** can also be effected by the use of $LiBF_{20}$ or $NaBPh_4$ as halide abstracting reagents. Both decrease the reaction time from days to hours as compared to TMSOTf. In all cases the chemical shifts vary only slightly, suggesting the anion has little association with the phosphine or phosphenium centers (Table 6.1).

Table 6.1 – ^{31}P NMR chemical shifts for derivatives of **6.2** (R = Dmp).

Compound	^{31}P chemical shifts (ppm)	$^{2}J_{P\text{-}P}$ (Hz)
6.2[$GaCl_4$]	160, 210	50.2
6.2[OTf]	159, 209	52.1
6.2[BF_{20}]	161, 210	52.1
6.2[BPh_4]	156, 208	54.0

Crystals of **6.2**[OTf] (R = Dmp) suitable for diffraction studies were grown and the structure is shown in Figure 6.3. Select structural parameters along with $(DmpNPCl)_2$ are listed in Table 6.2. The N_2P_2 cyclodiphosphazane core is retained in **6.2**[OTf] (R = Dmp), with one P-Cl bond replaced by a coordinative bond from the nitrogen in the pyridine ring of DMAP. Structurally, the internal P_2N_2 bond lengths and angles of **6.2**[OTf] (R = Dmp) are almost indistinguishable from $(DmpNPCl)_2$, even though one phosphine centre is now formally cationic.

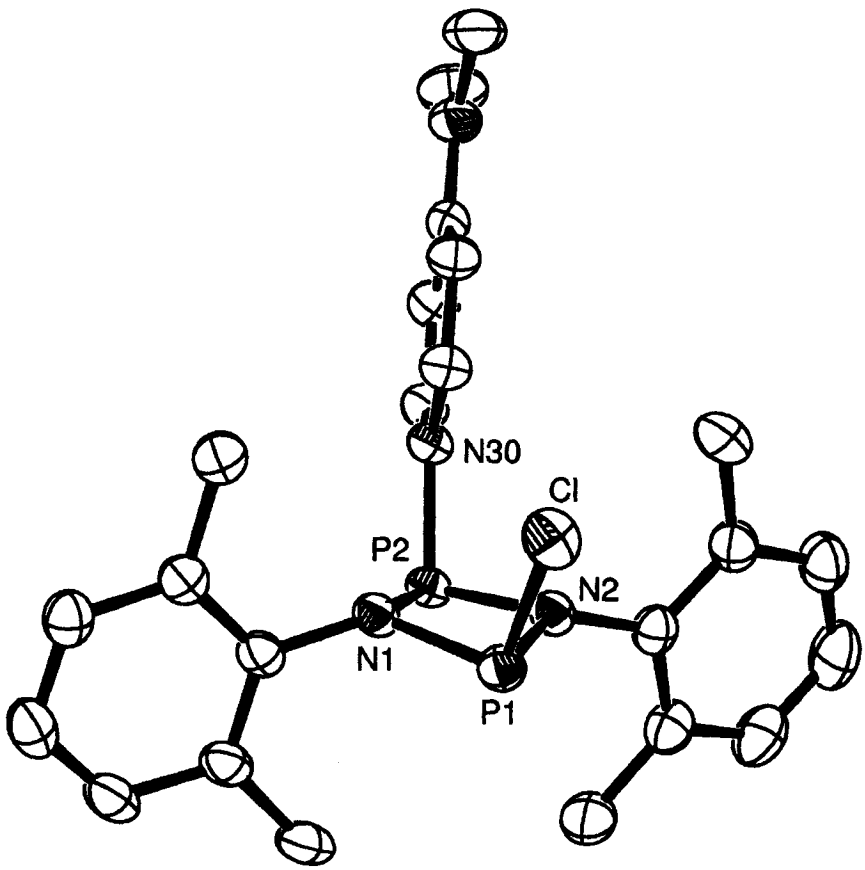

Figure 6.3 – Solid-state structure of **6.2**[OTf] (R = Dmp). Hydrogen atoms and triflate anion have been omitted for clarity. Thermal ellipsoids are drawn at 50 % probability.

The N-P2 bonds lengths of **6.2**[OTf] (R = Dmp) are not significantly different from the N-P1 bond lengths as might be expected. The mesomeric interaction between the lone pair of electrons on the adjacent nitrogen atoms and the empty 3p orbital of the phosphenium cation is insignificant due to the occupation of the 3p orbital of the phosphenium cation by the coordinative bond from DMAP. The N30-P3 bond length [1.773(2) Å] is only slightly longer than the covalent P-N bonds in the 4-membered ring and is short in the range of coordinative bonds from nitrogen to phosphenium centres [1.789(1) – 2.110(6) Å].[98] Any attempts to remove DMAP with $GaCl_3$ showed no change in the ^{31}P NMR over 24 hours, suggesting a very strong DMAP – phosphenium interaction.

Table 6.2 –Bond lengths (Å) and angles (°) for **6.2**[OTf] and $(DmpNPCl)_2$.

Structural Parameter	**6.2**[OTf]	$(DmpNPCl)_2$
N1–P1	1.717(2)	1.703(3)
N1–P2	1.712(2)	1.713(2)
N2–P1	1.704(2)	1.703(3)
N2–P2	1.711(2)	1.704(2)
P1–Cl1	2.134(1)	2.111(1)
P2–N30/Cl2	1.773(2)	2.111(1)
N1-P1-Cl1	103.19(6)	102.83(10)
N1-P2-N30/Cl2	105.45(8)	106.69(10)
N2-P1-Cl1	103.58(6)	105.57(9)
N2-P2-N30/Cl2	102.06(8)	102.18(9)
N2-P1-N1	81.69(8)	81.63(12)
N2-P2-N1	81.64(8)	81.28(12)
P1-N1-P2	97.13(9)	97.76(13)
P1-N2-P2	97.62(8)	98.18(12)

6.3 – Evidence for the existence of an iminopnictenium $[RNPn]^+$ as an intermediate during the ring expansion

The relationship between a dimer and trimer suggests a monomeric unit is likely to be involved in the reaction, which could include a neutral iminopnictine (RNPnX) and/or a cationic iminopnictenium (**6.3**). Beyond the intense colours seen when GaX_3 is added to derivatives of $(RNPnX)_2$ and the low intensity ^{31}P NMR peak associated with iminophosphenium cations (**6.3**P) (R = Dmp, Dipp) seen in chapter 3, further attempts were made to identify monomeric intermediates. While iminopnictines are a possible intermediate in the reaction, their identification would be difficult. With the ring expansion being Lewis acid induced, the identification of iminopnictenium cations (**6.3** or **6.4**) became the focus of attention.

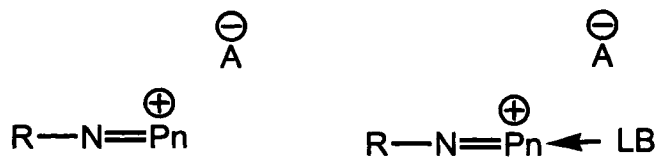

6.3 **6.4**

Isolation of **6.3**$[GaX_4]$ or **6.3**$[Ga_2X_7]$ (R = Dipp, Dmp, Pn = P, As) by adding excess GaX_3 (2 or 4 eq.) to $(RNPnX)_2$ produces uncharacterizable red oils. This is not unexpected as no free iminopnictenium cations (**6.3**) have been isolated in the solid-state, however they are readily coordinated by Lewis bases (LB)[37] to yield base stabilized

iminophosphenium cations (**6.4**). This approach was used in an attempt to identify and isolate monomeric intermediates during the ring expansion.

Identification of **6.2**[$GaCl_4$] provides optimism that derivatives of **6.4** may be seen in solution or the solid-state. The relative stability of Lewis acid/base complexes between the acidic GaX_3/pnictenium cation and basic LB/X^- would dictate if **6.4**[GaX_4] could be identified. Unfortunately, regardless of how or when DMAP was added to reactions of $(RNPX)_2$ and GaX_3, no examples of **6.4**[$GaCl_4$] (R = Dipp, Dmp, LB = DMAP) were observed, which would be expected to have a similar ^{31}P NMR chemical shift to **6.4**[OTf] (LB = DMAP, R = Mes*; δ 132 ppm).[112]

Consequently, other Lewis bases besides DMAP that are known to coordinate iminophophenium cations[69,112-115] were added to the reaction of $(RNPX)_2$ and 2 eq. of GaX_3. In almost all cases, ^{31}P NMR spectra implied the formation of a LB-GaX_3 adduct with the observation of $(RNPX)_2$ or $(RNPX)_3$. In some cases new ^{31}P NMR chemical shifts were observed but they could not be unquestionably identified as a derivative of **6.4**. Any attempts to isolate material from these latter solutions produced uncharacterisable oils or yielded LB-GaX_3, $(RNPX)_2$ or $(RNPX)_3$ in the solid-state. As with the attempted isolation of **6.2**[$GaCl_4$] it appears the Lewis acidity of GaX_3 makes the $[GaX_4]^-$ anion unsuitable to study coordination chemistry at an iminopnictenium centre. Therefore replacement of the $[GaX_4]^-$ (or X^-) with non-Lewis acidic anions was again studied.

Halide abstracting reagents (TMSOTf, $NaBPh_4$, $LiBF_{20}$) were added to reactions of $(RNPnX)_2$ and 2 eq. of GaX_3 in attempts to remove X^- in forming derivatives of **6.3**

(Scheme 6.1). Subsequently Lewis bases were used in attempts to coordinate **6.3**, to yield **6.4** without the labile X^- reverting back to the cationic pnictogen centre.

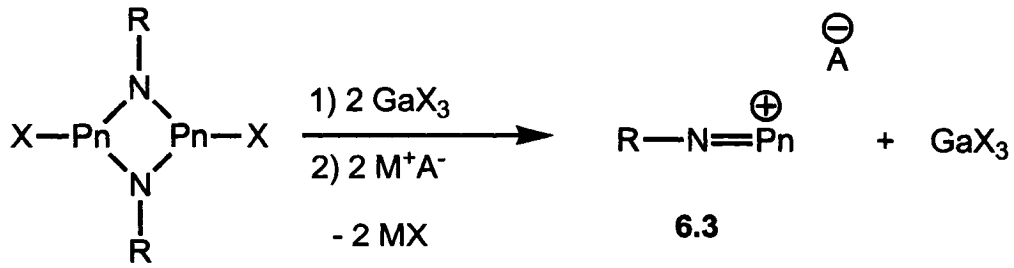

M^+A^- = TMSOTf, $NaBPh_4$, $LiBF_{20}$

Scheme 6.1 – Attempted synthetic routes to derivatives of **6.3**.

Combinations of $(RNPnCl)_2$ (R = Dipp, Dmp; Pn = P, As) with 2 eq. of $GaCl_3$ and TMSOTf or $LiBF_{20}$ were ineffective, producing no discernable changes in the reaction such as the production of TMSCl of LiCl. Subsequent addition of DMAP, did promote Cl^- loss, but rather formation of the DMAP-$GaCl_3$ adduct.

In the case when $(RNPnCl)_2$ (R = Dipp, Dmp; Pn = P) was reacted with 2 eq. of $GaCl_3$ followed by $NaBPh_4$, the reactions immediately changed from red to light yellow and a new precipitate formed, attributed to NaCl. The ^{31}P NMR spectrum where R = Dipp gave two chemical shifts; 197 and 264 ppm assigned to the *cis* and *trans* configurations of $(DippNPPh)_2$ resulting from the phenylation of a phosphenium centre by the $[BPh_4]^-$ anion, which is known for iminophosphenium cations.[116] At this point it is

not possible to determine which of the 4-membered cation **6.1** or the monomeric **6.3** is responsible for the phenyl abstraction, even though no evidence of phenylation reactions have been observed in the preparation of **6.2**[BPh_4].

For reactions of $(DmpNAsCl)_2$ with 2 eq. of $GaCl_3$, and $NaBPh_4$, it was postulated phenyl abstraction may not be as apparent for arsenium cations as the more electrophillic phosphorus analogs. The addition of $NaBPh_4$ to the reaction mixture yielded NaCl as was expected and unlike the phosphorus case, the colour of the reaction remained an intense red, which suggested that an iminoarsenium cation was retained. Filtration of the NaCl from reaction mixture, followed by allowing a concentrated solution to stand at - 30 °C, saw the colour fade to a light red with yellow crystals being deposited. Structural determination identified the new arsino-arsazene (**6.5**) as a major product in the reaction (Scheme 6.2).

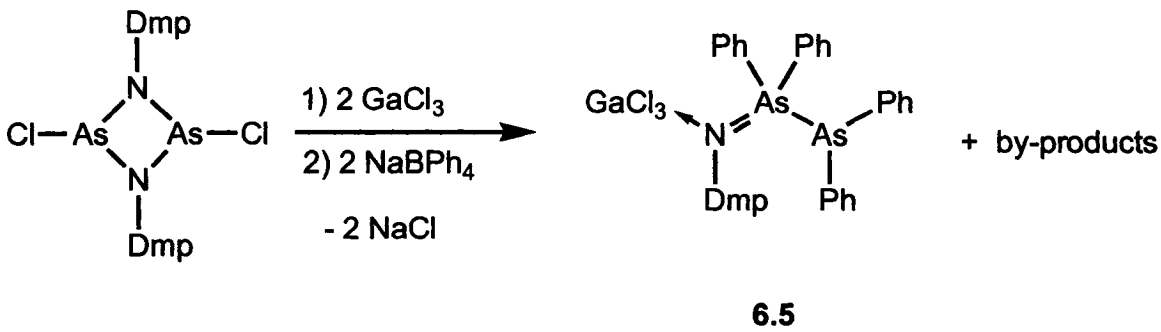

6.5

Scheme 6.2 – Preparation of the arsino-arsazene **6.5**.

As was observed with the phosphorus case, the $[BPh_4]^-$ anion is not stable in the presence of cationic arsenic centres. While the mechanism of the reaction is likely complex, it appears the cyclodiarsazane framework dissociates in the presence of $GaCl_3$, giving an iminoarsenium cation, whose general structure is retained in **6.5**. Another unit of cyclodiarsazane is also completely dissociated, breaking both N-As bonds and an arsenic "atom" is transferred to the iminoarsenium fragment. Phenyl abstraction is also occurring during this process but the point at which phenylation is occurring with respect to the decomposition of the cyclodiarsazane framework is not known. Preparation of **6.5** is also likely to involve the formation of nitrogen-boron compounds a by-products. However it is not possible to write a balanced equation based on the stiochiometry of the reaction. Further NMR studies are needed to determine the structures of the unidentified by-products.

The solid-state structure of **6.5** is shown in Figure 6.4 containing a 4-membered chain with a Ga-N-As-As backbone. The terminal gallium has a tetrahedral geometry while the internal nitrogen is trigonal planer. Terminal arsenic (As2) is trigonal pyramidal, indicating the presence of a lone pair of electrons and is best described as a As(III) centre. The internal arsenic (As1) is tetrahedral and As(V).

The N-As1 bond length (1.797 Å) is typical of nitrogen – arsenic double bonds in an arsazene [*c.f.* 2-MePhNAsPh$_3$; 1.721 Å][117] and significantly shorter than the As-N bonds in $(DmpNAsCl)_2$ [1.838(2) – 1.847(2) Å]. The As1-As2 bond length [2.4789(7) Å] is typical of an As-As single bond [*c.f.* $Ph_2AsAsPh_2$; 2.457 Å].[118]

To date, no molecules containing a N-As-As connectivity have been reported in the literature. The corresponding phosphorus analogues, iminobiphosphines

($RNP(R_2)PR_2$) are known but difficult to prepare due to their instability relative to the bis(phosphino)amines ($R_2PN(R)PR_2$).[119,120]

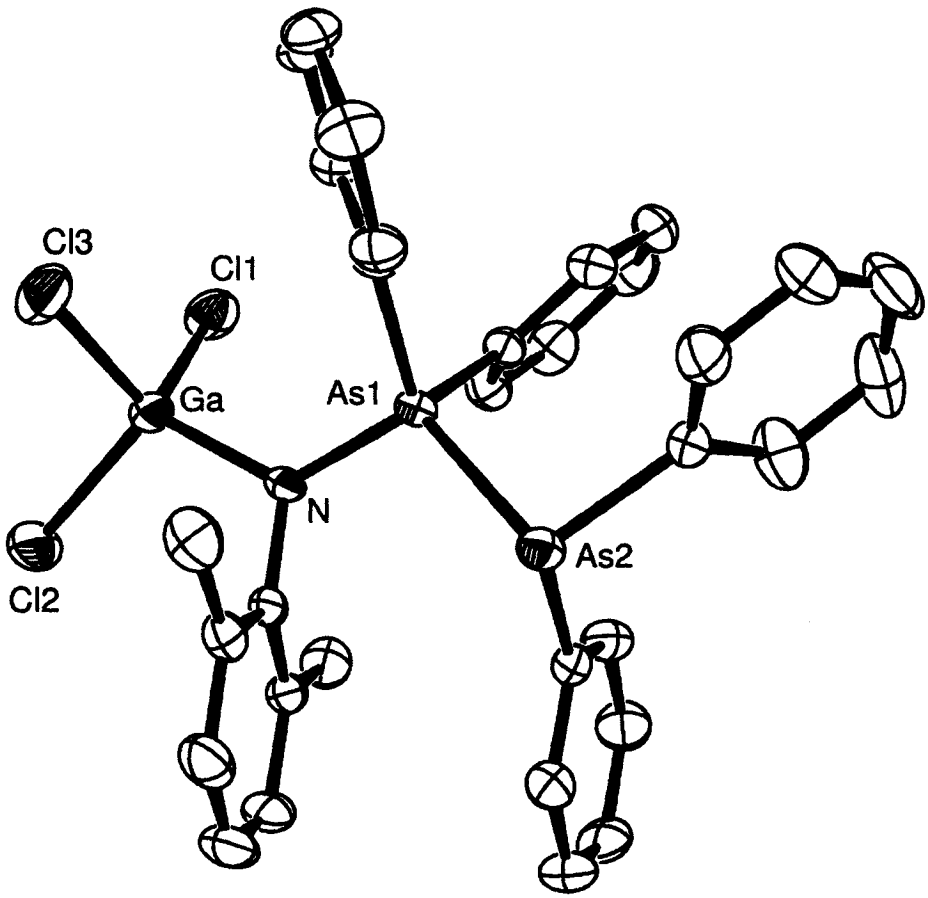

Figure 6.4 – Solid-state structure of **6.5**. Hydrogen atoms omitted for clarity. Thermal ellipsoids are drawn at 50 % probability.

While the synthesis of **6.5** may not have been predicted, it does suggest that a [DmpNAs] unit is formed in solution during the reaction as a consequence of the interaction of $(DmpNAsCl)_2$ and $GaCl_3$. Combined with the intense colouration during the ring expansion reactions and the spectroscopic identification of $[RNP]^+$ (R = Dipp and Dmp) by low temperature ^{31}P NMR, it appears that iminopnictenium cations are intermediates in the ring expansion.

6.4 – Speculation towards the ring expansion mechanism.

It appears the first step in the ring expansion is halide abstraction from $(RNPnX)_2$ (Step A, Scheme 6.3). Subsequent steps could take a variety of pathways and a few possibilities are discussed. **6.1** could undergo two possible fates, association/insertion with another molecule of $(RNPnX)_2$ to yield an 8-membered cationic ring (**6.6**) (step B) or the dissociation of **6.1** to yield a monomeric iminopnictenium (**6.3**) and iminopnictine (step C).

Decomposition of the cationic 8-membered ring **6.6** could occur in one of two ways, giving off neutral or cation species (steps D and E, respectively). In the case of step D, **6.6** would eject an iminopnictenium cation, however the result would be a trimer $(RNPnX)_3$. Since a cyclotriphosphazane has yet to be observed under any conditions by ^{31}P NMR without the addition of DMAP, this pathway seems unlikely.

6.6 could also decompose to eject a iminopnictine, with the formation of the 6-membered cyclic cation **6.7** (step E) which has been isolated from reaction of $(RNPX)_2$ and GaX_3. Ejection of the iminopnictine in this step circumvents the formation of an iminopnictenium cation which evidence suggests is in the reaction. The iminopnictine

could interact with GaX_3 before cycloaddition occurs back to the cyclodipnictazane, which could account for the observation of the iminopnictenium centre in solution.

The other possible outcome from **6.1** is the dissociation to yield the iminopnictenium **6.3**, which could insert into another unit of $(RNPnX)_2$, to yield **6.6**. While steps (A-D-F) and (A-B-C) are the most logical, conclusive evidence towards either pathway is not currently available.

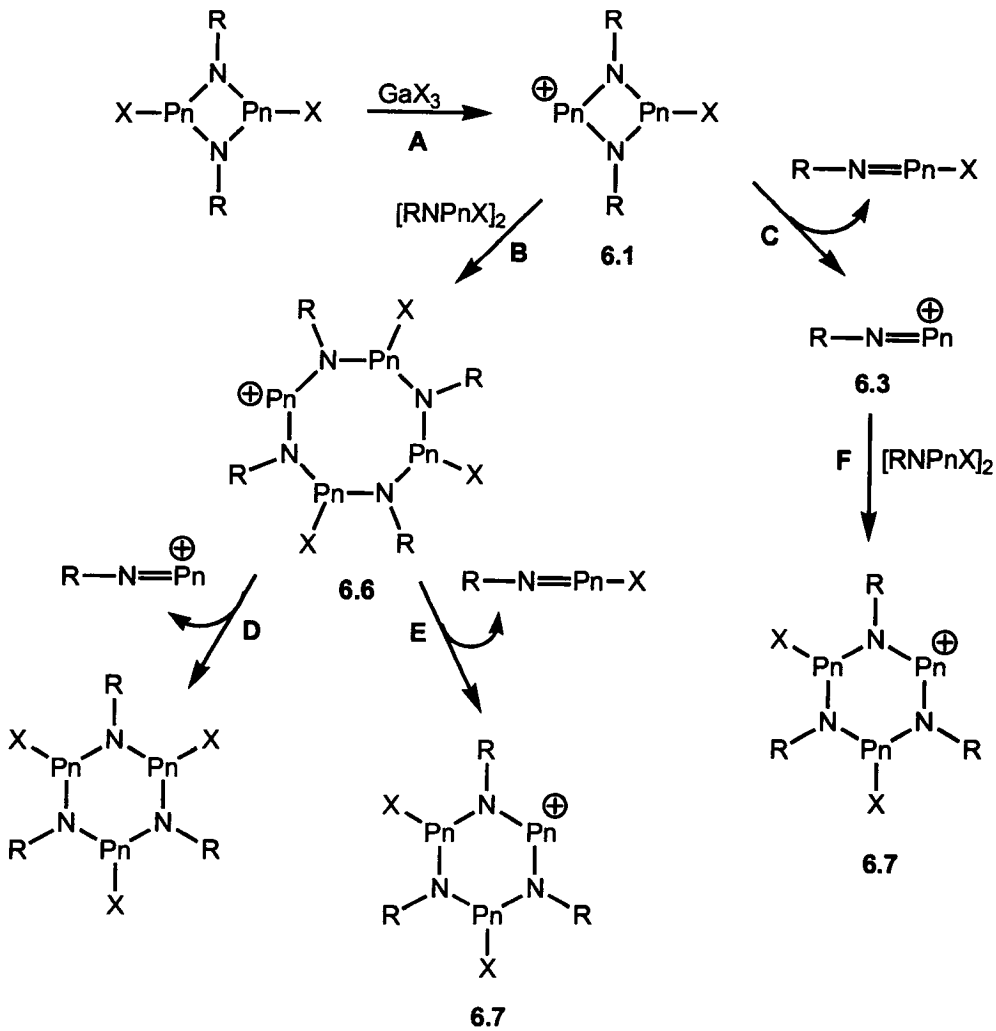

Scheme 6.3 – Potential pathways and intermediates in the ring expansion of dimeric $(RNPX)_2$ to the corresponding trimer $(RPNX)_3$.

Summary

Identification and isolation of intermediates in the ring expansion suggest the first step being the heterolytic cleavage of a P-X bond. Evidence also suggests that cationic, monomeric intermediates are involved in the reaction, however the pathway to their formation is still undetermined.

Chapter 7 - Reactions of $SbCl_3$ with $PhNH_2$, $DmpNH_2$ and $DippNH_2$

7.1 – Introduction

With the generality of the ring expansion shown for the conversion of both cyclodiphosphazanes and cyclodiarsazanes into their corresponding cyclotripnictazanes, extrapolation of the result to antimony derivates would continue to show the general applicability of the reaction. Currently only one example of a cyclodistibazane exists; $(t\text{-BuNSbCl})_2$ prepared from $t\text{-BuNH}_2$ and $SbCl_3$ which is also the only example of a dehydrohalide coupling reaction of a primary amine and SbX_3 to a cyclodistibazane framework.[48] Since no literature reports describing the dehydrohalide coupling of aryl primary amines and SbX_3 have been reported, reactions of $SbCl_3$ and RNH_2 (R = Ph, Dmp, Dipp) following the conditions observed for PCl_3, PBr_3 and $AsCl_3$ were explored in an attempt to prepare the cyclodistibazanes $(RNSbCl)_2$.

7.2 - Preparation of $SbCl_3$ – RNH_2 (R = Dmp, Dipp) coordination complexes

It is well established that reactions involving 2 RNH_2 (R = Dmp, Dipp) and PCl_3 undergo dehydrochloride coupling to yield the aminophosphine $RN(H)PCl_2$ which readily cyclizes to yield the cyclodiphosphazane $(RNPCl)_2$.[8] Similar approaches to synthesize the corresponding aminostibines upon reaction of 2 RNH_2 (R = Dmp, Dipp) and $SbCl_3$ show no evidence of dehydrochloride coupling, as ^1H NMR spectra are qualitatively consistent with the free amine.

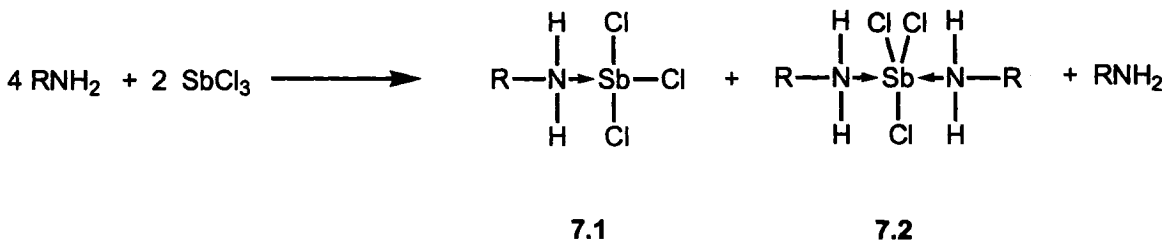

Scheme 7.1 – Formation of mono- and bis-adducts of $SbCl_3$ and RNH_2 (R = Dmp, Dipp).

Mixtures of $DmpNH_2$ with $SbCl_3$ lead to the isolation of a white solid, which upon recrystallization yields a mixture that has been characterized as co-crystallite of the mono- (**7.1**Dmp; Figure 7.1) and bis- (**7.2**Dmp) coordination adducts of the primary amine and antimony trichloride (Scheme 7.1). Similarly, mixtures of $DippNH_2$ and $SbCl_3$ show no evidence of dehydrohalide coupling by ^1H NMR; however **7.2**Dipp has been isolated in the solid-state (Figure 7.2). Structural parameters are shown in Table 7.1 for **7.1**Dmp, **7.2**Dmp, **7.2**Dipp and **7.1**Ph[121] the only previously reported example of a primary amine-stibine adduct.

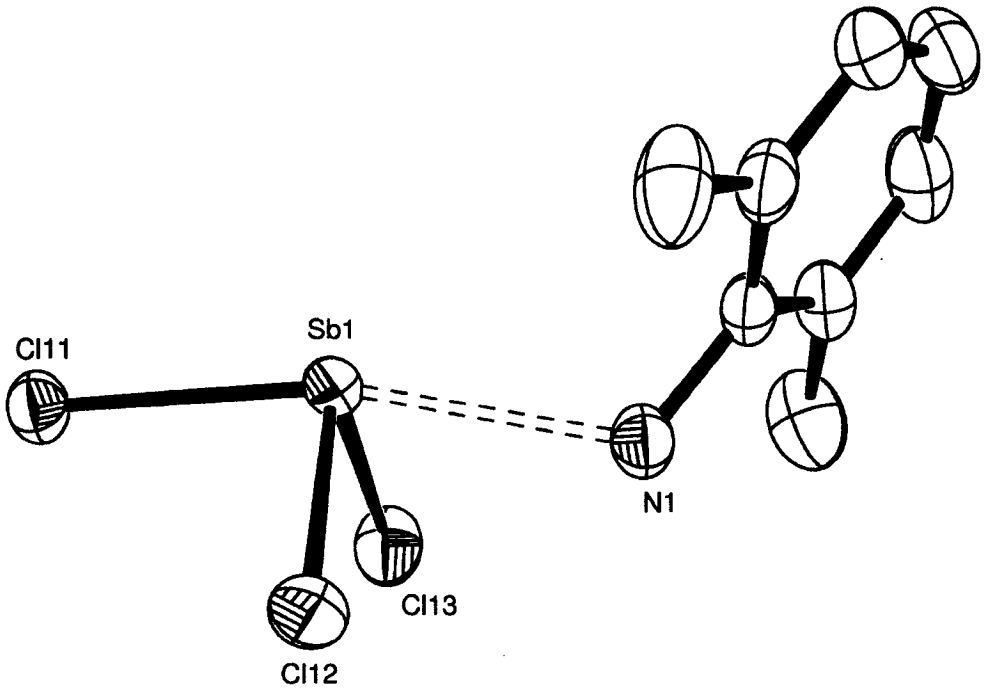

Figure 7.1 – Solid-state structure of **7.1**Dmp. Hydrogen atoms omitted for clarity. Thermal ellipsoids are drawn at 50 % probability.

Structurally, **7.1**Ph and **7.1**Dmp are very similar, adopting a disphenoidal environment around antimony as predicted by VSEPR theory for an AX_4E complex. Dative Sb-N bonds for **7.1**Ph [2.525(44) Å] and **7.2**Dmp [2.596(2) Å] are not significantly different indicating the increased sterics associated with the Dmp over phenyl substituent has no influence on the dative bond. Both structures have longer Sb-Cl bonds in the position *trans* to the dative Sb-N bond compared to the two remaining *cis* Sb-Cl bonds.

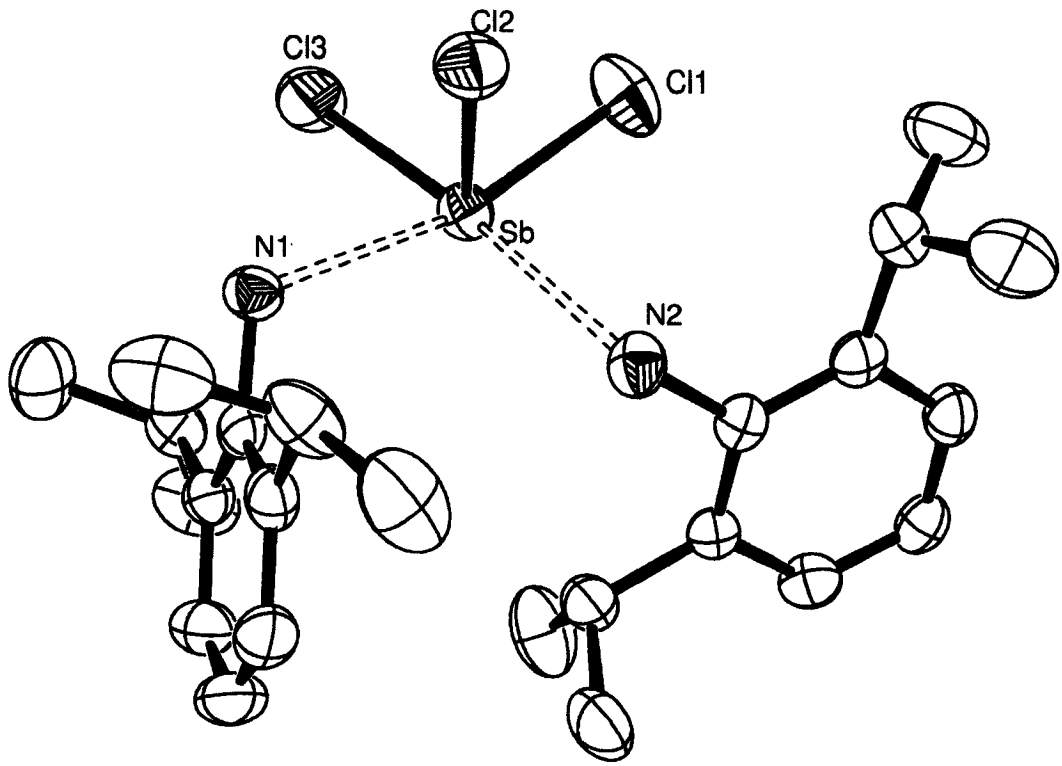

Figure 7.2 – Solid-state structure of **7.2**Dipp. Hydrogen atoms omitted for clarity. Thermal ellipsoids are drawn at 50 % probability.

7.2 Dmp and **7.2**Dipp adopt square pyramidal environments around antimony, typical of AX_5E complexes. The dative N-Sb distances in **7.2**Dmp [2.614(2); 2.799(2) Å] and **7.2**Dipp [2.6906(15); 2.981(10) Å] are longer than those found in **7.1**Ph and **7.1**Dmp due to crowding imposed by the increase in coordination number at antimony. For derivatives of **7.2** the increased steric presence of $DippNH_2$ over $DmpNH_2$ does have an impact on the associated N-Sb bond lengths.

Table 7.1 – Selected bond lengths (Å) for derivatives of **7.1** and **7.2**.

	7.1 Ph	**7.1**Dmp	**7.2**Dmp	**7.2**Dipp
Sb – N1	2.525(44)	2.596(2)	2.614(2)	2.6906(15)
Sb – N2	-	-	2.799(2)	2.981(10)
Sb – Cl1	2.516(16)	2.4711(6)	2.4519(6)	2.4256(6)
Sb – Cl2	2.323(14)	2.3813(6)	2.4419(6)	2.3804(5)
Sb – Cl3	2.335(18)	2.3581(6)	2.3836(6)	2.3701(5)

7.3 – Reactions of $SbCl_3$ and RNH_2 in the presence of NEt_3

For the case of Pn = P or As, addition of RNH_2 (R = Ph, Dmp or Dipp) to a mixture of $PnCl_3$ and excess NEt_3 proceeds directly to the formation of the corresponding cyclodipnictazane. Addition of RNH_2 (R = Ph, Dmp and Dipp) to combinations of $SbCl_3$ and NEt_3 yields different results depending on choice of R group.

In the case of R = Dipp, under typical reaction and work-up conditions, all observable products by ^1H NMR spectroscopy are consistent with the coordination adduct **7.2**Dipp and provides no evidence of dehydrohalide coupling.

When R = Dmp, the ^1H NMR spectrum show chemical shifts consistent with free $DmpNH_2$/coordination adducts, however new peaks are also seen in the spectrum. Notable are new peaks associated with the ortho-methyl groups of the Dmp substituents which are more shielded than those from the free amine/coordination adducts (2.50 – 2.80 ppm, *c.f.* $DmpNH_2$; 2.16 ppm). Assignment of the new peaks was not possible at that point; however after work up, two crystalline materials were isolated; clear colourless block crystals and a few yellow crystals.

In the region of 2.5 – 2.8 ppm, the ^{1}H NMR spectrum of the colourless crystals showed at 1:2:1:2 pattern, typical for ortho-methyl groups of the Dmp substituents in *cis, trans* cyclotripnictazanes. X-Ray crystallography confirmed the composition of the crystals to be $(DmpNSbCl)_3$, while the yellow crystals were identified as the acyclic distibazane **7.3** (Scheme 7.2).

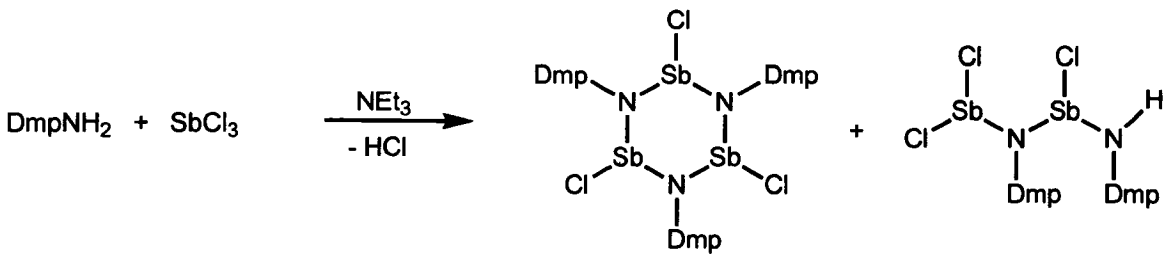

7.3

Scheme 7.2 – Isolated products form the dehydrohalide coupling of $DmpNH_2$ and $SbCl_3$ in the presence of NEt_3.

The solid-state structure of $(DmpNSbCl)_3$ is disordered at the Sb3 position as a 50:50 mixture of envelope and boat conformers (Figure 7.3). The chlorine substituents adopt a *cis, trans* configuration reminiscent of the phosphorus and arsenic analogues confirming the assignment by ^{1}H NMR spectroscopy. In the boat conformer a complete *cis, trans* configuration is not observed as the chlorine substituents at Sb1 and Sb2 are *trans* and ~ 180° to each other, however the Sb3b-Cl3b bond is ~ 90° to both Sb1-Cl1 and Sb2-Cl2 bonds.

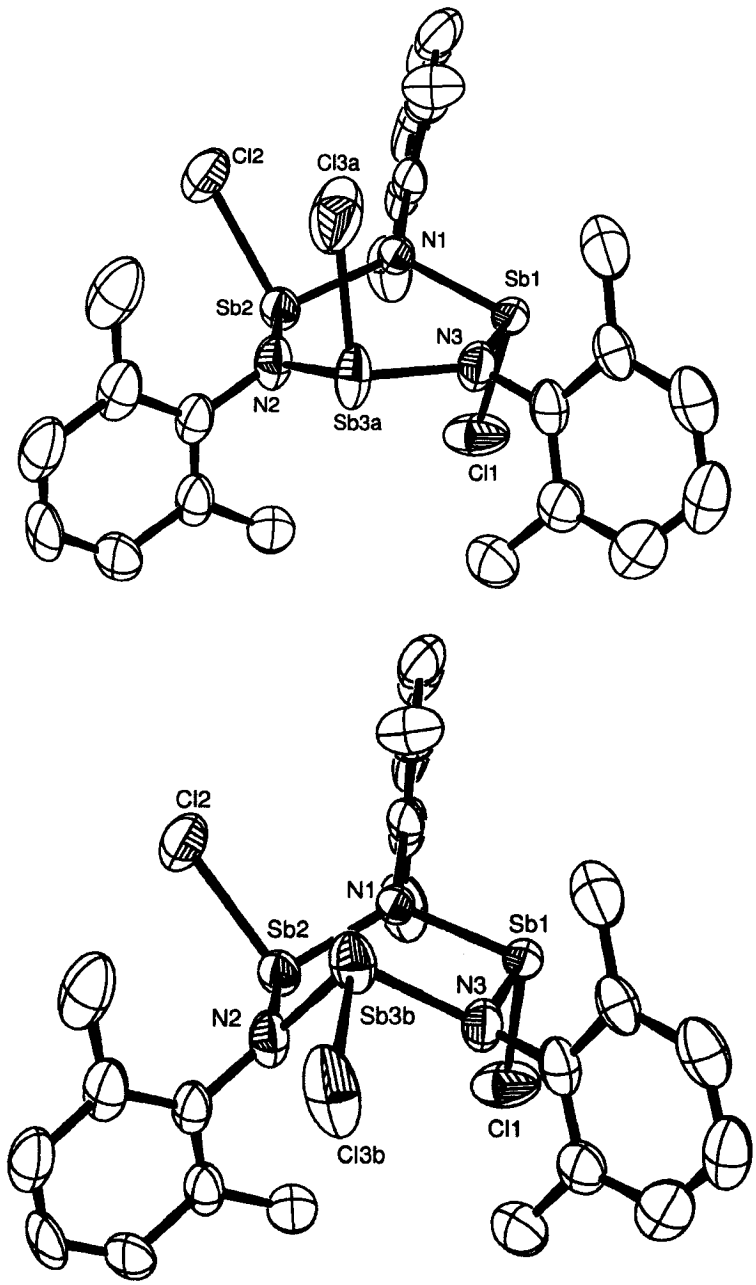

Figure 7.3: Solid-state structures of both envelope (top) and boat (bottom) conformers of $(DmpNSbCl)_3$. Hydrogen atoms omitted for clarity. Thermal ellipsoids are drawn to 50 % probability.

Structural parameters for $(DmpNSbCl)_3$ (envelope conformer only) and the corresponding phosphorus and arsenic derivatives are listed in Table 7.2. In comparison, no unexpected trends are observed as the size of the pnictogen is increased from phosphorus to antimony. As would be expected, the Sb-E bonds (E = N, Cl) are longer than the corresponding P-E and As-E bonds. Also as expected, the endocyclic N-Pn-N angles within the ring become smaller, followed by an increase in the Pn-N-Pn angles as the size of the pnictogen increases. This is expected as the hybridization of the valence orbitals become less pronounced for the heavier elements.

Table 7.2 – Select bond lengths (Å) and angles (°) for $(DmpNPnCl)_3$ (Pn = P, As, Sb).

Parameter	$(DmpNPCl)_3$	$(DmpNAsCl)_3$	$(DmpNSbCl)_3$
N1-Pn1	1.704(2)	1.834(3)	2.035(7)
N3-Pn1	1.693(2)	1.836(3)	2.020(8)
N1-Pn2	1.687(2)	1.846(3)	2.030(7)
N2-Pn2	1.717(2)	1.826(3)	2.012(8)
N2-Pn3	1.694(2)	1.828(3)	2.011(8)
N3-Pn3	1.703(2)	1.829(3)	2.017(8)
Pn1-Cl1	2.104(1)	2.255(1)	2.403(3)
Pn2-Cl2	2.116(1)	2.245(1)	2.390(3)
Pn3-Cl3	2.136(1)	2.232(1)	2.364(7)
N-Pn1-N	101.7(1)	100.2(1)	94.7(3)
N-Pn2-N	100.1(1)	98.5(2)	93.4(3)
N-Pn3-N	101.8(1)	100.7(1)	97.1(3)
Pn-N1-Pn	132.0(1)	134.0(2)	127.3(3)
Pn-N2-Pn	134.5(1)	131.9(2)	139.2(4)
Pn-N3-Pn	131.8(1)	128.6(2)	135.6(4)
Σ° at N1	360.0(1)	354.7(3)	352.6(5)
Σ° at N2	358.1(1)	359.9(2)	359.6(6)
Σ° at N3	359.6(2)	360.0(2)	360.0(6)
Σ° at Pn1	307.5(1)	300.2(1)	288.1(3)
Σ° at Pn2	305.5(1)	299.1(1)	287.5(3)
Σ° at Pn3	303.9(1)	300.3(1)	288.0(3)

The open chain distibazane **7.3** is only observed as a small amount of crystals that can be manually separated from $(DmpNSbCl)_3$ and represents the first known example of an extended pnictazane chain. The alternating N-Sb backbone of **7.3** is terminated by two Sb-Cl bonds and an N-H bond, but a close intra-molecular interaction occurs between these sites (N1 to Sb2) imposing a cyclic conformation that is reminiscent of the cyclodipnictazanes $(DmpNPnCl)_2$ (Pn = P, As). The N2-Sb bonds in **7.3** [2.023(2) – 2.039(2) Å] are comparable to those in the aminated cyclodistibazane $(DmpNSbN(H)Dmp)_2$ [2.033(4); 2.057(4) Å][53] and cyclotristibazane $(DmpNSbCl)_3$ [2.011(8) – 2.035(7) Å]. The N1-Sb bonds are significantly longer than those for N2-Sb, with the coordinative N1-Sb2 being the longest at 2.521(2) Å and comparable to the coordinative bonds found in derivatives of **7.1** and **7.2**. The slight increase in the Sb1-N1 bond length is also observed [2.108(2) Å] and is a consequence of the coordinative N1-Sb2 bond.

Samples of **7.3** appear to be only kinetically stable and decay slowly in solution preventing attempts to purify bulk samples for comprehensive spectroscopic characterization or to access further reactivity.

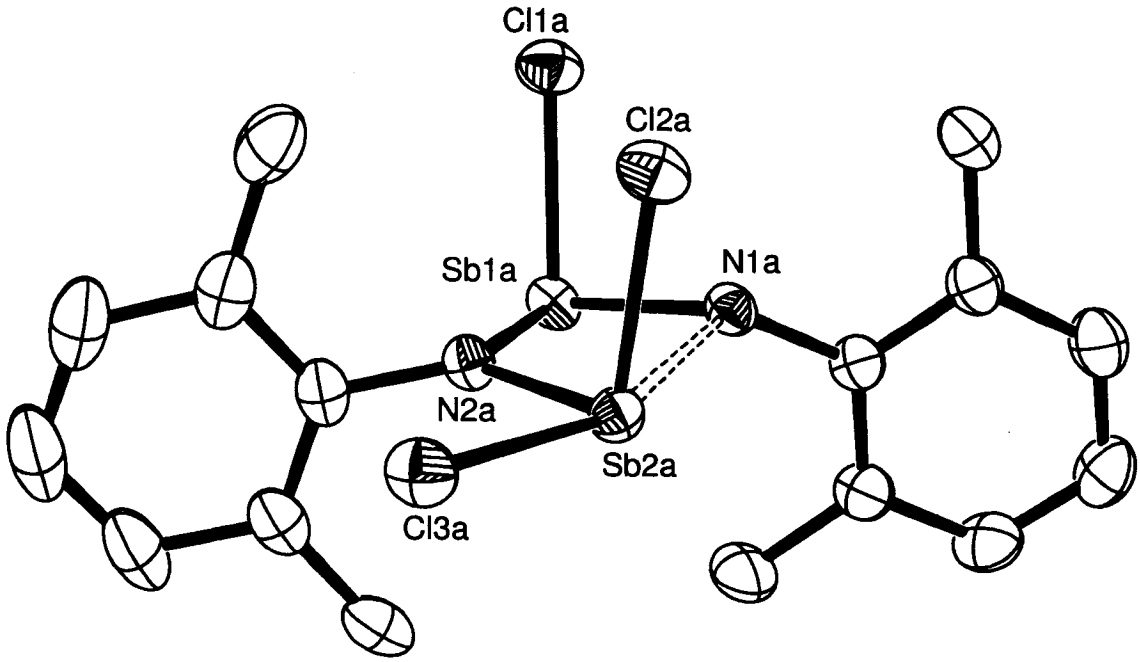

Figure 7.4: Solid-state structure of **7.3**. Hydrogen atoms omitted for clarity. Thermal ellipsoids drawn at 50 % probability.

While coordination adducts of $PhNH_2$ and $SbCl_3$ have been observed, no dehydrohalide coupling products have been identified in the literature, which is surprising considering the first cyclodiphosphazane $(PhNPCl)_2$ derived from $PhNH_2$ and PCl_3 was identified over 100 hundred years ago.[40] Reactions of $PhNH_2$ and $SbCl_3$ in the presence of NEt_3 yield a microcrystalline yellow solid after workup. ^1H NMR spectrum indicates the complete loss of $-NH_2$ protons, suggesting complete dehydrohalide coupling to a cyclic oligomer $(PhNSbCl)_n$ or a cage structure and precludes the possibility of a linear stibazane or aminated cyclodistibizane. In the regions associated with phenyl protons, the ^1H NMR spectrum shows a pattern that is more complicated than free $PhNH_2$ or

$(PhNPCl)_2$, and suggests multiple phenyl environments, which could be attributed to a *cis, trans* cyclotristibazane. Comparison to the previously observed $(DmpNSbCl)_3$ is not possible as phenyl protons in that case (and all other cyclotripnictazanes prepared) overlap and showing no readily distinguishable features. Direct comparison to $(PhNPnX)_3$ would be suitable however no such examples are known.

Electron ionization mass spectrometry of the yellow solid identified the cation $[PhNSb]^+$ and radical cation $[Ph_2N_2Sb]^{+\cdot}$, however at this point it is not possible to conclude the molecular source of these cations. No fragments were identified that could be attributed to molecules containing more than 3 antimony atoms, however the detection limit (maximum m/z^+ values) of the EI-MS spectrometer could not be tuned to include the molecular ion of $(PhNSbCl)_3$ (741 g/mol). Also considering the destructive nature of electron ionization methods, it is not surprising no fragments were seen that may be attributed to the cyclotristibazane $(PhNSbCl)_3$. Further studies using MALDI-TOF MS and crystallography will hopefully identify the nature of the oligomer $(PhNSbCl)_n$ or cage structure.

7.4 – Mechanistic insight into the dehydrohalide coupling of primary amines and tri-chloropnictines

Descending down the group, pnictogen – halide bonds are less prone towards substitution by amines in dehydrohalide coupling reactions as indicated by the decreased number of reports for antimony and bismuth. Subsequently, the kinetics associated with Pn-Cl bond cleavage reactions become slower for the heavier elements, which can be

exploited to isolate intermediates or products from different reaction pathways in the dehydrohalide coupling process.

Scheme 7.3 outlines the potential outcomes for association of a primary amine and PnX_3. The coordination of a primary amine to $PnCl_3$ (**7.4**) is likely the first step in the dehydrohalide coupling reaction towards pnictazanes. Coordination adducts between neutral tertiary amines and PX_3 are known,[122] however the reactivity of PCl_3 and $AsCl_3$ in the presences of primary amines prevents the isolation of **7.4**P or **7.4**As. Due to the increased Lewis acidity of $SbCl_3$ it appears the adduct **7.4**Sb is more thermodynamically stable with respect to HCl elimination than the corresponding phosphorus and arsenic analogues.

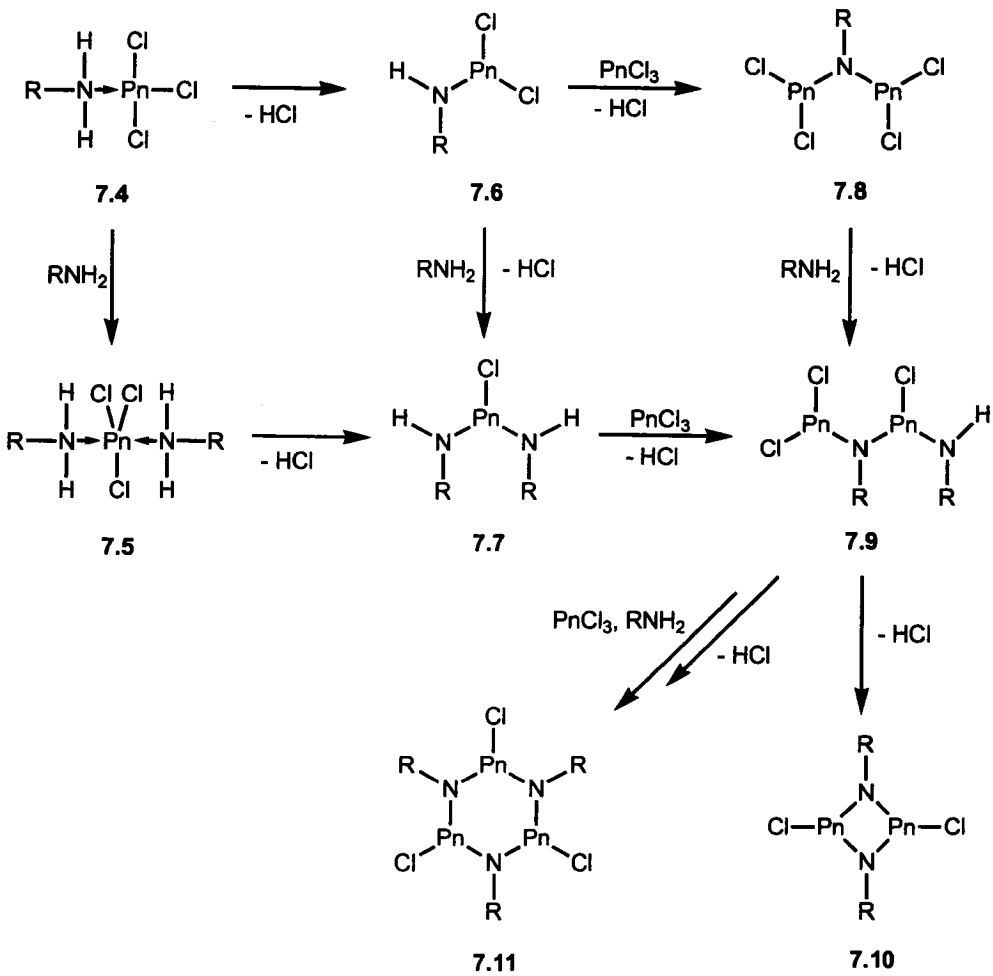

Scheme 7.3 – Potential outcomes for the association of RNH_2 and $PnCl_3$.

Compounds **7.4** and **7.5** represent kinetically stable adducts and the introduction of NEt_3 as a stronger Bronsted base than $DmpNH_2$, effects deprotonation of the adduct securing the N-Sb bond with subsequent chloride loss to **7.6** or **7.7**. Secondary processes could include further association of $PnCl_3$ with **7.6** or **7.7** to extend the chain to **7.8** or **7.9**. Alternatively, dehydrochloride coupling of two molecules of **7.6** provides access to **7.9**.

Isolation of **7.9** is rather unique considering the preference for reactions containing primary amines and $PnCl_3$ (Pn = P, As) to yield a cyclodipnictazane framework. Consider the conformation of **7.9**Sb/**7.3** as pseudo 4-membered ring, this suggests that for **7.9**P and **7.9**As the rapid intramolecular cyclization to **7.10**P and **7.10**As has a very low activation barrier, which is the reason kinetically stable cyclodiphosphazanes and cyclodiarsazanes are observed under these conditions. For the case of **7.9**Sb/**7.3** it appears the activation barrier yielding the cyclization product **7.10**Sb is larger than for phosphorus and arsenic, allowing intermolecular reactions with a further unit of **7.6**Sb or (RNH_2 and $SbCl_3$) to occur, providing a pathway to the thermodynamically favorable cyclotristibazane **7.11**Sb.

Summary

While access to cyclodiphosphazanes and cyclodiarsazanes through dehydrohalide coupling has proven to be a valuable synthetic method, access to the corresponding cyclodistibazanes has proven challenging. The resistance of the Sb-Cl towards dehydrohalide coupling alters the reaction pathway allowing the isolation of amine-$SbCl_3$ adducts en-route to the thermodynamically more favorable cyclotristibazane. A unique acyclic distibadiazane has also been identified in the reaction providing insight into the key pathways towards kinetic and thermodynamic products in the coupling of amines and pnictogen trihalides.

Chapter 8 – Conclusion and Future Work

8.1 – Conclusion

Kinetically stable cyclodipnictazanes $(RNPnX)_2$ (R = Dmp, Dipp; Pn = P, As; X = Cl, Br) can be prepared from the dehydrohalide coupling reaction of RNH_2 and PnX_3 in the presence of triethylamine. Their formation is a consequence of the rapid intramolecular cyclization reaction that occurs after a 4-membered dipnictidiazane chain is formed, which has been isolated for the case of Pn = Sb. Similar dehydrohalide coupling reactions between RNH_2 and $SbCl_3$ show that the kinetic barrier towards more thermodynamically favoured cyclotristibazanes is lower than for the phosphorus or arsenic analogues, which are not observed in the corresponding dehydrohalide coupling reactions.

The cyclodipnictazanes $(RNPnX)_2$ (R = Dmp, Dipp; Pn = P, As; X = Cl, Br) are readily transformed to their corresponding cyclotripnictazanes by a Lewis acid induced heterocyclic disproportionation, which occurs through cationic 4- and 6-membered pnictazane rings, containing di-coordinate pnictenium centres. The thermodynamic preference for the cyclotripnictazanes is a consequence of substituent steric strain and ring flexibility. The dimer to trimer relationship formally requires a monomeric intermediate and the process is viewed as the first step in an inorganic oligomerization reaction that draws similarities to the polymerization of ethylene.

8.2 – Future Work

Diversification of cyclic pnictazane chemistry to include examples of $(RNPnCl)_n$ (Pn = Sb, Bi; n = 2, 3), including the extrapolation of the Lewis acid induced ring expansion to stibazane and bismuthane chemistry would be the next progression of this research project. The key challenge would be the preparation of $(RNPnCl)_2$, (R = Dmp and Dipp). Transamination reactions of primary amines with $Sb(NMe_2)_3$ have already been used to prepare the bis(amino)cyclodistibazanes $(RNSbNMe_2)_2$ {R = Dipp,[54] 2-pyridyl(Me-4),[55] $C_6H_2(OMe)_3$-3,4,5[55]; Scheme 8.1 – Step 1}, which would be a starting point for preparation of the $(RNSbCl)_2$.

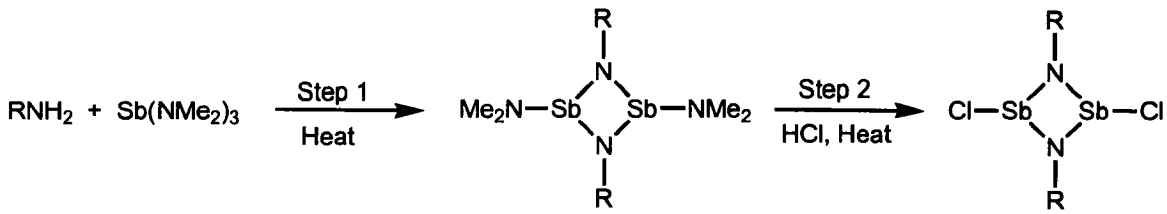

Scheme 8.1 – Transamination followed by amine/halide exchange to cyclodistibazanes

Preliminary evidence has shown that step 1 proceeds with $DmpNH_2$ to yield $(RNSbNMe_2)_2$, while both derivatives (R = Dmp and Dmp) react with HCl to give the cyclodistibazanes $(RNSbCl)_2$ (Scheme 8.1 – Step 2). With the transamination reactions likely having lower activation barriers than the corresponding dehydrohalide coupling reactions, the reaction proceeds more readily to the kinetically stable dimer rather the

thermodynamically stable trimer. The cyclotristibazane $(DmpNSbCl)_3$ has been isolated and identified from reaction outlined in scheme 8.1, however it appears to be only a minor product and the consequence of solubility issues with the product assigned to $(DmpNSbCl)_2$.

Extrapolation of the transamination reactions with $Sb(NMe_2)_3$, to the bismuth analogue $Bi(NMe_2)_3$ would be the next step in an attempt to prepare the cyclodibismuthane $(RNBiCl)_2$. Lewis acid induced ring expansion of both antimony and bismuth cyclodipnictazanes would be the final goal to show the general application of the reaction to all of the cyclodipnictazanes (Pn = P – Bi).

Chapter 9 – Experimental

9.1 - General information

All manipulations were carried out under oxygen- and moisture-free conditions using standard high vacuum,[123] Schlenk,[124] or dry box techniques. All solvents were dried using standard drying reagents[125] or by being degassed with nitrogen, prior to being passed through a solvent purification system. Propylamine, aniline, 2,6-dimethylphenylaniline, 2,6-diisopropylaniline, gallium trichloride, gallium tribromide, methyltrifluoromethylsulfonate, lithium tetrakispentafluorophenylborate, sodium tetraphenylborate were all used as received. Phosphorus trichloride, phosphorus tribromide and arsenic trichloride were distilled, while antimony trichloride was sublimed prior to use. Methylamine hydrochloride and ethylamine hydrochloride were recrystallized from methanol then pumped before use. 4-dimethylaminopyridine and ammonium chloride were pumped on prior to use. Triethylamine was purified by fractional distillation from potassium hydroxide and calcium hydride. $(DippNPCl)_2$[8] and $(DmpNPN(H)Dmp)_2$[87] were prepared as previously reported. Solvent volumes in reaction mixtures are approximate.

Infrared spectra were recorded as Nujol mulls on CsI plates using a Bruker Vector 22 FT-IR and are presented as wavenumber (cm-1) maxima with ranked intensity for each absorption given in parentheses and the most intense peak given a ranking of 1. Melting points were obtained using an Electro-thermal apparatus. Elemental analyses were performed by Desert Analytics, Tuscon, AZ; Guelph Chemical Company, Guelph, ON; Canadian Microanalytics, Vancouver, BC. Samples for analysis by solution NMR

spectroscopy were either flame-sealed or capped with a septa and parafilmed. Solution ^{1}H and ^{31}P NMR spectra were obtained at room temperature on a Bruker AC-250 NMR spectrometer. Chemical shifts are reported in ppm relative to a reference standard [$SiMe_4$ (^{1}H) and 85% H_3PO_4 (^{31}P)], with ^{1}H spectra calibrated to an internal reference signal ($CHDCl_2$, 5.32 ppm; $CHCl_3$, 7.26 ppm). X-Ray diffraction data were obtained on a Bruker PLATFORM diffractometer with a sealed tube generator and a SMART 1000 CCD detector using graphite-monochromated Mo-Kα (λ=0.71073) radiation on samples cooled to 193(2)K. The structures were solved by direct methods and refined by full-matrix least squares. Unit cell parameters were obtained from the refinement of the setting angles of reflections from the data collection. The choice of space groups was based on systematically absent reflections and was confirmed by the successful solution and refinement of the structures. Inert atmosphere MALDI analyses were performed on a Bruker Daltronics OmniFlex® MALDI TOF spectrometer equipped with a nitrogen laser (337 nm), and interfaced to an Mbraun LabMaster® 130 glovebox. Data were collected in positive reflectron mode, with accelerating voltage held at 20 kV for all experiments. Matrix (pyrene or anthracene) and analyte solutions were prepared in CH2Cl2 at concentrations of 25 mg/mL and 1 mg/mL respectively; samples were mixed in a matrix:analyte ratio of 20:1.

9.2 – Preparation/isolation procedures and characterization data

General for $(RNPnX)_2$: PnX_3 and NEt_3 were combined in benzene at 0°C and RNH_2 was added (15 minutes). The mixture was warmed to room temperature and stirred for 18 hrs giving a precipitate, which was filtered and washed twice with benzene (100 ml). Removal of the solvent from the combined filtrates under reduced pressure gave a pale orange solid, which was washed with pentane (10 – 50 ml) to leave a white powder, which in all case was suitable for further reactions. Purification for analytical and crystallography studies are specified below.

$(DmpNPCl)_2$: PCl_3 (10 ml, 120 mmol) and NEt_3 (33 ml, 460 mmol), $DmpNH_2$ (14 ml, 120 mmol), benzene (500 ml)

Purification: Re-crystallization from minimal toluene at - 30°C. Plate-shaped, X-ray quality crystals were grown by allowing a portion of the first filtrate to stand at room temperature for one week.

Yield: 8.0 g, 22 mmol, 38 %

Mp: 119 - 123 °C

$^{31}P\{^1H\}$ NMR (CD_2Cl_2): δ 211 ppm

^1H NMR (CD_2Cl_2): δ 2.69 ppm (s), 7.12ppm (s)

IR (cm^{-1}): 414(5), 463(7), 505(6), 533(10), 561(12), 580(18), 615(20), 740(13), 775(3), 895(1), 920(4), 976(14), 983(15), 1032(16), 1074(17), 1097(9), 1167(11), 1209(2), 1262(8), 1283(10)

EA: Calculated for $C_{16}H_{18}N_2P_2Cl_2$ (Found): C 51.77 (50.85), H 4.89 (5.03), N 7.55 (7.14)

Crystal data: $C_{16}H_{18}Cl_2N_2P_2$, M = 371.16 g Mol^{-1}, Monoclinic, $P2_1/n$, a = 11.2850(7) Å, b = 11.2343(7) Å, c = 14.3926(8) Å, β = 105.6520(10) °, V = 1757.02(18) $Å^3$, T = 193(2) K, Z = 4, μ(MoK_α) 0.71073 (Å), Reflections; 3564 unique, 3198 observed R (for 3198 reflections with (I > 2σ(I)) = 0.0587; wR(all) = 0.1391

(DmpNPBr)$_2$: PBr_3 (4.0 ml, 42 mmol) and NEt_3 (9.1 ml, 130 mmol), $DmpNH_2$ (5.20 ml, 42 mmol), benzene (80 ml)

Purification: Re-crystallization from minimal toluene at - 30°C. Rod-shaped, X-ray quality crystals were grown by allowing a portion of the first filtrate to stand at room temperature for one week.

Yield: 2.0 g, 4.4 mmol, 21 %

Mp: 226 - 230 °C

$^{31}P\{^1H\}$ NMR (CD_2Cl_2): δ 231 ppm

^1H NMR (CD_2Cl_2): δ 2.74 ppm (s); 7.13ppm (s)

IR (cm^{-1}): 410(8), 440(1), 496(4), 530(5), 559(13), 586(17), 670(20), 740(15), 770(2), 889(3), 920(7), 977(14), 1033(16), 1099(10), 1167(11), 1207(6), 1247(19), 1261(9), 1287(12), 1581(18)

EA: Calculated for $C_{16}H_{18}N_2P_2Br_2$ (Found): C 41.77 (42.64), H 3.94 (4.38), N 6.09 (6.22)

Crystal data: $C_{16}H_{18}Br_2N_2P_2$, M = 460.08 g Mol^{-1}, Monoclinic, $P2_1/c$, a = 15.7724(16) Å, b = 11.5131(12) Å, c = 20.513(2) Å, β = 104.628(2) °, V = 3604.3(6) $Å^3$, T = 193(2) K, Z = 8, μ(MoK_α) 0.71073 (Å), Reflections; 7334 unique, 5374 observed R (for 5374 reflections with (I > 2σ(I)) = 0.0346; wR(all) = 0.0780

$(DmpNAsCl)_2$: $DmpNH_2$ (4.4 ml, 36 mmol), $AsCl_3$ (3.0 ml, 36 mmol), NEt_3 (10 ml, 69 mmol), benzene (300 ml);

Purificaiton: Vapour diffusion of pentane into a CH_2Cl_2 solution yielding rod-shaped crystals

Yield 1.7 g, 3.7 mmol, 21 %

Mp: 207 - 209 °C

NMR ^1H ($CDCl_3$): 2.76 (s), 7.12 (m)

IR (cm^{-1}): 489(11), 521(5) 699(4), 774(3), 810(1), 882(6), 914(15), 974(12), 1030(10), 1096(7), 1166(9), 1203(2), 1256(8), 1535(14), 1587(13), 1624(20), 1748(19), 1867(18), 1944(17)

EA: Calculated for $C_{16}H_{18}N_2As_2Cl_2$ (Found): C 41.86 (42.89), H 3.95 (4.78), N 6.10 (6.11)

Crystal data: $C_{16}H_{18}As_2Cl_2N_2$, M = 459.06 g Mol^{-1}, Monoclinic, $P2_1/c$, a = 15.5906(9) Å, b = 11.4246(7) Å, c = 20.7190(12) Å, β = 104.2500(10) °, V = 3576.8(4) $Å^3$, T = 193(2) K, Z = 8, $\mu(MoK_\alpha)$ 0.71073 (Å), Reflections; 7289 unique, 6055 observed R (for 6055 reflections with $(I > 2\sigma(I)) = 0.0261$; wR(all) = 0.0690

$(DippNAsCl)_2$: $DippNH_2$ (6.7 ml, 36 mmol), $AsCl_3$ (3.00 ml, 36 mmol), NEt_3 (13 ml, 90 mmol), benzene (300 ml)

Purification: Slow solvent removal of toluene yielded plate-shaped crystals which were washed with toluene.

Yield: 3.4 g, 5.9 mmol, 34%

Mp: 231 - 234 °C

NMR ^{1}H ($CDCl_3$): 1.345 (d), 4.08 (m), 7.28 (s)

IR (cm^{-1}): 329(4), 354(2), 419(11), 455(15), 517(13), 702(19), 715(13), 788(1), 828(6), 873(9), 893(12), 933(17), 1041(18), 1055(14), 1101(8), 1191(3), 1241(7), 1316(5), 1384(10), 1578(20)

EA: Calculated for $C_{24}H_{34}N_2As_2Cl_2$ (Found): C 50.46 (50.36), H 6.00 (5.75), N 4.90 (5.06)

Crystal data: $C_{24}H_{34}As_2Cl_2N_2.2C_6H_6$, M = 727.49 g Mol^{-1}, Orthorhombic, Pnma, a = 22.8454(16) Å, b = 10.2167(7) Å, c = 15.6139(11) Å, V = 3663.0(14) $Å^3$, T = 193(2) K, Z = 4, $\mu(MoK_\alpha)$ 0.71073 (Å), Reflections; 3983 unique, 3316 observed R (for 3316 reflections with ($I > 2\sigma(I)$) = 0.0248; wR(all) = 0.0652

$H_2NP[\mu\text{-}DmpN]_2PCl$ (2.4): (0.50 g, 1.4 mmol) was added to NH_4Cl (0.29 g, 5.4 mmol) and dissolved in 10ml of benzene, to which 1ml of NEt_3 was added. After stirring for 18hrs at room temperature, the reaction mixture was filtered and solvent was removed under vacuum. The remaining white solid was taken up in minimal amount of toluene, concentrated by 10-15 % and a left at -30° for 2 days yielding colourless rod-shaped crystals.

Yield: (crude) 0.16 g, 0.46 mmol, 34%

Mp: 125 – 127 ° C

$^{31}P\{^{1}H\}$ NMR ($CDCl_3$): δ 144 ppm (d), 193 ppm (d), $^{2}J_{PP}$ = 44.6 Hz

Crystal data: $C_{16}H_{20}ClN_3P_2$, M = 357.74 g Mol^{-1}, Monoclinic, $P2_1/n$, a = 9.2189(6) Å, b = 16.7393(10) Å, c = 11.9119(7) Å, β = 92.2950(10) °, V = 1781.88(19) $Å^3$, T = 193(2) K,

Z = 4, $\mu(MoK_\alpha)$ 0.71073 (Å), Reflections; 3645 unique, 3247 observed R (for 3247 reflections with $(I > 2\sigma(I)) = 0.0349$; wR(all) = 0.1018

Typical Rxns of RNH_2 or RNH_3Cl with $[DmpNPCl]_2$: As general example, 0.50 g (1.4 mmol) of $(DmpNPCl)_2$ was dissolved in 10 ml of benzene and 0.40 ml of NEt_3 to which 0.43 g (5.4 mmol) of $EtNH_3Cl$ was added. The slurry was stirred at room temperature for 18hours, at which time the reaction was filtered. Removal of solvent under vacuum yielded an oily froth, which upon addition of 1 ml pentane precipitated into a white powder, which remained after removal of the pentane under vacuum.

General for $[R_3N_3As_3Cl_2][GaCl_4]$ (4.1[$GaCl_4$]): $(RNAsCl)_2$ and $GaCl_3$ were combined and dissolved in CH_2Cl_2 (~2 ml), immediately forming a dark red solution, which faded to light orange after hours. Vapour diffusion of pentane into CH_2Cl_2 gave orange plate crystals.

$[Dmp_3N_3As_3Cl_2][GaCl_4]$ (4.1Dmp [$GaCl_4$]): $(DmpNAsCl)_2$ (0.20 g, 4.4 mmol), $GaCl_3$ (0.052 g, 0.30 mmol)

Yield 0.12 g, 0.14 mmol, 48 %

Mp: 85 - 95 °C

IR: 445(16), 487(8), 523(3), 551(17), 628(14), 640(15), 700(7), 718(6), 736(9), 874(1), 914(4), 980(12), 1025(11), 1096(5), 1164(2), 1262(10), 1567(15), 1799(20), 1875(19), 1954(18)

EA: Calculated for $C_{24}H_{27}N_3As_3Cl_6Ga$ (Found): C 33.34 (33.51), H 3.15 (3.39), N 4.86 (4.61)

$[Dipp_3N_3As_3Cl_2][GaCl_4]$ (4.1Dipp $[GaCl_4]$): $(DippNAsCl)_2$ (0.10 g, 0.17 mmol), $GaCl_3$ (0.021 g, 0.12 mmol)

Yield: 0.049 g, 0.047 mmol, 40 %

Mp: 182 - 185 °C

IR: 463(19), 520(1), 537(9), 575(17), 693(13), 737(8), 799(4), 839(14), 877(16), 932(5), 1037(7), 1053(12), 1097(3), 1159(2), 1180(10), 1234(15), 1264(11), 1314(18), 1385(16), 1581(20)

EA: Calculated for $C_{36}H_{51}N_3As_3Cl_6Ga$ (Found): C 41.86 (41.19), H 4.98 (4.75), N 4.07 (3.60)

Crystal data: $C_{36}H_{51}As_3Cl_6GaN_3.CH_2Cl_2$, M = 1117.90 g Mol^{-1}, Triclinic, P-1, a = 10.5083(5) Å, b = 14.0826(6) Å, c = 16.5909(8) Å, α = 87.3630(10) °, β = 81.2030(10) °, γ = 79.0670(10) °, V = 2381.91(19) $Å^3$, T = 193(2) K, Z = 2, $\mu(MoK_\alpha)$ 0.71073 (Å), Reflections; 9698 unique, 8572 observed R (for 8572 reflections with $(I > 2\sigma(I))$ = 0.0264; wR(all) = 0.0742

General for $(RNPX)_3$: $(RNPX)_2$ was added to GaX_3, each dissolved in dichloromethane (10 mL), giving an orange solution. After stirring for 2 hours, DMAP was added to give a yellow solution. The solvent was removed under reduced pressure giving a frothy yellow oil, which was extracted with benzene (20 mL) which was removed yielding a slightly yellow solid.

$(DmpNPCl)_3$: $(DmpNPCl)_2$ (0.75 g, 2.0 mmol), $GaCl_3$ (0.31 g, 1.8 mmol), DMAP (0.21 g, 1.8 mmol).

Purification: Slow removal of solvent (benzene) under a static vacuum gave colourless rod-shaped crystals

Yield: 0.28 g, 0.50 mmol, 37 %

Mp: 135 - 138 °C

^{31}P $\{^1H\}$ NMR (CD_2Cl_2): 111 (s, 2P); 116 (s, 1P)

^1H NMR (CD_2Cl_2): 2.55 (s); 2.74 (s); 7.25 (m)

IR: 374(9), 449(3), 509(10), 530(16), 563(20), 578(13), 729(8), 776(5), 802(14), 856(12), 924(17), 964(1), 979(4), 1020(7), 1097(6), 1160(2), 1211(19), 1260(15), 1566(18), 1649(11)

EA: Calculated for $C_{24}H_{27}N_3P_3Cl_3$ (Found): C 51.77 (50.74), H 4.89 (5.07), N 7.55 (7.33)

Crystal data: $C_{24}H_{27}Cl_3N_3P_3.C_6H_6$, M = 634.85 g Mol^{-1}, monoclinic, $P2_1/c$, a = 8.6580(10) Å, b = 30.316(3) Å, c = 11.7922(14) Å, β = 96.593(2) °, V = 3074.7(6) $Å^3$, T = 193(2) K, Z = 4, $\mu(MoK_\alpha)$ 0.71073 (Å), Reflections; 6294 unique, 5504 observed R (for 5504 reflections with $(I > 2\sigma(I))$ = 0.0427; wR(all) = 0.1183

$(DmpNPBr)_3$: $(DmpNPBr)_2$ (1.0 g, 2.2 mmol), $GaBr_3$ (0.50 g, 1.6 mmol), DMAP (0.25 g, 1.6 mmol).

Purification: Re-crystallized from a minimum amount of toluene at –30 °C followed by vapour diffusion of pentane onto dichloromethane afforded colourless plate-shaped crystals

Yield: 0.23 g, 0.33 mmol, 23 %

Mp: 241 - 243 °C

$^{31}P\{^{1}H\}$ NMR ($CDCl_3$): 121 (s, 2P); 134 (s, 1P)

^{1}H NMR (CD_2Cl_2): 2.61 (s); 2.79 (s); 2.82 (s); 2.87 (s); 7.24 (m)

IR: 322(10), 426(6), 452(16), 503(15), 528(12), 576(13), 727(9), 747(17), 775(4), 854(8), 890(20), 910(7), 960(1), 975(3), 1023(11), 1096(5), 1156(2), 1260(14), 1562(19), 1648(18)

EA: Calculated. for $C_{24}H_{27}N_3P_3Br_3$ (Found): C 41.77 (40.63), H 3.94 (4.10), N 6.09 (5.95)

Crystal data: $C_{24}H_{27}Br_3N_3P_3$, M = 690.13 g Mol^{-1}, Monoclinic, $P2_1/n$, a = 15.3058(8) Å, b = 19.7985(11) Å, c = 17.9343(10) Å, β = 97.0275 °, V = 5393.8(5) $Å^3$, T = 193(2) K, Z = 8, $\mu(MoK_\alpha)$ 0.71073 (Å), Reflections; 11044 unique, 8517 observed R (for 8517 reflections with ($I > 2\sigma(I)$) = 0.0357 ; wR(all)= 0.0998

General for $(RNAsCl)_3$: $(RNAsCl)_2$ and $GaCl_3$ were combined and dissolved in toluene (~ 3ml), the formation of a dark red solution was immediate, but faded after 2 hours, with stirring for 18 hours. Addition of DMAP gave a light yellow solution. Partial removal of the solvent in vacuo deposited a yellow oil, which was separated from the solution.

$(DmpNAsCl)_3$: $(DmpNAsCl)_2$ (0.30 g, 0.65 mmol), $GaCl_3$ (0.077 g, 4.4 mmol), DMAP (0.052 g, 4.3 mmol)

Purificaiton: The solvent was removed under vacuum to give a white solid, which was dissolved in minimal CH_2Cl_2 and vapor diffusion with pentane gave rod shaped crystals; Yield: 0.14 g, 0.20 mmol, 47 %

Mp: 215 - 217 °C

^{1}H NMR ($CDCl_3$): 2.59 (s), 2.69 (s), 2.74 (s), 2.79 (s), 7.20 (s), 7.22 (s)

IR: 310(1), 336(3), 384(9), 449(14), 524(9), 534(19), 700(11), 718(8), 782(5), 868(2), 915(10), 979(15), 1025(12), 1098(6), 1163(4), 1256(13), 1559(17), 1628(18), 1797(20), 1954(16)

EA: Calculated for $C_{24}H_{27}N_3As_3Cl_3$ (Found): C 41.86 (41.59), H 3.95 (3.94), N 6.10 (5.87)

Crystal data: $C_{24}H_{27}As_3Cl_3N_3$, M = 688.60 g Mol^{-1}, Monoclinic, I2/a, a = 31.883(3) Å, b = 9.2627(8) Å, c = 18.7383(15) Å, β = 96.3590(10) °, V = 5499.9(8) $Å^3$, T = 193(2) K, Z = 8, μ(MoK_α) 0.71073 (Å), Reflections; 5605 unique, 4196 observed R (for 4196 reflections with ($I > 2\sigma(I)$) = 0.0423; wR(all) = 0.1100

(DippNAsCl)$_3$: (DippNAsCl)$_2$ (0.150 g, 0.262 mmol), $GaCl_3$ (0.090 g, 0.51 mmol), DMAP (0.065 g, 5.4 mmol)

Purification: The solution was filtered through a small column of silica, which was washed repeatedly with toluene (~1ml). Slow solvent evaporation of the toluene gave plate crystals

Yield: 0.065 g, 0.075 mmol, 43 %

Mp: 244 - 247 °C

^{1}H ($CDCl_3$) NMR: 1.14(d), 1.28-1.39 (m), 3.49 (sep), 3.83 (sep), 3.99 (sep), 4.10 (sep); 7.32-7.41(m)

IR: 303(6), 327(16), 355(4), 425(7), 523(11), 748(18), 800(2), 838(9), 877(1), 933(13), 1036(12), 1052(15), 1098(5), 1159(3), 1235(16), 1255(17), 1310(14), 1346(8), 1365(8), 1592(20)

EA: Calculated for $C_{36}H_{51}N_3As_3Cl_3$ (Found): C 50.46 (49.65), H 6.00 (5.74), N 4.90 (4.85)

Crystal data: $C_{36}H_{51}As_3Cl_3N_3$, M = 856.91 g Mol^{-1}, Monoclinic, $P2_1/n$, a = 12.2049(14) Å, b = 21.386(2) Å, c = 16.3283(19) Å, β = 111.852(2) °, V = 3955.7(8) $Å^3$, T = 193(2) K, Z = 4, μ(MoK_α) 0.71073 (Å), Reflections; 8104 unique, 6329 observed R (for 6329 reflections with ($I > 2\sigma(I)$) = 0.0310; wR(all) = 0.0752

(DMAP)P(μ-DmpN)$_2$PCl [OTf] (6.2[OTf]**):** $(DmpNPCl)_2$ (0.600 g, 1.6 mmol) and DMAP (0.20 g, 1.6 mmol) were dissolved in CH_2Cl_2 (5 ml), to this solution was added TMSOTf (0.35 ml, 1.9 mmol). The reaction was allowed to stir until the consumption of the starting material was observed by ^{31}P NMR. The solvent was then removed under reduced pressure and the subsequent solid was washed twice with toluene (2 ml). Plate-shaped crystals were obtained from the vapour diffusion of pentane onto a solution of the product in CH_2Cl_2.

Yield: (crude) 0.69 g, 1.1 mmol, 70 %

Mp. decomposition 190 – 210 ° C

^{31}P {^1H} NMR ($CDCl_3$): δ 159 ppm (d), 209 ppm (d), $^2J_{PP}$ = 52.1 Hz

^1H NMR ($CDCl_3$): 2.52(s), 3.42(s), 7.08 - 7.212 (m), 8.82 – 8.87 (m)

IR: 439(12), 468(11), 517(5), 572(10), 636(3), 718(6), 763(7), 889(13), 1028(4), 1099(19), 1146(15), 1220(15), 1269(2), 1322(16), 1400(9), 1586(80, 1643(1), 1708(17), 1791(18), 3270 (20)

Crystal data: $C_{24}H_{28}ClF_3N_4O_3P_2S$, M = 606.95 g Mol^{-1}, Monoclinic, $P2_1/c$, a = 14.0899(11) Å, b = 15.4119(12) Å, c = 12.9028(10) Å, β = 91.8988(10) °, V = 2800.3(4) $Å^3$, T = 193(2) K, Z = 4, μ(MoK_α) 0.71073 (Å), Reflections; 5721 unique, 4722 observed R (for 4722 reflections with (I > 2σ(I)) = 0.0411; wR(all) = 0.1066

$Cl_3Ga.DmpNAsPh_2AsPh_2$ (6.5): $(DmpNAsCl)_2$ (0.20 g, 0.44 mmol) and $GaCl_3$ (0.15 g, 0.88 mmol) were combined and dissolved in toluene (5 ml). After 20 minutes, $NaBPh_4$ (0.30 g, 0.88 mmol) was added, immediately producing a white precipiate, which was removed by filtration. The solution was then concentrated and left at – 30 °C, yielding needle-shaped crystals.

^1H NMR ($CDCl_3$): 2.38(s), 6.84 – 7.56 (m)

Crystal data: $C_{32}H_{29}As_2Cl_3GaN$, M = 753.47 g Mol^{-1}, Monoclinic, $P2_1/c$, a = 9.980(2) Å, b = 18.559(3) Å, c = 17.005(3) Å, β = 103.895(3) °, V = 3057.4(9) $Å^3$, T = 193(2) K, Z = 4, μ(MoK_α) 0.71073 (Å), Reflections; 6258 unique, 4434 observed R (for 4434 reflections with (I > 2σ(I)) = 0.0463; wR(all) = 0.1114

Reactions of $(DmpNPCl)_2$ and $(DmpNAsCl)_2$ with $GaCl_3$: In a typical reaction 1eq. of $(DmpNPnCl)_2$ was combined with 2eq. of $GaCl_3$ in 1ml of toluene and allowed to stir for 15 minutes at room temperature, to which a solution of 2eq. $(DmpNPn'Cl)_2$ (where Pn ≠ Pn') in ~ 1ml of toluene was added. The reaction was stirred for 2 hours, at which time

2eq. of DMAP was added. Removal of the solvent under reduced pressure yielded an oily yellow precipitate, which was extracted with toluene (~2ml) and filtered through a small column of silica. Removal of the solvent yielded a white powder which was then used for NMR or mass spectrometry studies. Block shaped crystals were obtained from vapour diffusion the pentane onto CH_2Cl_2.

Crystal data: $C_{24}H_{27}AsClN_3P_3$, M = 600.70 g Mol^{-1}, Monoclinic, $P2_1/n$, a = 15.1756(10) Å, b = 19.8864(13) Å, c = 17.9060(12) Å, β = 96.2210(10) °, V = 5372.0(66) $Å^3$, T = 193(2) K, Z = 8, μ(MoK_α) 0.71073 (Å), Reflections; 10976 unique, 8973 observed R (for 8973 reflections with ($I > 2\sigma(I)$) = 0.0578; wR(all) = 0.2104

($DmpNH_2$)$SbCl_3$ (7.1Dmp) and ($DmpNH_2$)$_2SbCl_3$ (7.2Dmp): $DmpNH_2$ (2.4 ml, 20 mmol) was added to $SbCl_3$ (1.8 g, 7.8 mmol) in toluene (50 ml). The solution was filtered and removal of solvent under reduced pressure gave a precipitate that was dissolved in minimal CH_2Cl_2 and vapour diffusion of pentane over 2 days gave crystals of empirical formula $(DmpNH_2)_3(SbCl)_2$-$0.5CH_2Cl_2$:

Yield: 0.98 g, 1.8 mmol, 45 %

Mp. 81-82° C

^1H NMR ($CDCl_3$): 2.18 (s), 3.86 (s), 6.69 (t), 6.94(d)

IR: 280(1), 326(5), 436(9), 494(14), 543(11), 670(13), 770(2), 769(3), 928(11), 1027(15), 1098(12), 1139(19), 1154(20), 1211(6), 1262(7), 1577(10), 1598(8), 3295(17), 3357(16), 3374(18); NMR: ^1H ($CDCl_3$): ^1H ($CDCl_3$): 2.18 (s), 3.86 (s), 6.69 (t), 6.94 (d);

EA: Calculated. for $C_{24}H_{33}N_3Cl_6Sb_2$ (Found): C 35.16 (33.01), H 4.06 (4.04), N 5.13 (5.97); Calculated for $C_{24.5}H_{34}N_3Cl_7Sb_2$ (Found): C 34.13 (33.01), H 3.97 (4.04), N 4.87 (5.97)

Crystal data: $C_{24.5}H_{34}Cl_7N_3Sb_2$, M = 862.20 g Mol^{-1}, Triclinic, P^-1, a = 9.9556(7) Å, b = 10.4211(7) Å, c = 16.9114(12) Å, α = 85.8918(10) °, β = 84.9494(10)°, γ = 73.7057(9) °, V = 1675.5(2) $Å^3$, T = 193(2) K, Z = 2, $\mu(MoK_\alpha)$ 0.71073 (Å), Reflections; 6811 unique, 6180 observed R (for 6180 reflections with $(I>2\sigma(I))$ = 0.0220; wR(all)= 0.0600.

$(DippNH_2)_2SbCl_3$ (7.2Dipp): $DippNH_2$ (3.3 ml, 18 mmol) was added to $SbCl_3$ (1.8 g, 9.2 mmol) in toluene (50 ml). The solution stirred overnight, followed by removal of the solvent under vacuum to yield a greenish oil. Washing with pentane (15 ml) removed the green colour, leaving a white solid, which was recrystallized from minimal toluene (5 ml) at – 25 °C, yielding colourless block crystals.

Yield: 0.81 g, 1.8 mmol, 19 %

Mp: 64 – 66 °C

^1H NMR ($CDCl_3$): 1.27 (d), 2.95(sept), 4.03(s), 6.87(t), 7.07(d)

IR: 447(3), 517(4), 543(2), 667(1), 918(9), 960(8), 1000(12), 1043(5), 1114(13), 1145(10), 1197(7), 1259(6), 1300(15), 1355(11), 1615(14), 1807(20), 1862(19), 1919(18), 3341(17), 3403(16)

Crystal data: $C_{18}H_{28.5}Cl_3N_{1.5}Sb$, M = 494.02 g Mol^{-1}, Triclinic, P^-1, a = 9.2092(6) Å, b = 10.6249(7) Å, c = 11.0555(8) Å, α = 94.0040(10) °, β = 93.9842(10) °, γ = 90.6394(10) °, V = 1676.36(13) $Å^3$, T = 193(2) K, Z = 2, $\mu(MoK_\alpha)$ 0.71073 (Å), Reflections; 4405

unique, 4405 observed R (for 4172 reflections with ($I > 2\sigma(I)$) = 0.0187; wR(all) = 0.0533

Isolation of $DmpN(H)Sb(Cl)N(Dmp)SbCl_2$ (7.3) and $(DmpNSbCl)_3$: $DmpNH_2$ (4.9 mL, 40 mmol) added to NEt_3 (5.7 mL, 40 mmol) and $SbCl_3$ (6.2 g, 27 mmol) in toluene (110 mL) at 0° C, stirred for 1.5 h at RT. Filtered and the solvent was removed in vacuo to 5 mL, addition of pentane (5 mL) gave a yellow precipitate after 4 days at -24°C, which was dissolved in minimal CH_2Cl_2 and vapour diffusion of pentane gave crystals with two distinct morphologies and colours, that were manually separated.

$DmpN(H)Sb(Cl)N(Dmp)SbCl_2$ (7.3): Pale yellow Crystals

Crystal Data: $C_{16}H_{19}Cl_3N_2Sb_2$, M = 589.18 g Mol^{-1}, Monoclinic $P2_1/c$, a = 13.0005(9) Å, b = 20.8528(14) Å, c = 15.5863(10) Å, β = 108.9580(10) °, V = 3996.2(5) $Å^3$, T = 193(2) K, Z = 8, μ(MoK_α) 0.71073 (Å), Reflections; 8121 unique, 7448 observed, R (for 7448 reflections with ($I > 2\sigma(I)$) = 0.0211; wR(all)= 0.0555.

$(DmpNSbCl)_3$: Colourless crystals

Mp. 269 – 271 °C

NMR: ^1H ($CDCl_3$): 2.60 (s), 2.66 (s), 2.69(s), 2.74(s), 7.02 - 7.17 (m)

IR: 229(5), 325(9), 373(11), 486(15), 522(8), 690(10), 707(7), 790(3), 811(2), 839(4), 901(16), 984(12), 1023(13), 1097(6), 1164(1), 1252(14), 1586(17), 1799(19), 1867(20), 1934(18); EA: Calculated for $C_{24}H_{27}N_3Cl_3Sb_3$ (Found): C 34.77 (31.52), H 3.28 (3.45), N 5.07 (5.25)

Crystal data: $C_{24}H_{27}Cl_3N_3Sb_3$, M = 829.09 g Mol^{-1}, Monoclinic, $P2_1/c$, a = 16.376(3) Å, b = 8.9041(14) Å, c = 19.122(3) Å, β = 96.817(3) °, V = 2768.6(7) $Å^3$, T = 193(2) K, Z = 4, μ(MoK_α) 0.71073 (Å), Reflections; 5572 unique, 4468 observed R (for 4468 reflections with ($I > 2\sigma(I)$) = 0.0687; wR(all) = 0.1960

References

(1) Kotz, J. C.; Treichel, P. *Chemistry and Chemical Reactivity*; 3rd ed.; Saunders College Publishing: Toronto, 1996.

(2) Wiberg, K. B. *Angew. Chem. Int. Ed.* **1986**, *25*, 312.

(3) Power, P. P. *Chem. Rev.* **1999**, *99*, 3463.

(4) Brook, A. G.; Nyberg, S. C.; Abdesaken, F.; Gutekunst, B.; Gutekunst, G., Krishna, R.; Kallury, M. R.; Poon, Y. C.; Chang, Y. M.; Wong-Ng, W. *J. Am. Chem. Soc.* **1982**, *104*, 5667.

(5) Tsang, C., Yam, M., Gates, D. P. *J. Am. Chem. Soc.* **2003**, *125*, 1480.

(6) Manners, I. *Angew. Chem. Int. Ed.* **1996**, *35*, 1602.

(7) Harvey, D. A.; Keat, R.; Rycroft, D. S. *Dalton Trans.* **1983**, 425.

(8) Burford, N.; Cameron, T. S.; Conroy, K. D.; Ellis, B.; Macdonald, C. L. B.; Ovans, R.; Phillips, A. D.; Ragogna, P. J.; Walsh, D. *Can. J. Chem.* **2002**, *80*, 1404.

(9) Ford, R. R.; Neilson, R. H. *Polyhedron* **1986**, *5*, 643.

(10) Markovskii, L. N.; Romanenko, V. D.; Ruban, A. V.; Drapailo, A. B.; Chernega, A. N.; Antipin, M. Y.; Struchkov, Y. T. *Zh. Obshch. Khim.* **1988**, *58*, 291.

(11) Markovskii, L.; Romanenko, V.; Ruban, A. *Zh. Obshch. Khim.* **1979**, *49*, 1908.

(12) Jones, P. G.; Fischer, A. K.; Maller, C.; Pinchuk, V. A.; Schmutzler, R. *Acta Cryst.* **1996**, *C52*, 2750.

(13) Ang, H. G.; Kwik, W. L.; Lee, Y. W.; Rheingold, A. L. *Dalton Trans.* **1993**, 663.

(14) Brandl, A.; Noth, H. *Chem. Ber.* **1988**, *121*, 1321.

(15) Scherer, O. J.; Glenel, W. *Chem. Ber.* **1977**, *110*, 3874.

(16) Balakrishna, M. S.; Reddy, V. S.; Krishnamurthy, S. S.; Nixon, J. F.; Burckett St.Laurent, J. C. T. R. *Coord. Chem. Rev.* **1994**, *129*, 1.

(17) Markovskii, L. N.; Romanenko, V. D.; Ruban, A. V.; Drapailo, A. B.; Reitel, G. V.; Chernega, A. N.; Povolotskii, M. I. *Zh. Obshch. Khim.* **1990**, *60*, 2453.

(18) Gynane, M. J. S.; Hudson, A.; Lappert, M. F.; Power, P. P.; Goldwhite, H. *Dalton Trans.* **1980**, 2428.

(19) Bender, H. R. G.; Niecke, E.; Nieger, M.; Westermann, H. *Z. Anorg. Allg. Chem.* **1994**, *620*, 1194.

(20) Briand, G. G.; Chivers, T.; Parvez, M. *Can. J. Chem.* **2003**, *81*, 169.

(21) Scherer, O. J.; Kuhn, N. *Chem. Ber.* **1974**, *107*, 2123.

(22) Raston, C. L.; Skelton, B. W.; Tolhurst, V. A.; White, A. H. *Polyhedron* **1998**, *17*, 935.

(23) Tarassoli, A.; Haltiwanger, R. C.; Norman, A. D. *Inorg. Chem.* **1982**, *21*, 2684.

(24) Burford, N.; Macdonald, C. L. B.; Robertson, K. N.; Cameron, T. S. *Inorg. Chem.* **1996**, *35*, 4013.

(25) Raston, C. L.; Skelton, B. W.; Tolhurst, V. A.; White, A. H. *Dalton Trans.* **2000**, 1279.

(26) Mitzel, N. W.; Smart, B. A.; Dreihnupl, K. H.; Rankin, D. W. H.; Schmidbaur, H. *J.A.C.S.* **1996**, *118*, 12673.

(27) Frenzel, A.; Gluth, M.; Herbst-Irmer, R.; Klingebiel, U. *J. Organomet. Chem.* **1996**, *514*, 281.

(28) Atwood, J. L.; Cowley, A. H.; Hunter, W. E.; Mehrotra, S. K. *Inorg. Chem.* **1982**, *21*, 1354.

(29) Romming, C.; Songstad, J. *Acta Chemica Scandinavica* **1980**, *A 34*, 365.

(30) Edwards, A. J.; Paver, M. A.; Raithby, P. R.; Russell, C. A.; Wright, D. S. *Dalton Trans.* **1993**, 2257.

(31) Hass, D. *Z. Anorg. Allg. Chem.* **1964**, *332*, 287.

(32) Clegg, W.; Compton, N. A.; Errington, R. J.; Norman, N. C.; Wishart, N. *Polyhedron* **1989**, *8*, 1579.

(33) Clegg, W.; Compton, N. A.; Errington, R. J.; Fisher, G. A.; Green, M. E.; Hockless, D. C. R.; Norman, N. C. *Inorg. Chem.* **1991**, *30*, 4680.

(34) Hill, T. G.; Haltiwanger, R. C.; Prout, T. R.; Norman, A. D. *Inorg. Chem.* **1989**, *28*, 3461.

(35) Niecke, E.; Nieger, M.; Reichert, F. *Angew. Chem. Int. Ed.* **1988**, *27*, 1715.

(36) Niecke, E.; Gudat, D. *Angew. Chem. Int. Ed.* **1991**, *30*, 217.

(37) Burford, N.; Ragogna, P. J. *Dalton Trans.* **2002**, 4307.

(38) Hitchcock, P. B.; Lappert, M. F.; Rai, A. K.; Williams, H. D. *Chem. Commun.* **1986**, 1633.

(39) Ahlemann, J. T.; Kanzel, A.; Roesky, H. W.; Noltemeyer, M.; Markovskii, L.; Schmidt, H. G. *Inorg. Chem.* **1996**, *35*, 6644.

(40) Michaelis, A.; Schroeter, G. *Chem. Ber.* **1894**, *37*, 490.

(41) Davies, A. R.; Dronsfield, A. T.; Haszeldine, R. N.; Taylor, D. R. *Perkin. Trans.I* **1973**, 379.

(42) Keat, R. *Top. Curr. Chem.* **1982**, *102*, 89.

(43) Stahl, L. *Coord. Chem. Rev.* **2000**, *210*, 203.

(44) Muir, K. W.; Nixon, J. F. *Chem. Commun.* **1971**, 1405.

(45) Bohra, R.; Roesky, H. W.; Noltemeyer, M.; Sheldrick, G. M. *Acta Cryst.* **1984**, *C40*, 1150.

(46) Ahlemann, J. T.; Roesky, H. W.; Murugavel, R.; Parisini, E.; Noltemeyer, M.; Schmidt, H. G.; Muller, O.; Herbst-Irmer, R.; Markovskii, L. N.; Shermolovich, Y. G. *Chem. Ber.* **1997**, *130*, 1113.

(47) Burford, N.; Cameron, T.S.; Macdonald, C.L.B.; Robertson, K.N.; Schurko, R.; Walsh, D.; McDonald, R.; Wasylishen, R.E. *Inorg. Chem.* **2005**, *44*, 8085.

(48) Haagenson, D. C.; Stahl, L.; Staples, R. J. *Inorg. Chem.* **2001**, *40*, 4491.

(49) Grocholl, L.; Stahl, L.; Staples, R.J.; *Chem. Commum.* **1997**, 1465.

(50) Axenov, K. V.; Kilpelainen, I.; Klinga, M.; Leskela, M.; Repo, T. *Organometallics* **2006**, *25*, 463.

(51) Burford, N.; Cameron, T. S.; Lam, K. C.; LeBlanc, D. J.; Macdonald, C. L. B.; Phillips, A. D.; Rheingold, A. L.; Stark, L.; Walsh, D. *Can. J. Chem.* **2001**, *79*, 342.

(52) Wirringa, U.; Roesky, H. W.; Noltemeyer, M.; Schmidt, H. G. *Inorg. Chem.* **1994**, *33*, 4607.

(53) Bryant, R.; James, S. C.; Jeffrey, J. C.; Norman, N. C.; Orpen, A. G.; Weckenmann, U. *Dalton Trans.* **2000**, 4007.

(54) Beswick, M. A.; Harmer, C. N.; Hopkins, A. D.; Paver, M. A.; Raithby, P. R.; Wright, D. S. *Polyhedron* **1998**, *17*, 745.

(55) Edwards, A. J.; Paver, M. A.; Rennie, M. A.; Raithby, P. R.; Russell, C. A.; Wright, D. S. *Dalton Trans.* **1994**, 2963.

(56) Avtomonov, E. V.; Megges, K.; Li, X.; Lorberth, J.; Wocadlo, S.; Massa, W.; Harms, K.; Churakov, A. V.; Howard, J. A. K. *J. Organomet. Chem.* **1997**, *544*, 79.

(57) Kokorev, G. I.; Litvinov, I. A.; Naumov, V. A.; Badrutdinov, S. K. *Zh. Obshch. Khim.* **1991**, *60*, 1852.

(58) Ross, B.; Belz, J.; Nieger, M. *Chem. Ber.* **1990**, *123*, 975.

(59) Kokorev, G. I.; Litvinov, I. A.; Naumov, V. A.; Badrutdinov, S. K.; Yambushev, F. D. *Zh. Obshch .Khim.* **1989**, *59*, 1556.

(60) Zeiss, W.; Barlos, K. *Z. Naturforsch.* **1979**, *34b*, 423.

(61) Zeiss, W.; Pointner, A.; Engelhardt, C.; Klehr, H. *Z. Anorg. Allg. Chem.* **1981**, *475*, 256.

(62) Murugavel, R.; Krishnamurthy, S. S.; Chandrasekhar, J.; Nethaji, M. *Inorg. Chem.* **1993**, *32*, 5447.

(63) Vetter, H. J.; Noth, H.; Jahn, W. *Z. Anorg. Allg. Chem.* **1964**, *328*, 144.

(64) Weiss, J.; Eisenhuth, W. *Z. Naturforsch.* **1967**, *22b*, 454.

(65) Garcia, F., Kowenicki, R.A., Riera, L., Wright, D.S., *Dalton Trans.* **2005**, 2495.

(66) Malavaud, C.; M'Pondo, T. N.; Lopez, L.; Barrans, J.; Legros, J. P. *Can. J. Chem.* **1984**, *62*, 43.

(67) Zeiss, W.; Schwarz, W.; Hess, H. *Angew. Chem. Int. Ed.* **1977**, *16*, 407.

(68) Burford, N.; Cameron, T. S.; Conroy, K. D.; Ellis, B.; Lumsden, M. D.; Macdonald, C. L. B.; McDonald, R.; Phillips, A. D.; Ragogna, P. J.; Schurko, R. W.; Walsh, D.; Wasylishen, R. E. *J.A.C.S.* **2002**, *124*, 14012.

(69) Burford, N.; Dyker, C. A.; Phillips, A. D.; Spinney, H. A.; Decken, A.; McDonald, R.; Ragogna, P. J.; Rheingold, A. L. *Inorg. Chem.* **2004**, *43*, 7502.

(70) Olah, G. A.; Oswald, A. A. *Can. J. Chem.* **1960**, *38*, 1428.

(71) Thompson, M. L.; Tarassoli, A.; Haltiwanger, R. C.; Norman, A. D. *Inorg. Chem.* **1987**, *26*, 684.

(72) Barendt, J. M.; Haltiwanger, R.C.; Norman, A.D. *J. Am. Chem. Soc.* **1986**, *108*, 3127.

(73) Barendt, J. M.; Bent, E. G.; Haltiwanger, R. C.; Norman, A. D. *J. Am. Chem. Soc.* **1989**, *111*, 6883.

(74) Barendt, J. M.; Bent, E. G.; Haltiwanger, R. C.; Norman, A. D. *Inorg. Chem.* **1989**, *28*, 2334.

(75) Bent, E. G.; Schaeffer, R.; Haltiwanger, R. C.; Norman, A. D. *Inorg. Chem.* **1990**, *29*, 2608.

(76) Barendt, J. M.; Haltiwanger, R. C.; Squier, C. A.; Norman, A. D. *Inorg. Chem.* **1991**, *30*, 2342.

(77) Katz, S. A.; Allured, V. S.; Norman, A. D. *Inorg. Chem.* **1994**, *33*, 1762.

(78) Young, S. M.; Barendt, J. M.; Carperos, V.; Haltiwanger, R. C.; Hands, R. M.; Norman, A. D. *Inorg. Chem.* **1995**, *34*, 5003.

(79) Helm, M. L.; Katz, S. A.; Imiolczyk, T. W.; Hands, R. M.; Norman, A. D. *Inorg. Chem.* **1999**, *38*, 3167.

(80) Beswick, M. A.; Davies, M. K.; Paver, M. A.; Raithby, P. R.; Steiner, A.; Wright, D. S. *Angew. Chem. Int. Ed.* **1996**, *35*, 1508.

(81) Wright, D. S.; Bashall, A.; Doyle, E. L.; Tubb, C.; Kidd, S. J.; McPartlin, M.; Woods, A. D. *Chem. Commun.* **2001**, 2542.

(82) Beswick, M. A.; Elvidge, B. R.; Feeder, N.; Kidd, S. J.; Wright, D. S. *Chem. Commun.* **2001**, 379.

(83) Scherer, O. J.; Klusmann, P. *Angew. Chem. Int. Ed.* **1969**, *8*, 752.

(84) Kamil, W. A.; Shreeve, J. M. *Inorg. Synth.* **1990**.

(85) Wright, D. S.; Bashall, A.; Bond, A. D.; Doyle, E. L.; Garcia, F.; Kidd, S. J.; Lawson, G. T.; Parry, M. C.; McPartlin, M.; Woods, A. D. *Chem. Eur. J.* **2002**, *8*, 3377.

(86) Moser, D. F.; Grocholl, L.; Stahl, L.; Staples, R.J.; *Dalton Trans.* **2003**, 1402.

(87) Conroy, K. D. B.Sc. Thesis, Dalhousie University, 2002.

(88) Jefferson, R.; Nixon, J. F.; Painter, T. M.; Keat, R.; Stobbs, L. *Dalton Trans.* **1973**, 1414.

(89) Bashall, A.; Elvidge, B. R.; Beswick, M. A.; Kidd, S. J.; McPartlin, M.; Wright, D. S. *Chem. Commun.* **2000**, 1439.

(90) Scherer, O. J.; Andres, K.; Krager, C.; Tsay, Y. H.; Wolmershnuser, G. *Angew. Chem. Int. Ed.* **1980**, *19*, 571.

(91) Doyle, E. L.; Garcia, F.; Humphrey, S.M.; Kowenicki, R.A.; Riera, L.; Woods, A.D.; Wright, D.S. *Dalton Trans.* **2004**, 807-812.

(92) Burford, N.; Clyburne, J. A. C.; Bakshi, P. K.; Cameron, T. S. *Organometallics* **1995**, *14*, 1578.

(93) Cowley, A. H.; Kemp, R. A. *Chem. Rev.* **1985**, *85*, 367.

(94) Burford, N.; Losier, P.; Macdonald, C.; Kyrimis, V.; Bakshi, P. K.; Cameron, T. S. *Inorg. Chem.* **1994**, *33*, 1434.

(95) Cowley, A. H.; Lattman, M.; Wilburn, J. C. *Inorg. Chem.* **1981**, *20*, 2916.

(96) Burford, N.; Ragogna, P. J.; McDonald, R.; Ferguson, M. J. *Chem. Commun.* **2003**, 2066.

(97) Burford, N.; Cameron, T. S.; Clyburne, J. A. C.; Eichele, K.; Robertson, K. N.; Sereda, S.; Wasylishen, R. E.; Whitla, W. A. *Inorg. Chem.* **1996**, *35*, 5460.

(98) Burford, N.; Losier, P.; Phillips, A. D.; Ragogna, P. J.; Cameron, T. S. *Inorg. Chem.* **2003**, *42*, 1087.

(99) Yoshifuji, M. *Bull. Chem. Soc. Jap.* **1997**, *70*, 2881.

(100) McWilliams, A. R.; Gates, D. P.; Edwards, M.; Liable-Sands, L. M.; Guzei, I.; Rheingold, A. L.; Manners, I. *J. Am. Chem. Soc.* **2000**, *122*, 8848.

(101) Rivard, E.; Lough, A. J.; Chivers, T.; Manners, I. *Inorg. Chem.* **2004**, *43*, 802.

(102) Burford, N.; Parks, T. M.; Royan, B. W.; Richardson, J. F.; White, P. S. *Can. J. Chem.* **1992**, *70*, 703.

(103) Burford, N.; Parks, T. M.; Royan, B. W.; Borecka, B.; Cameron, T. S.; Richardson, J. F.; Gabe, E. J.; Hynes, R. *J. Am. Chem. Soc.* **1992**, *114*, 8147.

(104) Burford, N.; Macdonald, C. L. B.; Parks, T. M.; Wu, G.; Borecka, B.; Kwiatkowski, W.; Cameron, T. S. *Can. J. Chem.* **1996**, *74*, 2209.

(105) Gates, D. P.; Manners, I. *Dalton Trans.* **1997**, 2525.

(106) Scherer, O. J.; Wokulat, J. *Z. Anorg. Allg. Chem.* **1968**, *361*, 296.

(107) Scherer, O. J.; Janssen, W.M. *J. Organometallic Chem.* **1969**, *20*, 111.

(108) Singh, J.; Burg, A.B. *J. Am. Chem. Soc.* **1966**, *88*, 718.

(109) Scherer, O. J.; Schnabl, G. *Z. Naturforsch.* **1976**, *31b*, 142.

(110) Schranz, G.L.P.; Stahl, L.; Staples, R.J.; Johnson, A. *Inorg. Chem.* **2000**, *39*, 3037.

(111) Burford, N.; Cameron, T. S.; Ragogna, P. J.; Ocando-Mavarez, E.; Gee, M.; McDonald, R.; Wasylishen, R. E. *J. Am. Chem. Soc.* **2001**, *123*, 7947.

(112) Burford, N.; Spinney, H. A.; Ferguson, M. J.; McDonald, R. *Chem. Commun.* **2004**, 2696.

(113) Burford, N.; Cameron, T. S.; Robertson, K. N.; Phillips, A. D.; Jenkins, H. A. *Chem. Commun.* **2000**, 2087.

(114) Burford, N.; Phillips, A. D.; Spinney, H. A.; Robertson, K. N.; Cameron, T. S.; McDonald, R. *Inorg. Chem.* **2003**, *42*, 4949.

(115) Burford, N.; Phillips, A. D.; Spinney, H. A.; Lumsden, M. D.; Werner-Zwanziger, U.; Ferguson, M. J.; McDonald, R. *J. Am. Chem. Soc.* **2005**, *127*, 3921.

(116) Niecke, E.; Nixon, J. F.; Wenderoth, P.; Passos, B. F. T.; Nieger, M. *Chem. Commun.* **1993**, 846.

(117) Kokorev, G. I.; Litvinov, I.; Musin, R.Z.; Naumov, V.A. *Zh. Obs. Khimi.* **1991**, *22*, 2713.

(118) Chaozhou, N.; Zhiming, Z.; Zuowei, X.; Changtao, Q.; Yaozeng, H. *Chinese J. Struct. Chem.* **1986**, *5*, 181.

(119) Fei, Z.; Biricik, N.; Zhao, D.; Scopelliti, R.; Dyson, P. J. *Inorg. Chem.* **2004**, *43*, 2228.

(120) Fei, Z.; Scopelliti, R.; Dyson, P.J. *Dalton Trans.* **2003**, 2772.

(121) Hulme, R.; Scruton, J. C. *J. Chem. Soc. A* **1968**, 2448.

(122) Muller, G.; Brand, J.; Jetter, S. E. *Z. Naturforsch.* **2001**, *56b*, 1163.

(123) Burford, N.; Muller, J.; Parks, T. M. *J. Chem. Educ.* **1994**, *71*, 807.

(124) Shriver, D. F.; Drezdzon, M. A. *The Manipulation of Air-Sensitive Compounds*; John Wiley and Sons: Toronto, 1986.

(125) Perrin, D. D.; Armarego, W. L. F. *Purification of Laboratory Chemicals*; Permagon Press: Toronto, 1989.